





**LONG WEAKLY NONLINEAR  
WAVES IN GEOPHYSICAL  
APPLICATIONS**

**KALEV RANNAT**



TARTU UNIVERSITY  
PRESS

The study was carried out at the Marine Systems Institute of the Tallinn University of Technology, Institute of Cybernetics at Tallinn University of Technology and Institute of Environmental Physics, University of Tartu, Estonia.

The dissertation was admitted on April 04, 2007, in partial fulfilment of the requirements for the degree of Doctor of Philosophy in physics (environmental physics), and allowed for defence by the Council of the Department of Physics, University of Tartu.

Supervisors: Prof. Tarmo Soomere, D.Sc., Institute of Cybernetics, Tallinn University of Technology, Tallinn, Estonia  
Assoc. Prof. Hanno Ohvril, PhD, Institute of Environmental Physics, University of Tartu, Tartu, Estonia

Opponents: Prof. Sirje Keevallik, PhD, Estonian Maritime Academy, Tallinn, Estonia  
Dr. Oleg Andrejev, PhD, Finnish Institute of Marine Research, Helsinki, Finland

Defence: May 29, 2007, at the University of Tartu, Estonia

ISSN 1024-6479

ISBN 978-9949-11-583-9 (trükis)

ISBN 978-9949-11-584-6 (PDF)

Autoriõigus Kalev Rannat, 2007

Tartu Ülikooli Kirjastus

[www.tyk.ee](http://www.tyk.ee)

Tellimus nr 137

# CONTENTS

<b>INTRODUCTION</b> .....	7
<b>PAPERS CONSTITUTING THE THESIS</b> .....	<b>9</b>
Contribution of the author to the joint papers .....	11
Main arguments proposed to defend .....	13
<b>1. WEAKLY NONLINEAR WAVES IN GEOPHYSICAL FLOWS ....</b>	<b>16</b>
1.1. Linear, weakly nonlinear and long waves .....	16
1.2. Kinetic theory of weakly nonlinear waves .....	19
1.3. Equations of long waves on the $\beta$ -plane.....	21
1.4. Multi-modal kinetic equations and the multi-layer ocean .....	24
1.5. Ship waves.....	26
<b>2. SPECTRAL EVOLUTION OF ROSSBY WAVES IN A TWO-LAYER OCEAN .....</b>	<b>29</b>
2.1. Kinetic equation for Rossby waves in a two-layer ocean.....	29
2.2. Solver of the kinetic equation.....	31
2.3. Reduction of collision integrals.....	32
2.4. Resonance curves and double resonance.....	34
2.5. Resonance curves for baroclinic Rossby waves .....	37
2.6. Numerical scheme: discretization and stability .....	40
2.7. Basic features of spectral evolution.....	44
2.8. Layer formation in stratified medium .....	53
2.9. Modelling of layer formation .....	56
<b>3. LONG WEAKLY NONLINEAR SURFACE WAVES .....</b>	<b>62</b>
3.1. Kinetic theory in surface wave modelling.....	62
3.2. Basic concepts of the linear surface wave theory.....	63
3.3. Long nonlinear surface waves .....	66
3.4. Wind wave observations and modelling in the Baltic Sea .....	68
3.5. Trends and extremes in wave fields of the Baltic Sea.....	70
3.6. Wave properties in the Gulf of Finland and in Tallinn Bay .....	71
3.7. Ship waves in Tallinn Bay.....	73
3.7.1 Possibilities of description of ship waves .....	73
3.7.2 Properties of ship-generated waves in the Tallinn Bay area .....	76
3.7.3 Multisensor analysis of the surface waves .....	82
3.7.4 Shape of long ship waves .....	84
3.8. Environmental implications of ship wave activity .....	87
<b>REFERENCES .....</b>	<b>91</b>
Approbation of results .....	99
Summary.....	100
Abstract.....	102
Pikad nõrgalt mittelineaarsed lained geofüüsikalistes rakendustes .....	103
Väitekirja tulemused .....	104
<b>ACKNOWLEDGEMENTS.....</b>	<b>107</b>
<b>CURRICULUM VITAE .....</b>	<b>108</b>

Keywords: Long waves, weak nonlinearity, kinetic theory, Rossby waves, shallow water, nonlinear surface waves, ship waves

# INTRODUCTION

In this thesis, the concepts and ideas of the weakly nonlinear long wave theory have been applied to two different wave systems – planetary-scale long waves (Rossby waves) in layered medium and long anthropogenic waves on the background of complex surface wave systems in shallow water. In studies of Rossby waves the central object of investigation is the kinetic equation whereas in studies into long surface waves in shallow water the results obtained with the use of the relevant kinetic equation serve as the starting point. Also, several complementary aspects such as the description of a specific mechanism of formation of layers in realistic conditions as well as problems of calibration of multi-sensor measurement equipment of complex geophysical processes have been analysed in the light of the two main frameworks.

The interrelations of the different physical systems discussed in the thesis are practically not reflected in the publications. Several recent developments in the framework of the used approaches such as the theory of multi-modal kinetic equations or the nonlinear aspects of the ship wave theory have been only published in research papers and have not been described on the textbook level yet. For the listed reasons Chapter 1 as well as some other sections of the thesis contains a relatively large amount of introductory material necessary to follow the presented results as well as extended discussion of interrelations of the different sections.

Chapter 2 is dedicated to the numerical and analytical studies (based on the kinetic approach) of nonlinear interactions of Rossby waves in a two-layer model ocean (Papers I, VII). The key development consists in (i) constructing an effective numerical solver for the kinetic equation for Rossby waves in two-layer ocean, and in (ii) establishing the basic tendencies of the spectral evolution. These papers are the first systematic studies of equation of this type in multimodal systems and have served as a basis for extensive later research (Soomere 1995, 1996 [112, 113]). For that reason these studies are presented in some detail.

The two-layer structure is the simplest representation of the vertical stratification of the ocean (Pedlosky 1998 [84]). Some aspects of the mechanisms leading to the formation of the more general layered structure are studied in Paper IV in the framework of a one-dimensional model describing layer formation resulting from an interplay of the double diffusion and the turbulent mixing.

The importance of twinning of the studies of the kinetic equation and long weakly nonlinear waves in shallow water, with equally important role of both the counterparts, becomes evident in Chapter 3 that is dedicated to a comparative study of anthropogenic and natural waves. Some basic concepts of the linear wave theory that are extensively used in Papers V, VI as well as a description of the non-linear approach used in the discussion of ship waves, a

short overview of wind wave modelling efforts in this area and numerically modelled wave climate of Tallinn Bay are also sketched.

The starting point of the main body of Chapter 3 is an important property of wind wave fields in the Baltic Sea, namely, that the periods of wind waves in this area are relatively small. The relevant analysis for the sea areas adjacent to Estonia is performed in Paper III based on long-term measurements at Almagrundet. This feature has been numerically established for the Tallinn Bay conditions in (Soomere 2005 [121]) with the use of the WAM wave model, kernel of which is the kinetic equation for surface waves (Komen 1994 [55]). Since wave models based on the kinetic approach cannot correctly treat ship waves, their basic properties are extracted from the results of field experiments in 2002–2004 (Papers II, V, and VI). Some aspects of building and calibration of complex measurement systems are described in Paper VIII. The key development is that waves from high-speed ferries may serve as a qualitatively new forcing factor of local ecosystem of the bay because the periods of the highest waves excited by fast ferries greatly exceed typical periods of wind waves in this area (Paper II).

The description of ship wave properties in Paper V suggests that both the linear theory and the higher-order Stokes theory fail to adequately describe their properties, and that the cnoidal wave theory probably is an adequate tool. This suggestion is verified based on *in situ* measured surface time series (Paper VI). The influence of ship waves (that is already high at certain depths owing to the difference of periods) has been shown to be even higher because of their highly cnoidal and at times even solitonic nature (Paper VI). Finally, some environmental implications of specific properties of ship waves are discussed based on Paper II.



## PAPERS CONSTITUTING THE THESIS

- I. T. Soomere, **K. Rannat**, A numerical method for solving the kinetic equation for Rossby waves in two-layer ocean, *Oceanology*, **32**, 181–189 (in Russian), 129–134 (English translation), 1991.
- II. T. Soomere, **K. Rannat**, J. Elken, K. Myrberg. Natural and anthropogenic wave forcing in the Tallinn Bay, Baltic Sea, in *Coastal Engineering 2003 (Brebba, C.A., Almorza, D. and López-Aguayo, F., Eds.)*, WIT Press, Southampton, Boston, 2003, 273–282.
- III. B. Broman, T. Hammarklint, **K. Rannat**, T. Soomere, A. Valdmann. Trends and extremes of wave fields in the north-eastern part of the Baltic Proper, *Oceanologia* **48**, S, 2006, 165–184.
- IV. P. Miidla, **K. Rannat**, J. Heinloo. Numerical stability in a model of the layered structure of thermohaline fields. *Proc. Estonian Acad. Sci. Phys. Math.*, **50**, 1, 49–62, 2001.
- V. T. Soomere, **K. Rannat**. An experimental study of wind waves and ship wakes in Tallinn Bay, *Proc. Estonian Acad. Sci. Eng.* **9**, 3, 157–184, 2003.
- VI. T. Soomere, R. Pöder, **K. Rannat**, A. Kask, Profiles of waves from high-speed ferries in the coastal area, *Proc. Estonian Acad. Sci. Eng.* **11**, 3, 2005, 245–260.
- VII. T. Soomere, **K. Rannat**, On the evolution of the energy spectrum of weak geostrophic turbulence on the  $\beta$ -plane, in *Proc. XVII Conference of Baltic Oceanographers*, SMHI, Norrköping, Sweden 1990, 563–575.
- VIII. A. Luik, L. Kulmar, **K. Rannat**, V. Reedik, Fast Kalman filter for data processing in distributed mechatronic systems, in: *The 7th Mechatronics Forum International Conference and Mechanics Education Workshop, Atlanta, 6th – 8th September 2000*, Elsevier 2000 (CD), 6pp.

### I Papers listed in the ISI Science Citation Index

- 1a.** T. Soomere, **K. Rannat**, A numerical method for solving the kinetic equation for Rossby waves in two-layer ocean, *Okeanologiya*, **32**, 1991, 181–189. (in Russian) (ISI Science Citation Index, Cambridge Scientific Abstracts, Inspec).
- 1b.** T. Soomere, **K. Rannat**, A numerical method for solving the kinetic equation for Rossby waves in two-layer ocean, *Oceanology*, **32**, 1991, 129–134. (English translation.) (ISI Science Citation Index).
- 2.** T. Soomere, **K. Rannat**, J. Elken, K. Myrberg. Natural and anthropogenic wave forcing in the Tallinn Bay, Baltic Sea, in *Coastal Engineering 2003 (Brebba, C.A., Almorza, D. and López-Aguayo, F.,*

- Eds.*), WIT Press, Southampton, Boston, 2003, 273–282. (ISI Proceedings, SCOPUS, Cambridge Scientific Abstracts).
3. B. Broman, T. Hammarklint, **K. Rannat**, T. Soomere, A. Valdmann. Trends and extremes of wave fields in the north-eastern part of the Baltic Proper, *Oceanologia* **48**, S, 2006, 165–184. (ISI Science Citation Index Expanded).

II Papers published in the Proceedings of the Estonian Academy of Sciences – a peer-reviewed internationally distributed journal with international editorial board.

4. P. Miidla, **K. Rannat**, J. Heinloo. Numerical stability in a model of the layered structure of thermohaline fields. *Proc. Estonian Acad. Sci. Phys. Math.*, **50**, 1, 49–62, 2001. (Cambridge Scientific Abstracts, EBSCO, Inspec, Math. Reviews, etc.)
5. T. Soomere, **K. Rannat**. An experimental study of wind waves and ship wakes in Tallinn Bay, *Proc. Estonian Acad. Sci. Eng.* **9**, 3, 157–184, 2003. (Cambridge Scientific Abstracts, Inspec, Applied Mechanics Review, ASFA, etc.)
6. T. Soomere, R. Põder, **K. Rannat**, A. Kask, Profiles of waves from high-speed ferries in the coastal area, *Proc. Estonian Acad. Sci. Eng.* **11**, 3, 2005, 245–260. (Cambridge Scientific Abstracts, Inspec, Applied Mechanics Review, ASFA, etc.)

II Paper in proceedings of international conferences published by leading international publishing houses

7. A. Luik, L. Kulmar, **K. Rannat**, V. Reedik, Fast Kalman filter for data processing in distributed mechatronic systems, in: *The 7th Mechatronics Forum International Conference and Mechanics Education Workshop, Atlanta, 6th – 8th September 2000*, Elsevier 2000 (CD), 6pp.

II Paper published in proceedings of international conferences

8. T. Soomere, **K. Rannat**, On the evolution of the energy spectrum of weak geostrophic turbulence on the  $\beta$ -plane, in *Proc. XVII Conference of Baltic Oceanographers*, SMHI, Norrköping, Sweden 1990, 563–575. (Cited 3 times from the papers indexed/abstracted in the ISI Web of Science.)

## Contribution of the author to the joint papers

1) T. Soomere, **K. Rannat**, A numerical method for solving the kinetic equation for Rossby waves in two-layer ocean, *Oceanology*, **32**, 181–189 (in Russian), 129–134 (English translation), 1991.

Extending the numerical scheme and the code for solving the barotropic kinetic equation for the two-layer case. Performing of the computations on different platforms (both mainframe and PC). Coding software tools for data processing, sorting and graphical representation. Testing the validity of conversions of the model equations. Analysis of the resonant curves and the location of the double resonance points for validating the particular choice of the computational grid. Interpretation of the results in terms of motions in the two-layer ocean. Participation in the preparation of the manuscript, writing the parts reflecting the numerics.

2) T. Soomere, **K. Rannat**, J. Elken, K. Myrberg. Natural and anthropogenic wave forcing in the Tallinn Bay, Baltic Sea, in *Coastal Engineering 2003 (Brebba, C.A., Almorza, D. and López-Aguayo, F., Eds.)*, WIT Press, Southampton, Boston, 2003, 273–282.

Organizing and performing the wave measurements in Tallinn Bay, particularly at Aegna, incl. planning of the experiments, installing and servicing the instruments, and data preprocessing. Participation in the interpretation of the results and in preparation of the whole manuscript, writing the parts reflecting the measurement procedure.

3) B. Broman, T. Hammarklint, **K. Rannat**, T. Soomere, A. Valdmann. Trends and extremes of wave fields in the north-eastern part of the Baltic Proper, *Oceanologia* **48**, S, 2006, 165–184.

Preprocessing the wave data from Almagrundet, analysis of the frequency of occurrence of waves with different heights and periods, establishing the problems with the recorded wave periods starting from 1995, testing the validity of the rest of the analysis. Participation in the preparation of the manuscript, writing the parts reflecting the distribution of wave periods and its consequences.

4) P. Miidla, **K. Rannat**, J. Heinloo. Numerical stability in a model of the layered structure of thermohaline fields. *Proc. Estonian Acad. Sci. Phys. Math.*, **50**, 1, 49–62, 2001.

Construction of the numerical scheme analysed in the paper (in cooperation 50:50 with dr. P. Miidla), writing the code in Fortran and in Matlab, performing numerical experiments in order to practically estimate the stability properties of different versions of the numerical scheme, validating the estimates of the stability criteria. Participation in the preparation of the manuscript, writing the parts reflecting the discretization of the model equations.

5) T. Soomere, **K. Rannat**. An experimental study of wind waves and ship wakes in Tallinn Bay, *Proc. Estonian Acad. Sci. Eng.* **9**, 3, 157–184, 2003.

Organizing and performing the wave measurements in Tallinn Bay, incl. planning of the experiments, installing and servicing the instruments, and data pre-processing. Analysis of differences of appearance of ship waves in different sections of the coast. Participation in the interpretation of the results, preparation of the manuscript, writing the parts describing the experiments and the spatial variability of ship wave properties.

6) T. Soomere, R. Põder, **K. Rannat**, A. Kask, Profiles of waves from high-speed ferries in the coastal area, *Proc. Estonian Acad. Sci. Eng.* **11**, 3, 2005, 245–260.

Organizing and performing the wave measurements in Tallinn Bay, particularly at Aegna, incl. design and testing of new pressure-sensor-based measurement devices, planning of the experiments, installing and servicing the instruments and pre-processing of pressure data. Constructing and testing the steel-plastic pillar to hold the meter scale and wave height detector(s). Participation in the preparation of the whole manuscript, writing parts reflecting the setup and procedure of the experiments.

7) T. Soomere, **K. Rannat**, On the evolution of the energy spectrum of weak geostrophic turbulence on the  $\beta$ -plane, in *Proc. XVII Conference of Baltic Oceanographers*, SMHI, Norrköping, Sweden 1990, 563–575.

Extending the numerical scheme and the code for solving the barotropic kinetic equation for the two-layer case. Performing of the computations on different platforms (both mainframe and PC). Coding software tools for data processing, sorting and graphical representation. Testing the validity of conversions of the model equations (reduction of the delta functions and simplification of the system of equations). Analysis of the resonant curves and the location of the double resonance points. Interpretation of the results in terms of motions in the two-layer ocean. Participating in the preparation of the manuscript, writing the parts reflecting the numerics.

8) A. Luik, L. Kulmar, **K. Rannat**, V. Reedik, Fast Kalman filter for data processing in distributed mechatronic systems, in: *The 7th Mechatronics Forum International Conference and Mechanics Education Workshop, Atlanta, 6th – 8th September 2000*, Elsevier 2000 (CD), 6pp.

Analysis of different data filtering procedures for a system of distributed sensors in a wider context of distributed mechatronic systems. Estimate of the practical usability of the method based on the Kalman Filtering theory for real-time statistical calibration of the sparsely distributed sensors. Writing most of the paper, partially based on drafts presented by the co-authors.

## **Main arguments proposed to defend**

1. An efficient numerical solver for the kinetic equation for Rossby waves in a two-layer ocean has been constructed. This development includes treating of several nontrivial technical problems such as geometrical description of resonance curves, conversion of the collision integrals with singular kernels over an infinite domain to integrals with regular kernels over a finite domain, establishing the double resonance points and avoiding them in the solver, usage of a higher spectral resolution in a part of the computational domain, and the choice of an optimal computational domain.

2. The basic features of the potential final stage of the evolution of different Rossby wave systems have been identified based on numerical studies of the long-term evolution of largely different initial fields of Rossby waves (including initially isotropic, with initially dominating zonal flow component, and with initially dominating meridional flow component). The computations have been performed for the typical two-layer ocean conditions where the ratio of the depths of the upper and the lower layer is approximately 1:5.

3. Shown is that the main features of the temporal evolution of the barotropic mode in Rossby wave systems in a two-layer ocean follow the analogous features of barotropic Rossby wave systems. An appreciable part of the wave energy is transferred to the nearly zonal flow in all the considered cases. In other words, it is demonstrated that resonant interactions cause the generation of a nearly-zonal flow (that is, a flow mostly directed along parallels) also in the Rossby-wave systems in a two-layer medium.

4. A specific feature of the two-layer evolution of Rossby wave systems is that the nearly-zonal flow is practically barotropic whereas the baroclinic flow may remain or become practically isotropic. This sort of flow is generated from very different initial conditions. The majority of the energy of the zonal flow is concentrated in wave components, the length of which matches the baroclinic (internal) Rossby radius that characterises the typical scale of synoptic motions in realistic conditions. The typical wavelength of components of the nearly zonal flow is therefore about 100 km and the typical period a few tens of days in open ocean conditions. In the Baltic Proper the internal Rossby radius is smaller and the classical beta-effect is overridden by the topographic beta-effect; for that reason generation of motions along bottom isolines is probable, in which the dominating wavelength may be about 10–20 km (in the Gulf on Finland even 1–5 km).

5. Based on above calculations it is hypothesized that Rossby-wave systems in multi-layered media tend to evolve towards a specific final state consisting in a

superposition of strong barotropic nearly zonal flow and more or less isotropic system of motions of higher modes. (Remark: parallel studies with the use of the same numerical method have shown the possibility of exciting of meridional anisotropy in higher modes and a multi-stage evolution towards the thermodynamical equilibrium state, see details in Soomere, *Phys. Rev. Lett.* 1995). The described mechanism may be used, for example, in the analysis and forecast of the position of the polar front and its meanders, or flows directed along bottom isolines in the Baltic Sea.

6. The simulations demonstrate that the evolution of multi-modal (in this case consisting of the barotropic and one baroclinic mode) Rossby-wave systems is faster than the evolution of purely barotropic systems with an equal energy. In other words, the presence of the layers and the baroclinic mode serves as a "catalyst" for evolution of Rossby wave systems.

7. The properties of a one-dimensional model (developed by Dr. Jaak Heinloo) that reproduces the layer-formation process owing to the interplay of the double diffusion and the turbulent mixing are analysed. Shown is that for the typical values of temperature and salinity in both open ocean and in the Baltic Sea, and for roughly estimated extreme values of the turbulent kinetic energy, the relevant numerical scheme is stable provided  $(\Delta h)^2 / \Delta \tau > 0.01$ , where  $\Delta h$  is the step of the spatial grid and  $\Delta \tau$  is the time step. It is numerically demonstrated that for typical ocean conditions a sort of layered structure may be formed within an appreciable time.

8. The typical and extreme properties of wind waves in the northern Baltic Proper have been established based on factually measured wave data near Almagrundet (Sweden) during about 25 years (1978–2003). Shown is that the typical periods of wind waves in the Baltic Sea are relatively small: usually 4–6 s and reach about 10 s only in extreme storms. The basic conclusion is that dominating periods of wind waves are clearly smaller than the periods of the highest waves from fast ferries.

9. The parameters of waves from fast ferries have been established based on extensive wave measurements in the coastal area of Tallinn Bay. The heights of such waves are moderate: the daily highest examples are usually about 1 m high. Shown is that the majority of ship wave energy in Tallinna Bay is concentrated in very long waves, with periods of 10–15 s and with heights up to 1 m.

10. An extensive comparison of the parameters of ship waves and wind waves in Tallinn Bay has been performed. The reference data form the simulated wind wave properties obtained with the use of the WAM wave model that is based on

the kinetic equation for wind waves. The main outcome from the comparison is that:

- the wind wave climate is, in average, so mild that the daily highest waves from fast ferries belong to the annual highest 1–5% wind waves;
- the probability of occurrence of about 1 m high waves that have periods of 10–15 s is extremely small; for that reason the waves from fast ferries eventually serve as a qualitatively new component of hydrodynamic activity in the Tallinn Bay area.

11. Shown is that nonlinear effects become important for the highest and longest components of ship waves (the height above 0.5 m, period over 10 s) already at a depth of 10–15 m. Based on experimentally recorded time series of water surface in ship wakes it is demonstrated that:

- the shape of long and high waves from fast ferries well matches the shape of cnoidal waves – the periodical solutions to the Korteweg-de Vries (KdV) equation;
- the shape of the highest examples of waves from fast ferries nearly perfectly matches the shape of the Korteweg-de Vries solitons.

Based on the listed features it can be recommended to use the KdV equation for description of long waves from fast ferries also in realistic conditions in the coastal zone.

12. Comparison of properties of sine and cnoidal waves shows that the near-bottom velocities excited by the highest and longest examples of waves from fast ferries at certain depths considerably exceed the estimates of these velocities obtained in the framework of the linear surface wave theory.

# 1. WEAKLY NONLINEAR WAVES IN GEOPHYSICAL FLOWS

## 1.1. Linear, weakly nonlinear and long waves

Wave motion is one of the most important constituents of energy and an essential agent of energy redistribution in geophysical flows. Different kinds of waves and wave-like motions have been an important subject for studies in various areas of geophysics for centuries. To the first approximation, wave motion is frequently assumed to be linear, that is, governed by linear differential equations. The primary property of linear waves is that any superposition of such waves satisfies the governing equation. Another basic feature is that they propagate independently of other waves of the same class. The properties of linear waves, the mechanisms governing their generation, propagation and damping in the oceans and the atmosphere have been studied in great detail (*e.g.* LeBlond and Mysak 1978 [60]).

Although the linear approximation is acceptable in many cases, wave motion in nature is seldom perfectly linear. Apart from the highly nonlinear phenomena such as turbulent flows (Heinloo 1984 [37]) or violent wind wave breaking (Longo *et al.* 2002 [64]) there exist situations of considerable practical interest when disturbances of the medium are mostly independent of each other but yet their nonlinear interplay is a decisive factor of the evolution of the whole system in long-term run. Certain features of such wave systems are the subject of a large part of this thesis.

Heuristically, weakly non-linear waves can be defined as a class of motions, for which non-linear effects are negligible in the time scale comparable with their characteristic period but for longer time scales non-linearity may have significant impact. They are thus "intermediate" motions between linear waves and non-linear motions. Such motions are frequently described by the equations in which the nonlinear terms are much smaller than the linear terms. In nondimensional form, such equations contain small parameters (that sometimes are called the measure(s) of non-linearity, cf. Eq. (1) below) at the nonlinear terms. To the first approximation, motions described by such equations are governed by the linear terms.

The nonlinear terms, whatever small they are, contribute to the motion to some extent. Under certain conditions, such a contribution may be cumulative. In the kinetic theory of weakly nonlinear waves the cumulative effects become evident as slow energy exchange (equivalently, changes in wave amplitudes) between wave components whereas the shape of the waves, the dispersion relation and the propagation properties do not change. The equation describing the energy exchange usually is a strongly non-linear equation called kinetic equation.



Probably the most well-known class of nonlinear wavelike motions form structures described by the Korteweg-de Vries equation (*e.g.* Drazin and Johnson 2002 [19]). This equation has a nondimensional form  $\eta_t + 6\eta\eta_x + \eta_{xxx} = 0$  and describes, among other physical phenomena, the evolution of the surface elevation  $\eta$  in long waves of finite height in shallow water. The wave propagation occurs in conditions where the nonlinear  $6\eta\eta_x$  and the linear dispersive terms  $\eta_t$ ,  $\eta_{xxx}$  have the same magnitude. For that reason, it is frequently said that the KdV equation describes the situation where the dispersive properties are balanced by the nonlinearity. This balance is the reason for the modification of the wave shape that generally is no more sinusoidal and, for very long waves, leads to the soliton formation.

The periodic solutions of the KdV equation are called cnoidal waves. Formally, the short-wave limit of the cnoidal wave solutions to the KdV equation is a linear sine wave and the long-wave limit is a soliton. KdV solitons are known to interact in a very complex manner (*e.g.* Drazin and Johnson 2002 [19]). Interactions of wavelike solutions of this equation and its spatial generalization (the Kadomtsev-Petviashvili equation) may lead to other manifestations of nonlinearity such as essential changes of the wave shape and height, or extensive phase shifts (*e.g.* Hammack *et al.* 1989 [28], Soomere and Engelbrecht 2005 [122]). Yet the wave systems described by the KdV and Kadomtsev-Petviashvili equations are also frequently called weakly nonlinear (Segur and Finkel 1985 [107]).

The fact that different scientific schools use the same term for different things is sometimes confusing; yet in both cases the central objects of study are progressive waves. The benefit from the use of both the described approaches becomes evident in the comparative analysis of wind waves (that can be interpreted as a random wave field, evolution of which is described by the kinetic equation) and wakes from fast ferries that consist of a few wave crests localised in time and space.

From the variety of weakly nonlinear motions in the geophysics, this thesis is concentrated to long weakly nonlinear waves. This wave class is particularly relevant to the use of the methods and ideas of the weak nonlinear theory. On the one hand, long waves frequently are ‘nonlinear’ enough to initiate effective balance between dispersive and nonlinear effects (*e.g.* long surface waves of finite amplitude in shallow regions (Hammack *et al.* 1989, 1995 [28, 29])). This feature is important in the analysis of long waves from fast ferries that obtain clearly nonlinear character in the coastal area (Paper VI). On the other hand, certain features of the energy exchange between the components of several motion systems only become evident when the disturbances are long enough for the wavelike behaviour to dominate. The classical example is the conversion of the practically isotropic two-dimensional geostrophic turbulence (which is

strongly nonlinear *a priori*) to a system of weakly nonlinear Rossby waves at a certain stage of the scale-increasing process (Rhines 1979 [101]).

The definition of a long wave crucially depends on the underlying physical system. For Rossby waves and surface waves the relevant length scales differ considerably. The typical length scale of barotropic Rossby waves in the ocean is, at least, a few hundreds of kilometres, thus they are long intrinsically. Surface waves are treated as long if their length greatly exceeds the water depth. Thus for shallow coastal areas already waves with a length of a few tens of metres may be very long whereas the same waves in the deep ocean are short waves.

Long waves are particularly important in geophysical flows where the characteristic horizontal and vertical scales frequently differ considerably. The description of long waves often is considerably simpler than the general theory of waves of the same type. In the classical shallow-water theory, for example, the horizontal velocity is independent of the location of the water particles, and the vertical velocity is a linear function of the location (Dean and Dalrymple 2004 [17]). The same idea is used in the mathematical description of Rossby waves in the quasi-geostrophic approximation: a relatively simple equation is obtained for the vertical velocity (Kamenkovich *et al.* 1986 [48]) and the equations for the horizontal velocity components are split into a separate system of equations. Since motions in the oceans and the relevant physical fields are intrinsically three-dimensional (denoted as 3D in what follows), the basic advantage of the approach of long waves consists in the possibility of splitting the general 3D equations of motions into a system of two-dimensional (2D) equations and an additional equation for the vertical velocity. This feature allows considering many geophysical systems as a superposition of 2D motions with an acceptable accuracy.

From the viewpoint of the long wave theory, the possibly layered structure of the physical fields in the ocean and the atmosphere has a particularly important role. It frequently allows considering motions within a specific layer only. The ratio of the horizontal and the vertical scales of the motion in one layer obviously is larger than for the motions in the whole water (air) column. Thus the long wave theory is even more appropriate in the layered ocean. A large part of the results of this thesis have been obtained for stratified environment in the form of a layered ocean. Thus the processes governing layer formation are an important topic of long wave studies in geophysical applications and are also analysed to some extent.

## 1.2. Kinetic theory of weakly nonlinear waves

The basic contribution of interactions of weakly nonlinear waves to the evolution of wave fields is the change of wave amplitudes in a time scale of the order of many wave periods (Zakharov *et al.* 1992 [145]). The idea behind is that the nonlinearity is so weak that it practically does not affect single disturbances but is strong enough to cause certain coupling of different wave components that meet each other in some area of the physical space. The nonlinear coupling in this framework only affects the energy of disturbances, but not their shape or other features.

Long-term evolution of weakly nonlinear wave systems can be described, to the first approximation, in the kinetic framework. The natural motion system is assumed to consist of a vast number of wavelike harmonics so that it can be treated as a random wave field with continuous spectral density (spectrum) of energy (*e.g.* Reznik 1986 [100]; Zakharov *et al.* 1992 [145]; Komen *et al.* 1994 [55]). In such a case the behaviour of particular wave components is usually of no interest. The changes of the general properties of such motions are determined by the temporal behaviour of their statistical moments or cumulants. The evolution of cumulants is described by an infinite system of coupled equations similar to the BBGKY system (Tapp 1989 [130]). Usually (for example, in the analysis of turbulent motions) this system cannot be truncated because of the incessant generation of the higher moments by the nonlinear coupling (Monin and Yaglom 1967 [75]). Truncation is possible only in specific cases; for example, in the case of the Gaussian systems when the third and higher order cumulants are identically zero.

For weakly nonlinear waves the system of equations for cumulants can be truncated in a consistent manner. Hasselmann (1962 [33]) pointed out that the initial correlations between the harmonics of weakly nonlinear surface waves are damped relatively fast by dispersive effects in comparison with the rate of growth of the correlations by nonlinear effects. In other words, changes of the wave field owing to linear wave propagation over sea surface are much faster compared to the nonlinear changes. Consequently, he argued, a weakly nonlinear dispersive wave field can be assumed to be approximately Gaussian. He assumed that the second and third order cumulants govern the motion and the fourth and higher order cumulants can be discarded. This assumption leads to a closed equation describing the evolution of the energy spectrum of such wave fields. This equation is called kinetic equation. The relevant approach is called the kinetic theory of waves. Such wave fields are sometimes also called wave turbulence or weak turbulence (Zakharov *et al.* 1992 [145]). The derivation of the kinetic equation was revisited by Reznik (1984 [97]) who showed that it is correct under certain more general restrictions. Although the assumptions made in deriving of the kinetic equation are not perfect (Majda *et al.* 1997 [66]), applications based on the kinetic equation or on its simplified

versions frequently show excellent results in applications (*e.g.* Komen *et al.* 1994 [55], Zakharov *et al.* 1992 [145], Zakharov and Pushkarev 1999 [146]).

From this description it follows that the magnitude of non-linearity has a fundamental importance for the mathematical modelling of wave evolution. On the one hand, without non-linearity several fundamental changes in the wave properties such as gradual increase of dominating periods of storm waves are impossible. On the other hand, the weakness of non-linearity is a key issue, because for stronger non-linearity the truncation of the sequence of equations for cumulants may be impossible.

The kinetic equation may be interpreted as a hydrodynamical analogue of the Boltzmann equation for an idealized gas. This analogy becomes evident when one considers a wave field as a superposition of a huge number of localized wave packets, each associated with its mean wave vector and frequency (Hasselmann 1967 [35], Soomere 1992b [110]). As distinct from the classical kinetic theory, interaction (collision) between packets may occur only if at least three packets meet each other. Although a continuum of different packets may coexist at any given point, an appreciable energy exchange occurs only if the wave vectors and frequencies of a set of packets satisfy certain geometrical conditions called resonance conditions (see below, Sections 2.4 and 2.5). These conditions serve as another important difference from the classical kinetic theory and ensure that interactions of this type are relatively rare. As a result, the time of free propagation of the packets is much longer than the duration of the ‘collisions’; consequently, energy exchange occurs slowly compared with the wave propagation.

The coupling of wave components in this framework is a specific case of resonance. The relevant energy exchange mechanism is called resonant interaction. The presence of small nonlinear terms in the governing equation means that evolution of a certain wave component depends on other wave components. If this wave component satisfies the resonance conditions together with a certain set of other waves, its amplitude may grow linearly in time. Physically, this is only possible during a short time interval, and some other mechanism should limit this growth. The kinetic equation can be interpreted as the mathematical description of the relevant limiter.

Although the mechanism of resonant interactions is common for a wide variety of wave classes in geophysics, in the initial stage of formation of the kinetic theory, there was no common understanding of the properties of the kinetic equations. The derivation of this equation and establishing its basic properties was performed separately for each wave class (*cf.* Hasselmann 1962, 1963 [33, 34], Kenyon, 1964 [49], Longuet-Higgins and Gill 1967 [65]). The simple form of the dispersion relation for Rossby waves made this wave class one of the most important model systems for studies of the kinetic theory in the 1960s–1980s. The kinetic equation for Rossby waves has a relatively simple structure, which reflects several interesting physical phenomena and for which many results can be proved analytically.

Rapid progress in understanding of the physics of the kinetic equations was gained through extensive studies in 1980s (see Zakharov *et al.* 1992 [145] for overview). One of the main outcomes was the perception that the form of the kinetic equations, the methods of their handling and their basic properties are universal (Zakharov *et al.* 1992 [145], Soomere 2001 [114]). The conservation laws, the law of increase of entropy (reflecting the tendency of the system to evolve towards the thermodynamically equilibrated state), the basic features of the thermodynamically equilibrated spectra and other exact solutions are valid for all wave systems governed by kinetic equations. The number of exceptions is small and usually connected with specific geometric features of the resonance conditions and the corresponding curves or surfaces (*e.g.* Balk 1997 [8], Soomere 2001 [114]). Only the physical meaning and appearance of several coefficients are different, because they are defined jointly by the dispersion relation and the appearance of the nonlinear terms in the governing equation (Zakharov *et al.* 1992 [145], Soomere 2003 [116]).

This progress allowed to correctly link the results obtained with the use of the classical asymptotic analysis of solutions to the primitive wave equations (used in most of the references above) with the more general results obtained with the use of the Hamiltonian approach in studies of V.E. Zakharov and his school. This feature also allows to transfer many results proved for one particular wave system (admitting *e.g.* extensive analytical study or simple numerical models) to all systems allowing kinetic description. In other words, particular results obtained, for example, for Rossby waves were, with some restrictions, directly applicable in surface wave theory. The methods of constructing of numerical solvers of the kinetic equations as well as the problems with their implementation are also similar to each other. In particular, results and experience obtained in the first part of this thesis for numerical simulation of the energy exchange between Rossby waves have been particularly useful for simulating spectral evolution of surface waves in a theoretically and numerically much more complicated situation.

### 1.3. Equations of long waves on the $\beta$ -plane

Many processes in astrophysics [18], plasma physics [31], and geophysics [101] can be reduced to a problem of free (quasi) 2D anisotropic turbulence. Under some restrictions, this phenomenon can be described by the 2D Charney-Obukhov equation (frequently called Hasegawa-Mima equation after Japanese scientists who re-derived it for certain applications in plasma [32]):

$$\partial(\Delta\psi - a^2\psi)/\partial t + \beta \partial\psi/\partial x + \varepsilon J(\psi, \Delta\psi) = 0. \quad (1)$$

Here  $J(f, g) = f_x g_y - g_x f_y$  is the 2D Jacobi operator; the function  $\psi = \psi(x, y)$  usually has the meaning of the stream function,  $t$  is the physical time and the meaning of parameters  $a, \varepsilon, \beta$  depends on the physical system.

In geophysical applications, Eq. (1) describes evolution of so-called synoptic- scale barotropic<sup>1</sup> motions in the ocean (atmosphere) of constant depth in Cartesian coordinates  $(x, y)$  in the  $\beta$ -plane approximation. The  $x$ -axis is directed to the North and the  $y$ -axis to the East. These motions (synoptic rings in the ocean; cyclones or anticyclones in the atmosphere) have the horizontal scale  $L$  of order of the external or barotropic Rossby deformation radius  $L_R = a^{-1} \approx 100$  (2000) km in the ocean (atmosphere), the vertical scale of the depth of the ocean (thickness of the atmosphere) and the time scale  $\tau \geq$  several dozens of days (a few days). The Earth's surface is assumed to be an infinite even plane, where the Coriolis parameter  $f = f_0 + \beta y$  (the vertical component of the Earth's rotation) varies linearly in the North-South direction. This variation is usually called  $\beta$ -effect, the typical value of the Coriolis parameter at mid-latitudes is  $f_0 \approx 10^{-4} \text{ s}^{-1}$ , and  $\beta \approx 10^{-11} \text{ s}^{-1} \text{ m}^{-1}$  is the North-South derivative of the Coriolis parameter.

The wave solutions of linearised Eq. (1) have the dispersion relation  $\omega(\vec{k}) = -\beta k / (\kappa^2 + a^2)$  (here  $\vec{k} = (k, l)$  is the wave vector and  $\kappa = |\vec{k}|$ ) and are called Rossby waves. They exist because of the interplay of rotation and sphericity of the Earth. This interplay is reflected by the term proportional to  $\beta$  in Eq. (1), the presence of which admits wave solutions to this equation. Without this term, Eq. (1) is equivalent to the equation of 2D isotropic turbulence that has no wave solutions.

The specific role of Rossby waves among other wavelike processes in the ocean is that they carry about 80% of the wave energy in the open ocean (Kamenkovich *et al.* 1986 [48]). Rossby waves also form an appreciable fraction of the total energy of motions in the ocean since about 10% of the total kinetic energy of all the motions in the ocean belongs to synoptic processes (Kamenkovich *et al.* 1986 [48]). Rossby waves serve as a particularly rich in content wave system of direct geophysical interest. They possess several important properties: the 2D nature, the anisotropy of the dispersion relation (i.e. the wave properties depend also on the propagation direction), the possibility of double resonance, and the existence of an additional conservation law of enstrophy. Owing to their relatively simple dispersion relation (an

---

<sup>1</sup> Barotropic motions frequently are interpreted as vertically nearly homogeneous flows. In fact, the motions are called barotropic when the isopycnal surfaces are horizontal, equivalently, the density of fluid only depends on the pressure.

explicit algebraic polynomial rational function of the wave vector components) and the possibility of triad resonant interactions they admit extensive analytical studies into the properties of the corresponding kinetic equation.

The role of synoptic-scale motions has been intensely investigated since MODE and POLYMODE experiments in the 1970s. Such *in situ* studies as well as laboratory studies of the synoptic scale motions (*e.g.* Read *et al.* 2004 [94]) are time consuming and extremely expensive. The approximation of weakly non-linear Rossby waves is a feasible way to study the long-term behaviour of synoptic-scale motions in the oceans (atmosphere). In the nondimensional form of Eq. (1),  $a = \beta = 1$  and  $\varepsilon = U / (\beta L^2) \ll 1$  can be interpreted as the measure of non-linearity (here  $U$  is the characteristic velocity scale). For small values  $\varepsilon \ll 1$ , motions governed by Eq. (1) can be interpreted as consisting of a large number of wavelike components that are coupled only through the term  $\varepsilon J(\psi, \Delta\psi)$ . If this term is small, the coupling is weak and waves behave practically independently of each other.

To the first approximation, the influence of nonlinearity can be described in terms of resonant interactions, equivalently, with the use of the kinetic theory of weakly nonlinear waves. This theory has been first formulated for four-wave interactions of surface waves (Hasselmann 1962 [33]) and a few years later generalised to three-wave interactions of barotropic Rossby waves (Kenyon 1964 [49]). If the system of synoptic motions can be treated as a random weakly nonlinear wave field with continuous energy spectrum, the kinetic equation describes slow (as compared to the characteristic wave period) evolution of the wave system owing to interactions between wave harmonics satisfying so-called resonance conditions  $\omega(\vec{k}) + \omega(\vec{k}_1) + \omega(\vec{k}_2) = 0$ ,  $\vec{k} + \vec{k}_1 + \vec{k}_2 = \vec{0}$ .

Extensive numerical experiments with the kinetic equation for barotropic Rossby waves have been performed in the 1980s (Reznik and Kozlov 1981 [95], Reznik and Soomere, 1984a,b [98, 99], Reznik 1986 [100]). The basic features of the evolution of these wave systems are well known by now. The most important feature is that they tend to evolve towards a specific thermodynamically equilibrated state, consisting of a superposition of a zonal flow (*i.e.* flows along parallels in the Earth's oceans) and a 'classical' isotropic equilibrium state of the 2D isotropic turbulence (Reznik 1986 [100]).

## 1.4. Multi-modal kinetic equations and the multi-layer ocean

Interactions of waves from different classes may provide an efficient way of energy redistribution in geophysical flows where frequency domains often are interlapping (*e.g.* interactions of two inertial waves with a Rossby wave, Wiklund 1999 [143]). The derivation of the relevant kinetic equation (sometimes called multi-modal kinetic equation) describing interactions of several wave classes was probably first presented in (Zakharov and Schulman 1980 [144]) and was extended to the Rossby waves in (Soomere 2003 [116]). However, such systems have been studied in detail only in a particular case when frequencies of the waves are essentially different (Zakharov *et al.* 1992 [145], Section 3.2.2). In the general case of comparable frequencies and/or a larger number of wave types, the properties of multi-modal kinetic equations have not been analysed numerically until studies described in Papers I and VII (Piterbarg 1998 [92]). Only some preliminary experiments for Rossby waves in a two-layer medium have been reported in (Kozlov *et al.* 1987 [56]).

The barotropic model of geophysical flows often inadequately represents the vertical structure of the oceans and the atmosphere because these media usually are stratified. The vertical structure of synoptic-scale motions in a stratified fluid can be described in terms of a linear combination of a barotropic and a (maybe infinite) number of baroclinic modes (Phillips 1966 [90]). This decomposition is equivalent to a model, consisting of several non-mixing vertically homogeneous layers whereas the motion in each layer is effectively depth-independent. This leads to a certain de-coupling of motions in different layers that are only coupled through the motions of the interfaces. The simplest representation of a stratified medium is a 2-layer model of synoptic-scale motions. It serves as the first approximation of 3D motions in terms of the basically 2D description of motions in a thin water layer on a  $\beta$ -plane. This is frequently an acceptable approximation, because most of the ocean normally contains, at least, two layers separated by the main thermocline (*e.g.*, Pedlosky 1998 [84]). In medium latitudes, the seasonal thermocline occasionally creates a three-layer structure. In some areas (*e.g.* in the Baltic Sea, Aitsam *et al.* 1984 [2]) the barotropic mode is damped and the Rossby-wave energy is mostly concentrated in the first and the second baroclinic modes. To resolve the vertical structure in such situations, at least three-layer model is necessary (Soomere 2003 [116]).

Rossby waves in a stratified medium serve as an example of a set of wave components with different dispersion relations but with comparable frequencies. The advantage of the layered model as compared with the models with continuous vertical density alteration (Piterbarg, 1998 [92]) is that the coefficients of the kinetic equation and many basic features of the energy transfer can be established analytically. Also, the important question – whether



the kinetic approach reproduces the properties of the governing equations – can be clarified to some extent. For example, kinetic models are irreversible and may possess additional motion invariants as compared with the physical systems (Reznik 1984 [97], Balk 1991 [7]). Moreover, their solutions may evolve towards principally different final states as compared to those of the governing equations (cf. results of Carnevale 1982 [12], Vallis and Maltrud 1993 [136], Reznik 1986 [100]).

The derivation of the kinetic equation for Rossby waves in the two-layer case is presented in (Kozlov *et al.* 1987 [56]). Its derivation for the multi-layer case has been studied in (Piterbarg 1998 [92]) on the basis of Hamiltonian approach, and in (Soomere 2003 [116]) for the three-layer model. The generalisation of this procedure for the multi-layer case is straightforward; however, calculation of the relevant coefficients is nontrivial. The resulting effects of the strong layering in some cases create particularly interesting phenomena such as the double resonance and multiple scenarios of approaching the thermodynamical equilibrium, or even multiple near-equilibrium states (Soomere 1995, 1996 [112, 113]).

In order to use the kinetic framework in the case of a multi-modal wave systems (incl. multi-layered model ocean), the equations for the motions excited by different wave classes (resp. motion in each layer) must first be modified so that each linear part contains one unknown function. Doing this is equivalent to introducing normal modes, or diagonalisation of the linear parts of the equations (Soomere 2003 [116]). The resulting nonlinear parts consist of certain combinations of nonlinear terms from various initial equations. The coefficients at these terms are called coupling coefficients because they determine how the different modes (wave classes) are coupled with each other. (At times, interaction coefficients are also called coupling coefficients, *e.g.* Axelsson, 1998 [6]. Such a distinguishing is only important in motion systems described by two or more coupled equations). Their appearance depends on the structure of both the linear and the nonlinear parts of the governing equations.

The properties of the coupling coefficients (that are of modest interest in studies into dynamical properties of motions) are particularly important in the kinetic theory. They enter into the collision integrals of the kinetic equation and determine the relative role of triads of various types in the energy exchange. For example, in the two-layer model of Rossby waves with a proper scaling of all types of triads have equal relative energy exchange intensity, except triads containing three baroclinic waves (Kozlov *et al.* 1987 [56], Papers I, VII). The intensity of self-interactions of the baroclinic mode crucially depends on the ratio of the depths of the layers and fully ceases in the widely used case of layers of equal depth (Kozlov *et al.* 1987 [56]; Papers I, VII, Soomere, 1996 [113]). As a consequence, the baroclinic zonal flow and the following large-scale meridional anisotropy do not emerge and the motion tends to a final state consisting of purely barotropic zonal flow and an isotropic wave system (Papers

I, VII, Soomere 1995; 1996 [112, 113]). Thus, an improper choice of the model may result in a completely different evolution scenario of the whole system.

The calculation of the coupling coefficients for the two-layer model is straightforward (Kozlov *et al.* 1987 [56]). Their analytic expressions for the three-layer model, their role in the energy exchange, and their dependence on the particular physical background are analysed in (Soomere 2003 [116]). Certain types of interactions totally vanish in several realistic situations. For Rossby waves they vanish if and only if an eigenvector of the governing system of equations possesses a zero component (Soomere 2003 [116]). The largest possible number of vanishing interactions occurs in a specific case of the three-layer model with the equal depths of the topmost and the lowest layers. Such a stratification is not typical in the open ocean but frequently occurs in the Baltic Sea (*e.g.* Aitsam *et al.* 1984 [2]).

One might argue that the kinetic framework is not a proper tool for describing the evolution of multi-modal Rossby wave systems, because the barotropic mode generally propagates much faster than the baroclinic ones. This feature is implicitly represented in the kinetic equation where certain classes of interaction involving the barotropic harmonics actually do not redistribute energy, because the corresponding coupling coefficients vanish.

An important reason for the numerical modelling of the long planetary-scale waves (Rossby waves) in a layered structure consists in establishing a more adequate picture about long-term evolution of synoptic scale motions (in particular, generation of zonal flows) in realistic conditions.

## 1.5. Ship waves

Waves excited by contemporary ships form a substantial part of surface wave activity in many water bodies. The importance of their contribution to the local hydrodynamic activity in rivers, inland channels and narrow straits has been recognised for a long time. Ship wakes can essentially contribute to the shoreline erosion, cause erosion and resuspension of bottom sediments, trigger ecological disturbance, cause harm to the aquatic wildlife etc. (Guidelines 2003 [26], Soomere *et al.* 2003 [118]). Ship-generated waves have become an environmental problem of growing concern in restricted waters and estuaries during the last years. In particular, in Scandinavia and in the United Kingdom, studies of various aspects of fast ferry operation, including properties of their wakes, have been carried out already in the middle of the 1990s (Forsman 1997 [25], Kirk McClure Morton 1998 [51], Kofoed-Hansen and Kirkegaard 1996 [53], Kofoed-Hansen and Mikkelsen 1997 [54]). Recently, analogous studies have been performed (or are in progress) in many countries (Guidelines 2003 [26], Parnell and Kofoed-Hansen 2001 [83], Varyani and Krishnankutty 2002 [137], Whittaker *et al.* 2001 [142]).

The introduction of high-speed vessels sailing in open sea areas extended the above threats from inland waterways, narrow straits, and archipelagos to much larger confined sea areas with low natural wave and tide activity (Parnell and Kofoed-Hansen 2001 [83]). These vessels have a high ratio of propulsion power to vessel displacement. They are able to sail at speeds comparable with the hump speed (that occurs when the half-length of ship waves is close to the vessel's length) or with the critical speed (that is, the maximum phase speed of surface waves in finite depths). Additionally to an increase of wave heights and periods with the increase of the sailing speed, the ship sailing at near-critical speeds may generate highly nonlinear waves and KdV solitons (Li and Sclavonuos 2002 [61]).

The kinetic theory employs very weak non-linearity which only contributes to wave evolution in long-term run whereas the wave shape and other properties coincide with those of perfectly linear waves. This assumption implicitly means that wave amplitudes have to be small. For description of spectral evolution of storm waves the violation of this assumption probably is not essential, because the wave models based on the kinetic approach (Komen *et al.* 1994 [55]) show good results also for rough windseas where wave amplitudes and steepness are substantial.

This and some other basic principles of the kinetic theory (that the wave field consists of a large number of wave harmonics which are spread over large sea areas, that the wave systems have a continuous spectrum, and that the kinetic equation is only valid when group velocities of resonantly interacting waves are different, see below) are completely violated for ship wakes. In many cases of practical interest the wake waves have considerable heights, are localised in small groups and, in particular in shallow water, have nearly equal group velocities. Therefore, generally they cannot be considered as a part of the surface wave system in the kinetic approach. For the listed reasons, the kinetic theory (more specifically, contemporary wind wave models that are based on the kinetic description) is used in the context of ship wave studies for estimates of the wind wave activity in the areas of interest whereas other approaches are used for analysis of the ship waves.

Numerical studies of wind wave properties in Tallinn Bay with the use of the WAM model (based on the relevant kinetic equation, Komen *et al.* 1994 [55]) have shown that the typical periods of wind waves usually do not exceed 6–7 s in this area (Soomere 2005 [121]). The specific feature of waves from fast ferries is that typical periods of the highest ship-induced waves are much longer than wind wave periods (Paper V). The length of ship waves frequently exceeds 100 m. Since such waves also have considerable heights, they cannot be considered as linear in shallow water. The KdV equation is shown to be a proper model for such waves in coastal areas.

The stratification of media, which plays a certain role in the general theory of ship wakes (Chung and Lim 1991 [14], Watson *et al.* 1992 [140]), is not taken into account in the studies of ship wakes below. Instead, the attention is

paid on their non-linear properties that modify the shape of wake waves and enhance certain properties of waves and wave-induced motions.

The nonlinear properties of ship waves may cause additional severe effects because of some specific features of nonlinear interaction of solitonic surface waves in shallow water (Miles 1977 [72, 73], Peterson *et al.* 2003 [86], Soomere and Engelbrecht 2005 [122]). The impact on the bottom ecosystem is equally important (Erm and Soomere 2004 [20]). The investigation of fast ferry waves thus has a great practical importance in quantifying the impact of intense ship traffic on the coastline and sediment transport in shallow waters.

## 2. SPECTRAL EVOLUTION OF ROSSBY WAVES IN A TWO-LAYER OCEAN

### 2.1. Kinetic equation for Rossby waves in a two-layer ocean

Let us consider large-scale motions in the infinite ocean of constant depth on the  $\beta$ -plane consisting of two non-mixing homogeneous layers with densities  $\rho_1 < \rho_2$  and mean thicknesses  $h_1, h_2$ , respectively. The subscript “1” refers to the upper layer, “2” – to the lower layer.

In the kinetic theory it is traditionally assumed that there exist such a great number of weakly nonlinear waves that we are allowed to speak about the system of waves with a continuous energy spectrum. In this case one is usually no more interested in the behaviour of single waves but in the evolution of the statistical characteristics of the whole system. The slow evolution of the most important statistical quantities – the energy spectra  $F_0(\vec{k}, \tau)$  and  $F_1(\vec{k}, \tau)$  of the baroclinic and the barotropic mode of the motion, respectively – is then described by the following system of integro-differential equations (Kozlov *et al.* 1987 [56]):

$$\frac{\partial F_p(\vec{k}, \tau)}{\partial \tau} = \sum_{m,n=0}^1 8\pi \tilde{I}_{pmn}, \tilde{I}_{pmn} = \int \tilde{K}_{pmn} N_{pmn}^{-1} \delta(\omega_{pmn}^{012}) \delta^2(\vec{\kappa}_{012}) d\vec{\kappa}_{12}, \quad (2)$$

where  $\vec{k} = (k, l) \equiv (\kappa \cos \varphi, \kappa \sin \varphi)$  is the wave vector,  $\tau$  is slow time,  $\tilde{I}_{pmn}$ ,  $p, m, n = 0, 1$  are frequently called collision integrals and describe the changes of energy of the wave with  $\vec{k}$  of mode  $p$  due to interactions with waves belonging to modes  $m$  and  $n$ ,  $\omega_{pmn}^{012} \equiv \omega_p(\vec{k}) + \omega_m(\vec{k}_1) + \omega_n(\vec{k}_2)$ ,  $\omega_p(\vec{k}) = -k / (\kappa^2 + a_p^2)$  is the dispersion relation and  $\omega_p$  is the angular frequency of the Rossby waves of the  $p$ -th mode,  $\vec{\kappa}_{012} = \vec{k} + \vec{k}_1 + \vec{k}_2$ ,  $d\vec{\kappa}_{12} = dk_1 dl_1 dk_2 dl_2$ , and integration is performed over the whole 4-dimensional space  $R^2(k_1, l_1) \otimes R^2(k_2, l_2)$ . The kernel of the collision integrals contains three delta-functions, because  $\delta^2(\vec{\kappa}_{012})$  is a product of two delta-functions applied to the components of the vector  $\vec{\kappa}_{012}$ . The functions  $\tilde{K}_{pmn}$  and  $N_{pmn}$  in the kernel of the collision integrals are as follows:

$$\tilde{K}_{pmn} = \tilde{C}_{\vec{k}_1 \vec{k}_2}^{pmn} \left( \tilde{C}_{\vec{k}_1 \vec{k}_2}^{pmn} F_m^1 F_n^2 + \tilde{C}_{\vec{k} \vec{k}_1}^{pmn} F_p F_m^1 + \tilde{C}_{\vec{k} \vec{k}_2}^{pmn} F_p F_n^2 \right), \quad (3)$$

$$N_{pmn} = (\kappa^2 + a_p^2)(\kappa_1^2 + a_m^2)(\kappa_2^2 + a_n^2).$$

Here  $\tilde{C}_{\vec{\kappa}_i \vec{\kappa}_j}^{pmn} = \frac{1}{2} \gamma_{mn}^p (k_i l_j - k_j l_i) (\kappa_i^2 + a_n^2 - \kappa_j^2 - a_m^2)$  are the interaction coefficients,  $F_p = F_p(\vec{\kappa}, \tau)$ , and  $F_p^i \equiv F_p(\vec{\kappa}_i, \tau)$ . The coupling coefficients  $\gamma_{mn}^p$  can be found as  $\gamma_{00}^0 = s_1(1 + s_1)$ ;  $\gamma_{11}^0 = s_0(1 + s_0)$ ;  $\gamma_{01}^0 = \gamma_{10}^0 = -s_0(1 + s_1)$ ;  $\gamma_{00}^1 = s_1(1 + s_1)$ ;  $\gamma_{11}^1 = s_1 + s_0^2$ ;  $\gamma_{01}^1 = \gamma_{10}^1 = -s_1(1 + s_0)$ , where  $s_0, s_1$  are the solutions of the equation  $h_1 \rho_1 s^2 / \rho_2 + (h_1 - h_2)s - h_2 = 0$ . The quantities  $a_0^{-1}$  and  $a_1^{-1}$  have the meaning of the barotropic and the baroclinic Rossby radii, respectively, and can be found from the equations

$$a_p^2 = \frac{f_0^2}{g'} \left( \frac{1}{h_1} - \frac{\rho_1 s_p}{\rho_2 h_2} \right); \quad a_p^2 s_p = \frac{f_0^2}{g'} \left( \frac{s_p}{h_2} - \frac{1}{h_1} \right), \quad (4)$$

where  $f_0$  is the mean value of the Coriolis parameter,  $g$  is the gravity acceleration and  $g' = g(\rho_2 - \rho_1) / \rho_2$ . We consider no energy source and dissipation.

Equations (2) serve as a generalization of the classical kinetic equation for barotropic Rossby waves and together are also called kinetic equation. Equations (2) are the simplest version of the multi-modal kinetic equation where only two different modes of motion – the barotropic and the (first) baroclinic mode appear. The details of derivation of Eqs. (2) and the corresponding dynamical equations can be found in (Kozlov *et al.* 1987 [56], Soomere 2003 [116]).

In the numerical experiments with the kinetic equation for Rossby waves the measure of non-linearity only appears in the definition of the “slow” time  $\tau = \varepsilon^{-2} t$  and, therefore, only affects the intensity of energy exchange between different wave components. If  $t$  is interpreted as the typical time scale (*e.g.* period) of synoptic-scale motions (a few weeks in the ocean) and the measure of nonlinearity is  $\sim 0.1$ , each “slow” time unit corresponds to several years of physical time.

The kinetic equation itself is valid only for limited time intervals  $\tau \ll \varepsilon^4$  and for the limited lengths of the wave vectors  $\kappa \ll \varepsilon^2$ . If  $\tau$  is of greater value, the higher order interactions will become significant and spectral evolution will be described by another equation (Benney and Newell 1969 [10]). For very short waves the initial assumption of weak nonlinearity is not valid (Reznik 1984, 1986 [97, 100]).

## 2.2. Solver of the kinetic equation

Papers I and VII contain description of a fast numerical solver for the kinetic equation for Rossby waves in a two-layer ocean, and a description of the basic evolution tendencies of the relevant waves system. The investigation of the slow evolution of the energy spectra of barotropic and baroclinic modes is reduced to the numerical solution of the Cauchy problem for the kinetic equation with initial conditions  $F(k, l, 0) = f(k, l)$ ,  $G(k, l, 0) = G(k, l)$ . The simulations were performed during 5 to 10 "slow" time units, that is, during several tens to a few hundreds physical years. Only spectral evolution governed by the homogeneous kinetic equation was studied. Equivalently, evolution of freely evolving (i.e. without energy sources or sinks) wave systems towards an equilibrium state was considered.

The solver was initially constructed for medium-size personal computers at the end of 1980s. The first numerical experiments, described in Papers I, VII were performed with the use of an 8 MHz CPU. Later studies based on this solver were performed with the use of CRAY supercomputers (Soomere 1995, 1996 [112, 113]) and revealed some other interesting features of multi-modal wave systems. However, extensive numerical studies of multi-modal kinetic equation are, until today, computationally extremely expensive and the need for numerical efficiency has not lost its actuality.

Equations (2) and the relevant interaction and coupling coefficients have been derived in (Kozlov *et al.* 1987 [56]) in a general form without any assumptions about the quantities  $h_1, h_2, \rho_1, \rho_2$ . For synoptic motions in the real ocean, these equations can be greatly simplified based on the fact that the density of water masses in the Earth's oceans varies insignificantly. The vertical variation usually does not exceed a few ‰, and only in extremely strongly stratified basins such as the Baltic Sea reaches 1–2‰. Therefore, for practical use it is allowed to disregard in Eqs. (2) the quantities of the order of  $O((\rho_1 - \rho_2)/\rho_2)$ , to replace  $\rho_1/\rho_2$  by 1 and  $\rho_1, \rho_2$  by  $\rho = (\rho_1 + \rho_2)/2$ . Using these approximations, we have (Kozlov *et al.* 1987 [56]):

$$s_0 = \frac{h_2}{h_1}; \quad s_1 = -1; \quad a_0^2 = \frac{f_0^2}{g(h_1 + h_2)}; \quad a_1^2 = \frac{f_0^2(h_1 + h_2)}{g'h_1h_2};$$

$$\gamma_{00}^1 = \gamma_{01}^0 = \gamma_{10}^0 = 0;$$

$$\gamma_{00}^0 = \gamma_{01}^1 = \gamma_{10}^1 = 1 + \frac{h_2}{h_1} \equiv Q; \quad \gamma_{11}^1 = \frac{h_2^2}{h_1^2} - 1 \equiv P; \quad \gamma_{11}^0 = \frac{h_2}{h_1} \left( \frac{h_2}{h_1} + 1 \right) = \frac{h_2}{h_1} Q.$$

In particular, we obtain  $\tilde{I}_{001} \equiv \tilde{I}_{010} \equiv \tilde{I}_{100} \equiv 0$ . This result reflects the well known fact that the interactions between two barotropic and one baroclinic wave in the ocean are much less intensive than other resonant interactions

(Jones, 1979 [42], Mirabel, 1985 [74], Kozlov *et al.* 1987 [56]). In numerical experiments we use nondimensional values  $a_0 = 0$  and  $a_1 = 1$ .

### 2.3. Reduction of collision integrals

For practical numerical analysis of the evolution of Rossby waves in the Earth's oceans the kinetic equation in question can be further simplified. Within the bounds of the 2-layer model of the Earth's ocean the natural boundary between the layers is the main thermocline, usually located on the depth of the order of 1 km ( $h_1$ ). The mean depth  $h_1 + h_2$  of the ocean is about 5 km. With the use of these values, several collision integrals in the kinetic equation are multiplied by the quantities  $Q^2 = 40$ ;  $P^2 = 20$ . In order to remove these relatively great factors a new time scale  $T$  was introduced as follows:

$$T = \tau(h_2 / h_1 + 1)^2 = \tau Q^2. \quad (5)$$

Using this time scale, replacing  $F_0$  by  $F$  and  $F_1$  by  $G = s_0^{-2} F_1$ , and after some algebra we obtain

$$\frac{\partial F}{\partial T} = 8\pi(\hat{I}_{000} + \alpha \hat{I}_{011}); \quad \frac{\partial G}{\partial T} = 8\pi(1 - \alpha)^2 \hat{I}_{111} + 16\pi \hat{I}_{110}, \quad (6)$$

where  $\alpha = h_1 / h_2$  and the collision integrals are modified in a straightforward manner. The relevant analytical expressions are given in Papers I and VII.

It can be shown that the Eqs. (6) have the same conservation laws as the full kinetic equation (2) (Kozlov *et al.* 1987 [56]). Namely, wave systems described by Eqs. (6) conserve total energy  $E$ , enstrophy  $Y$  and wave momentum  $L$ :

$$\begin{aligned} E &= \int (F + \alpha G) dkdl = \text{const}; \\ Y &= \int [(\kappa^2 + \alpha_0^2)F + \alpha(\kappa^2 + \alpha_1^2)G] dkdl = \text{const}; \\ L &= \int \left[ \frac{lF}{\omega_0(\vec{\kappa})} + \frac{\alpha lG}{\omega_1(\vec{\kappa})} \right] dkdl = \text{const}. \end{aligned} \quad (7)$$

Also, the so-called  $H$ -theorem  $\frac{dH}{dT} = \frac{d}{dT} \int \ln FG dkdl \geq 0$  holds. Equivalently the law of increase of the system entropy is valid for Eqs. (6). Therefore, this approximation maintains all the basic features of the full kinetic equation (2).



The direct use of four-dimensional collision integrals  $\hat{I}_{pmn}$ , taken over the infinite space of the wave vectors is inconvenient for numeric experiments. Since each collision integral contains three delta-functions, the factual integration is performed over a set of wave vectors lying at a certain curve and representing wave components, resonantly interacting with each other. The integral apparently can be reduced to a specific one-dimensional (1D) integral basically in the same way as the collision integral of the barotropic kinetic equation has been reduced to a 1D integral over a bounded segment (Reznik and Kozlov 1981 [95], Reznik and Soomere 1984a [98]).

In Papers I and VII this philosophy and some relevant results from (Kozlov *et al.* [56]) are used in order to reduce Eqs. (6) to equivalent ones but allowing discretization in a more convenient manner. First, the almost trivial integration over  $k_2, l_2$  is performed. After doing this, the new integration variables  $\kappa_0, \varphi'$  are introduced so that

$$\vec{\kappa}_1 = \frac{1}{2}(\vec{\kappa}_0 - \vec{\kappa}); \quad \vec{\kappa}_2 = \frac{1}{2}(-\vec{\kappa}_0 - \vec{\kappa}), \quad \varphi' = \angle(\vec{\kappa}, \vec{\kappa}_0), \quad \vec{\kappa}_0 = |\vec{\kappa}_0| \quad (8)$$

In new variables the expression  $\omega_{pmn}^{012}$  can be written as  $\omega_{pmn}^{012} = -kP_{pmn}N_{pmn}^{-1}/16$ , where

$$P_{pmn} = -\frac{16N_{pmn}^{012}}{\kappa \cos \varphi} \omega_{pmn}^{012} = \kappa_0^4 + 2A_{pmn}\kappa_0^2 + 4B_{pmn}\kappa_0 + C_{pmn} = 0.$$

The new integration variable  $\kappa_0$  is determined as a positive solution of the equation  $P_{pmn}(\kappa_0) = 0$ . As different from the barotropic kinetic equation where a unique  $\kappa_0 \geq 0$  exists for each set of interacting waves, in the baroclinic case there may exist from 0 to 3 positive solutions of this equation. The described simplifications allow expressing Eqs. (6) as follows:

$$\frac{\partial F}{\partial T} = I_{000} + \alpha I_{011}; \quad \frac{\partial G}{\partial T} = I_{111} + I_{110}. \quad (9)$$

Analytical expressions for the collision integrals in Eqs. (9) are given in Papers I, VII. The integrals  $I_{000}$  and  $I_{111}$  have no singularities and basically coincide with the collision integral of the kinetic equation for the barotropic Rossby waves. The integral  $I_{011}$  has only integrable singularities and always converges (Soomere 1992a [109]). These singularities are avoided in the solver by a proper choice of the grid points in the numerical integration.

The most complex problems arise in numerical representation of the integral  $I_{110}$ . It generally has non-integrable singularities corresponding to the double

resonance conditions (Soomere 1992a, 1993 [109, 111]). Mathematically, these singularities correspond to the case when simultaneously  $\omega_{pmn}^{012} = 0$ ,  $\kappa_{pmn}^{012} = 0$  and  $\nabla\omega_m(\kappa_1) = \nabla\omega_n(\kappa_2)$ . According to (Reznik 1984 [97]), the general conditions for validity of the kinetic equation are not satisfied in this case and the collision integral may diverge. Physically, the above conditions mean that resonantly interacting waves with the vectors  $\vec{\kappa}_1, \vec{\kappa}_2$  have also equal group velocities. Such a case is called double resonance and the relevant points  $\vec{\kappa}_1$  - the double resonance points. In this case, an underlying hypothesis of the kinetic theory – the assumption of stochastic phases of the interacting waves (Hasselmann 1962 [33], Majda *et al.* 1997 [66]) – is violated. Indeed, wave groups with equal group velocities remain in contact for a long time.

Baroclinic Rossby waves are one of the few wave systems where double resonance may have essential influence on the spectral evolution (Soomere 1992a [109]). It can be shown that the double resonance points form a finite curve  $S_{2R}$  on the  $(k, l)$ -plane (Soomere 1992a, 1993 [109, 111]). The fact that integral  $\int_{S_{2R\epsilon}} I_{110} dk dl$ , computed over some narrow  $\epsilon$ -vicinity of  $S_{2R}$ , approaches zero when  $\epsilon \rightarrow 0$  suggests that the inaccuracy made by excluding a certain narrow area nearby  $S_{2R}$  from the computations most probably will not distort essentially the evolution of the whole spectrum (Soomere 1993 [111]). In other words, although double resonance may locally distort the spectrum, its influence on the evolution of the whole system apparently is negligible. A rigorous proof of this fact was given by Amundsen and Benney (2000 [3]) for a particular case of 1D wave systems. Double resonance can generate a delta-like peak in the spectral space, but does not cause any huge amplification in the wave amplitudes (at least, in the 1D case). Thus it can be ignored as it causes some negligible error but probably has not substantial impact on the system behaviour. Although the general proof for multi-dimensional wave classes such as Rossby waves is still missing, the result obtained by Amundsen and Benney (2000 [3]) suggests that double resonance has a limited influence on the spectral evolution. Based on these results, the interaction of waves close to double resonance is simply neglected in the numerical solver.

## 2.4. Resonance curves and double resonance

The problem of detecting double resonance can be reduced to a purely geometric problem of topology of the sets of wave vectors, over which the integration in collision integrals is performed (Soomere 1992a [109]). This is the main reason of revisiting the classical studies of the properties of the set of vectors of waves, resonantly interacting with a given wave. The relevant studies

have been performed starting from 1960s (Longuet-Higgins and Gill 1967 [65]), and lead to interesting nontrivial geometric problems.

In the framework of the kinetic theory, the most intensive energy exchange of a given Rossby wave (either barotropic or baroclinic) with a wave vector  $\vec{\kappa}$  occurs when it interacts with waves, vectors of which  $\vec{\kappa}_1$  and  $\vec{\kappa}_2$  satisfy the resonance conditions

$$\vec{\kappa}_{012} = \vec{0}; \quad \omega_{pmn}^{012} = \omega_p(\vec{\kappa}) + \omega_m(\vec{\kappa}_1) + \omega_n(\vec{\kappa}_2) = 0 \quad (10)$$

together with the vector  $\vec{\kappa}$ . Here we assume that the waves with the wave vectors  $\vec{\kappa}, \vec{\kappa}_1, \vec{\kappa}_2$  represent the modes (either barotropic or baroclinic) with the numbers  $p, m$  and  $n$ , respectively. In the case of 2D waves and three-wave interactions, Eqs. (10) define three conditions for six components of wave vectors  $\vec{\kappa}, \vec{\kappa}_1$  and  $\vec{\kappa}_2$ . If any two of these components, say,  $\vec{\kappa} = (k, l)$ , are given, Eqs. (10) define three conditions for the remaining four components of the wave vectors.

These conditions generally define curves  $G_1 = G_1(\vec{\kappa}_1)$ ,  $G_2 = G_2(\vec{\kappa}_2)$  on the planes of wave vectors  $\vec{\kappa}_1$  and  $\vec{\kappa}_2$ . These curves are called resonance curves for wave vector  $\vec{\kappa}$ . The wave corresponding to vector  $\vec{\kappa}$  can only exchange energy with waves, vectors of which lie on these curves. The appearance of the resonance curves is a critical issue in the numerical solver for the kinetic equation, because integration in the collision integrals is factually performed along these curves.

In the case of barotropic Rossby waves the resonance curves for  $\vec{\kappa}_1$  and  $\vec{\kappa}_2$  coincide, are usually smooth oval, egg-like or hourglass-shaped curves, and have two axes of symmetry (Longuet-Higgins and Gill 1967 [65]). They have a singularity only in the case of interactions with the zonal flow that are void anyway (Longuet-Higgins and Gill 1967 [65]). The concurrence of curves  $G_1$  and  $G_2$  in the barotropic case (or, more generally, in the case of interactions of Rossby waves of belonging to the same mode) is not unexpected, because all waves satisfy the same dispersion relation which only depends on the Rossby deformation radius. These features allow essential reducing the amount of calculation in numerical evaluation of the barotropic collision integrals (Reznik and Kozlov 1981 [95], Reznik and Soomere 1984a [98]).

In the case of a baroclinic ocean certain sets of interacting waves contain waves from different modes that satisfy different types of dispersion relations. Expression  $\omega_{pmn}^{012}$  in this case is a sum of different expressions for the angular frequency for different modes (see Section 2.1). The expressions are similar to each other, but may contain different values of the Rossby radii. The most important outcome from this feature consists in the possibility of concentration of energy of different modes at different wavelengths that may lead to various

scenarios of evolution towards the equilibrium state (Soomere 1995, 1996 [112, 113]).

Further study of the resonance curves has been performed in (Jones 1979 [42]) for the particular case of interaction of one barotropic wave with two baroclinic harmonics. The corresponding resonance curves for  $\vec{\kappa}_1$  and  $\vec{\kappa}_2$  also coincide and have two axes of symmetry; thus the reduction of the amount of calculations owing to these features is still possible. For certain combinations of the wave vectors and Rossby radii the resonance curves may contain singularity points. The situation is still favourable: all singularities arising in the collision integral  $I_{011}$  are integrable.

In a more general case of interactions of a baroclinic wave with one barotropic and one baroclinic component the latter waves satisfy different dispersion relations. Therefore, it is natural that resonance curves for  $\vec{\kappa}_1$  and  $\vec{\kappa}_2$  do not coincide in this case (Papers I, VII), and that they generally have no axes of symmetry. Moreover, these curves may have singularity points corresponding to non-integrable singularities of collision integral  $I_{110}$ .

Although the presence of singularities apparently does not essentially disturb the evolution of the spectrum as a whole (see above), it is mandatory to incorporate the information about geometry of the resonant curves into the solver in order to avoid these singularities. The results of the relevant studies that have been essentially used in the construction of the solver for the baroclinic kinetic equation have been reported on various conferences<sup>2</sup>.

From representation (8) it follows that the resonant curves  $G_1 = G_1(\vec{\kappa}_1)$ ,  $G_2 = G_2(\vec{\kappa}_2)$  are always congruent, and can be obtained from each other via a rotation around the point  $-\frac{1}{2}\vec{\kappa}$ . This allows us without a loss of generality to consider only one curve, say,  $G = G_1$ . This curve only crosses the origin if  $a_m = a_n$ , i.e. in the symmetric cases analysed by Longuet-Higgins and Gill 1967 [65] and Jones 1979 [42].

Double resonance occurs exclusively for the waves that have singularity points of the resonance curves (Soomere 1992a, 1993 [109, 111]). Indeed, for a

---

<sup>2</sup> T. Soomere and K. Rannat, On the resonance curves for Rossby waves in two-layer ocean, in *IV USSR Conference "Contribution of young scientists and specialists towards solving contemporary problems of oceanology and hydrobiology"*, **2**, 47–48 Sevastopol, 1989 (in Russian), T. Soomere and K. Rannat, On the spectral evolution of baroclinic Rossby waves, in *III USSR Conference "Vortices and turbulence in the oceans"*, Kaliningrad, 1990, 44 (in Russian), T. Soomere and K. Rannat, On the numerical investigation of the spectral evolution of baroclinic Rossby waves, in *III USSR symposium "Fine structure and synoptic variability of seas and oceans"*, Tallinn, 1990, 146–147 (in Russian).

given  $\vec{k}$  the curves  $G_1 = G_1(\vec{k}_1)$ ,  $G_2 = G_2(\vec{k}_2)$  are differentiable everywhere except for the points  $\vec{k}_1$  or  $\vec{k}_2$ , satisfying the condition

$$\Delta = \left| \vec{\nabla} \omega_m(\vec{k}_1) - \vec{\nabla} \omega_n(\vec{k}_2) \right| = 0, \quad (11)$$

which is the condition of double resonance. The sets  $\vec{k}, \vec{k}_1, \vec{k}_2$ , satisfying simultaneously Eqs. (10) and Eq. (11) are called double resonance triplets and the corresponding points of  $\vec{k}$  on the  $(k, l)$ -plane - points of double resonance.

This connection between the double resonance (equivalently, the validity of the kinetic equation) and the occurrence of singularity points of the resonance curves is valid for all wave systems with three-wave resonant interactions. On the one hand, this feature motivates further studies of the shape of the resonance curves for different wave classes for which the set of the double resonance points cannot be found explicitly. On the other hand, it greatly simplifies the classification of the topological shapes of the resonance curves and their possible singularities provided the set of double resonance point has been determined. Namely, a displacement of a wave vector  $\vec{k}$  causes only a smooth deformation of the resonance curve unless this vector passes through a point for which the resonance curve contains a singularity (Soomere 1992b [110]).

## 2.5. Resonance curves for baroclinic Rossby waves

The resonance curves and their singularities for baroclinic Rossby waves are presented on figures 2.5.1 and 2.5.2 for several combinations of the values of  $a_p$ ,  $a_m$ ,  $a_p$  and the wave vector  $\vec{k}$ . Figure 2.5.1 illustrates the shape of the resonant curves for interactions of a baroclinic wave with one barotropic and one baroclinic component in the case  $a_p = a_m = 1$ ,  $a_n = 0$ . The corresponding set of double resonant points consists of two branches in the neighbourhood of the  $l$ -axis. One branch of this curve crosses the  $l$ -axis at a certain point with  $l > 0$  whereas the other one goes through the origin. Together they form a fishhook-like curve in each quadrant of the  $(k, l)$ -plane (Soomere 1992a [109]). The common point of the branches is a singularity point of the set of double resonant points, which is missed in the analysis in (Soomere 1992a [109]).

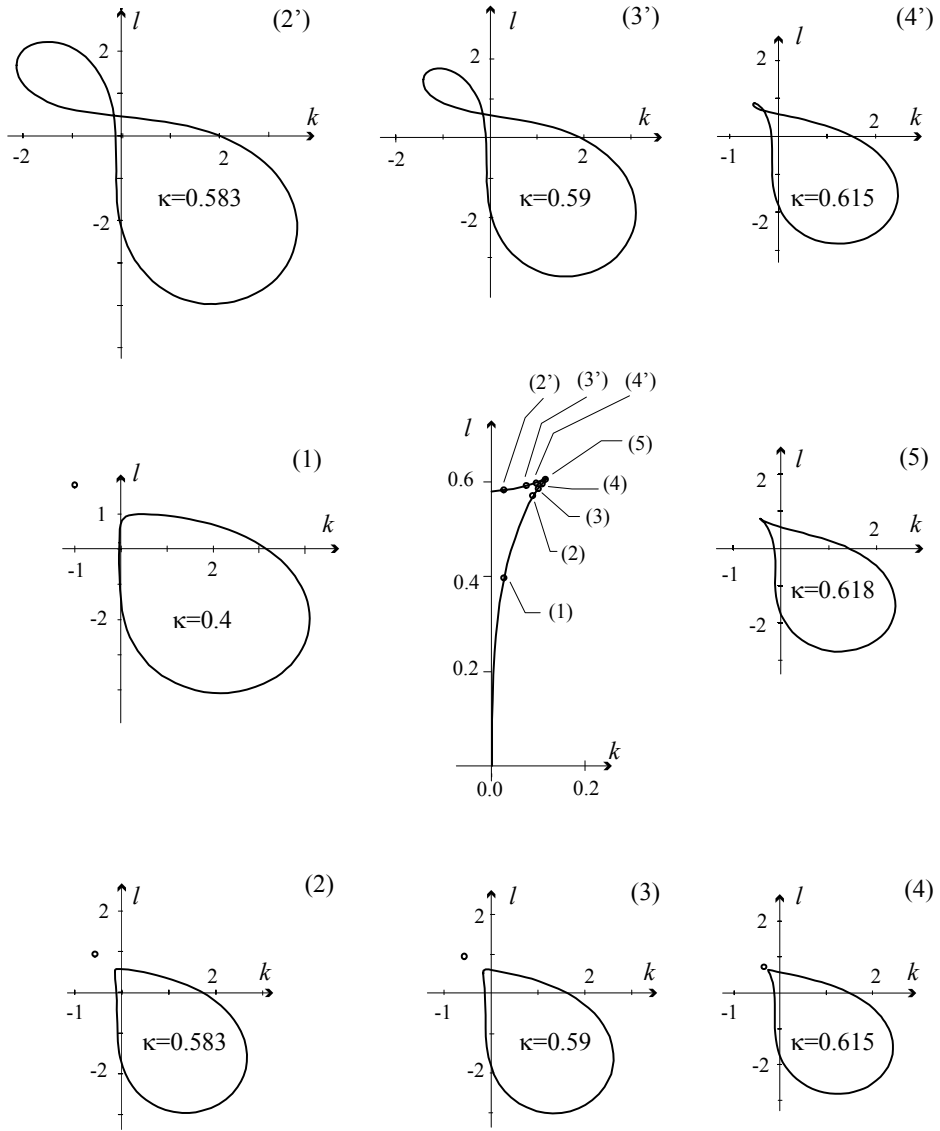


**Figure 2.5.1.** Resonance curves corresponding to wave vectors lying at the different points of the double resonance curve (the central panel) in the case  $a_p = a_m = 1$ ,  $a_n = 0$ . The position of the wave vector at the double resonance curve is shown using *small filled circles*. The *small circles* mark the separated singularity points of the double resonance curve (cases 2, 3 and 4).

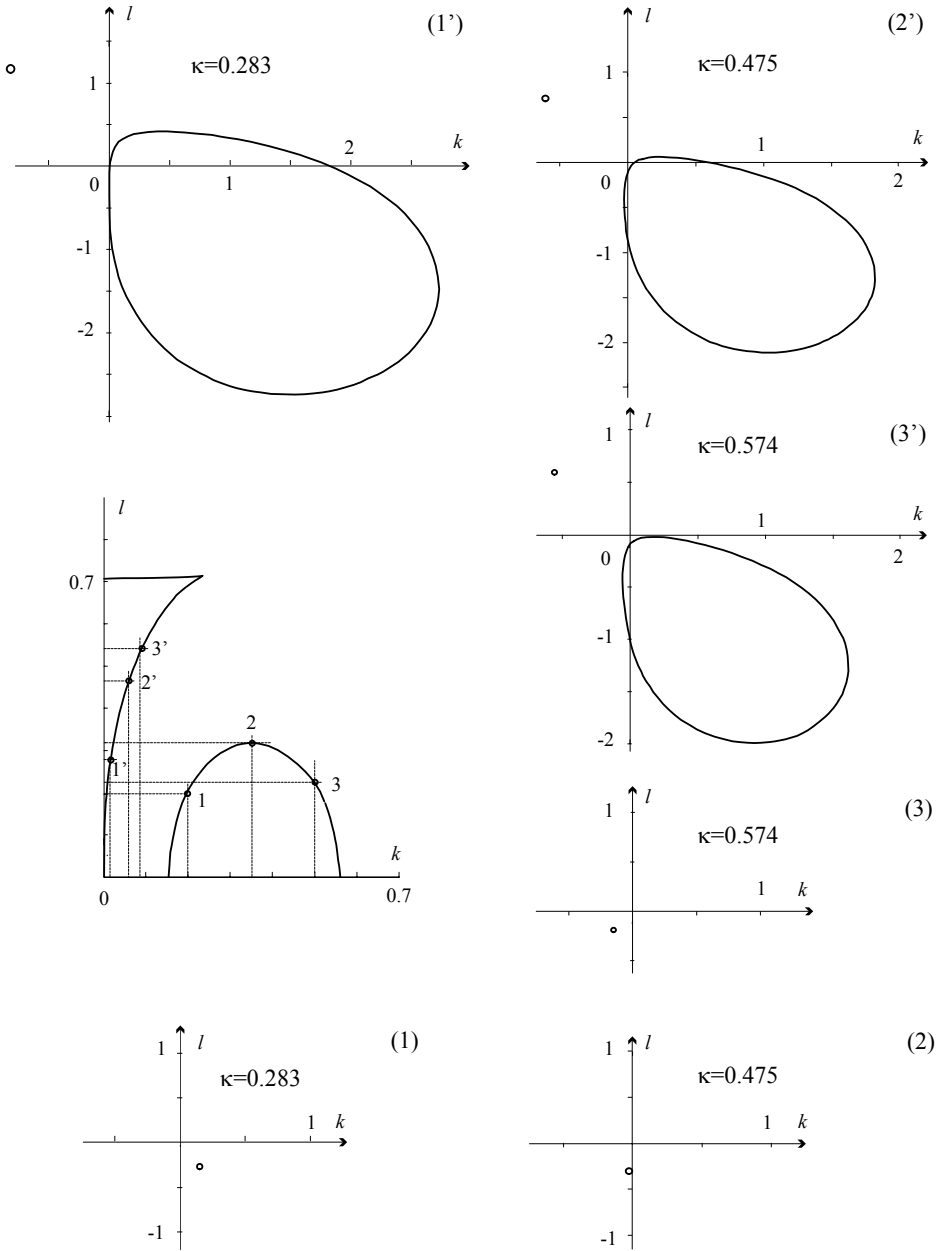


**Figure 2.5.2.** Resonance curves for  $a_p^2 = 0.5$ ,  $a_m^2 = 1.0$ ,  $a_n^2 = 0.6$ . The position of the wave vector at the double resonance curve is shown using *small filled circles*. The *small circles* mark the single points of the resonance curves, corresponding to the points 1', 2', 3' at branch II of the double resonance curve and one-point resonance curves corresponding to points 1, 2, 3 at branch III of the double resonance curve.

The resonant curves for waves, vectors of which lie on the former branch of this curve, are hourglass-shaped (at points 2', 3', 4') and contain a self-crossing point. The resonance curve for waves with vectors lying on the latter branch (points 1, 2 and 3) consists of a single point and a smooth egg-like curve. The resonance curve corresponding to the common point (5) of the branches contains a turning point.

In a more general case  $a_m \neq a_n$ ,  $a_m, a_n > 0$ ,  $a_p \leq a_m$ , additional oval branch of the double resonance curve lies near the  $k$ -axis. The resonance curve corresponding to a wave vectors lying at this branch consists of a single point (Fig. 2.5.2). Resonance curves corresponding to waves, vectors of which lie at the above-described branches of the double resonance curve are qualitatively similar to the ones presented on Fig. 2.5.1.

## 2.6. Numerical scheme: discretization and stability

The numerical scheme used in Papers I and VII is an extension of an analogical scheme for the barotropic kinetic equation (Reznik and Soomere 1983, 1984a [96, 98]). The problem consists now in solving the Cauchy problem for the system of integro-differential equations (9) in the infinite domain.

The functions  $F$  and  $G$  are calculated at the nodes of a rectangular grid covering the bounded region  $\Omega$  of the  $(k, l)$ -plane. Collision integrals (which were reduced to certain 1D integrals over a bounded interval by introducing the polar coordinates  $\kappa_0$ ,  $\varphi'$  and by making use of the delta-functions, as described in the previous sections) are approximated by using the Gauss' quadrature formula. The values of  $F(\vec{\kappa}_1)$ ,  $F(\vec{\kappa}_2)$ ,  $G(\vec{\kappa}_1)$ ,  $G(\vec{\kappa}_2)$  at points  $\vec{\kappa}_1$ ,  $\vec{\kappa}_2$ , corresponding to the nodes of the Gauss' formula but not coinciding with the grid points on the  $(k, l)$ -plane, are found with the use of a double linear interpolation.

The resulting system of ordinary differential equations with respect to spectra of the baroclinic and the barotropic modes at the grid points is not closed because in any finite region  $\Omega$  there exist waves, which interact with waves, vectors of which lie outside  $\Omega$ . The simplest way to handle such interactions consists in setting both the energy spectra identically zero outside this domain. Physically, this is equivalent to the introduction of infinite viscosity outside of  $\Omega$ . Since the energy spectrum of Rossby wave systems with finite energy must decay as  $F, G = o(\kappa^4)$  when  $\kappa \rightarrow \infty$ , for a sufficiently large region  $\Omega$  the error introduced by this truncation is expected to be very small (cf. (Reznik and Soomere 1983, 1984a [96, 98])).



Another simple truncation scheme (also used in earlier studies) consists in complete ignoring of all interactions involving vectors lying outside  $\Omega$ . This is equivalent to replacing the infinite region of integration in Eq. (10) by a finite region  $\Omega(\vec{\kappa}_1) \times \Omega(\vec{\kappa}_2)$ . Although this method has less clear physical interpretation, it is more relevant to the goals of the study of free evolution of wave systems, because the conservation laws of the kinetic equation as well as the  $H$ -theorem exactly hold in this approximation.

An important difference of the solver in question from the one for the barotropic case is that the integrands of  $I_{011}$  and  $I_{110}$  may contain singularities at the double resonance points. For integrable singularities, it was checked if the nodes of quadratic formula are located far enough from the singularity points of resonant curves. As discussed above, the presence of non-integrable singularities apparently does not distort the spectral evolution much. The actual behaviour of the spectrum in the vicinity of the double resonance curve is neglected, and its values in the grid points very close to this curve are estimated with the use of a double linear interpolation on the basis of the values of spectra at adjacent points.

The greatest difficulty in the development of the numerical scheme was the proper choice of the grid size, the interpolation method, the quadrature and the finite-difference representation of the time derivative, all of which together determine the operational effectiveness of the scheme. The listed parameters were optimized according to the demand that the rms. error of the calculations must be less than 1% per unit of slow time.

Most of the calculations were carried out for a regular rectangular grid with 97 points in the direction of the  $l$ -axis and 114 points in the direction of the  $k$ -axis, covering the region  $\kappa \leq 4$ . The grid has a finer resolution in the vicinity of the  $l$ -axis (Fig. 2.6.1), because an intense concentration of energy in this area was detected both in earlier studies of the barotropic spectra as well as in preliminary experiments.

In earlier studies, the collision integral was replaced by the Gauss' quadrature formula with 24 nodes in each segment with a length of  $\pi$ . For the baroclinic kinetic equation, the integration interval is divided into subintervals with the length of  $\pi/4$  and the 6-node Gauss formula is used in each subinterval. The resulting system of ordinary differential equations was solved by using the predictor-corrector method. The 2<sup>nd</sup> order explicit Adams' scheme is used as a predictor and the 3<sup>rd</sup> order implicit Adams' formula as a corrector.

The total energy was normalized to  $E = 1$  at  $T = 0$ . A permanent check was made on the proper operation of the scheme from the behaviour of the conservation integrals and the law of increasing in total entropy (Papers I, VII). The identity  $L \equiv 0$  (Eq. (7)) is maintained numerically, because all the initial spectra are symmetrical with respect to both the co-ordinate axes. Typically, the total energy  $E$  alters less than by 1% per time unit. At the beginning of most of

the runs described in this thesis as well as in the further studies with the use of this solver (Soomere 1995, 1996 [112, 113]), the energy alteration rate  $|dE/dT|$  is approximately 0.3% per time unit and somewhat increases in their final phases (Fig. 2.6.2). Also the value for  $H$  (entropy) was increasing monotonically.

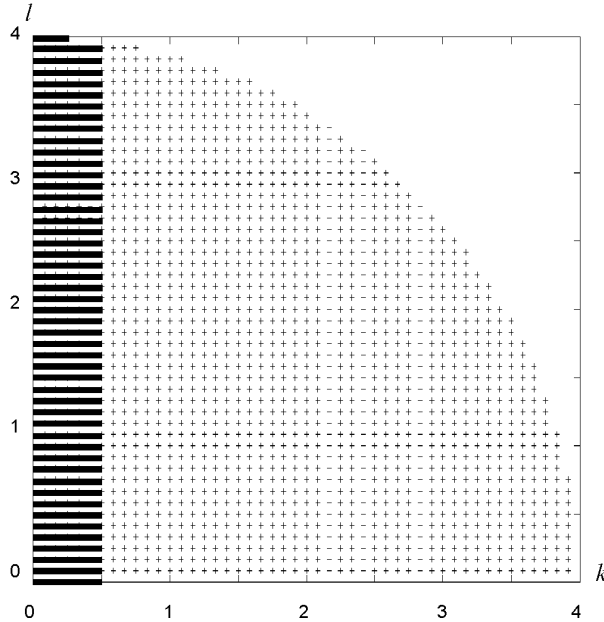


**Figure 2.6.1.** The computational grid.

The system enstrophy  $Y$  is more sensitive to computational errors because of the factor  $\kappa^2 + a_p^2$  in its spectral representation. Since the spectra are evidently most distorted near the boundary of the computational area, the enstrophy of shorter waves may be computed relatively inexactly. Indeed, the total enstrophy usually alters by 1–2% per time unit. Its alteration rate often increases in the final phases of evolution, achieving in extreme cases values of  $|Y^{-1}dY/dT|$  up to 0.04–0.05. Thus the variation of both the constraints is quite satisfactory. As the Adams scheme conserves both the energy and the enstrophy, their behaviour indicates that with time the total accuracy of the quadrature and the interpolation procedures decreases to some extent.

Another property that indirectly permits judging the operational correctness of the scheme in the barotropic case is the total spectral width (Reznik and Soomere 1984a [98]). Generally, nonlinearity destroys sharp spectral peaks and works towards widening the total spectrum with respect to a certain wave

number  $k^*$ . The relevant hypothesis is called defocusing or spreading assumption (Merilees and Warn 1975 [70]). For the barotropic case this assumption is  $E^{-1} \left[ d \int (\kappa - \kappa_c)^2 F dk dl \right] / dT > 0$ . Here  $\kappa_c = E^{-1} \int \kappa F dk dl$  is the average modulus (mean wave number) of the wave vector.

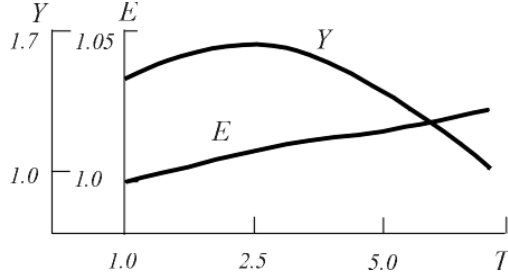


**Figure 2.6.2.** Evolution of the total energy  $E$  and enstrophy  $Y$  for the Rossby wave field with initial conditions  $F(\vec{\kappa}, 0) = G(\vec{\kappa}, 0) = [2\pi^{3/2}(1 + \alpha)]^{-1} \kappa \exp(-\kappa^2)$ ,  $\alpha = 0.2$ .

For inviscid nonforced 2D flows, the spreading assumption is equivalent to  $d\kappa_c/dT < 0$ , i.e. to the scale-increasing process (Merilees and Warn 1975 [70]). The effect of spectral widening is caused by the nonlinearity, which is supposed to be small in the kinetic theory. Yet in barotropic experiments this effect was observed in all cases in spite of the incessant generation of certain spectral peaks (Reznik and Soomere 1984a [98]).

Stratified motion possesses an additional degree of freedom and the defocusing and the scale-increasing processes are not necessarily active. For 2-layer flows the relevant spreading assumption (Marshall 1986 [67]) reads  $\frac{d}{dT} \int [(\kappa - \kappa_{c0})^2 F + \alpha(\kappa - \kappa_{c1})^2 G] dk dl > 0$ , where  $\kappa_{c0}$ ,  $\kappa_{c1}$  are the mean wave numbers of the barotropic and the baroclinic mode, respectively. This inequality does not yield a decrease in the mean wave number. For example, it is shown in (Soomere 1996 [113]) that the mean wave number of a 2-layer beta-plane flow must decrease only if the baroclinic energy increases. For the described reasons the temporal behaviour of the total spectral width is not used as an indicator of the correctness of computations.

## 2.7. Basic features of spectral evolution

Spectral evolution of weakly nonlinear Rossby wave systems is studied based on numerical integration of a large number of various initial spectra. The initial energy distributions are proportional to  $\kappa \exp(-\kappa^2)$ . Additionally to isotropic spectra, predominantly zonal motion systems were modelled with the use of the ‘spreading’ factor  $\sin^4 \varphi$ . An analogous factor  $\cos^4 \varphi$  was used to simulate initially mostly meridional motion systems. The relevant maximum of energy spectra in Figs. 2.7.1, 2.7.2 nearby  $k$ -axis corresponds to nearly meridional flow and the maximum nearby  $l$ -axis corresponds to the nearly zonal flow.

Integration was usually performed until the total intensity of interactions  $I = \int (|\partial F / \partial T| + \alpha |\partial G / \partial T|) dkdl$  decreases at least ten times compared with its maximum value. This quantity is expected to fully decay for systems in thermodynamical equilibrium. Its substantial decrease during the computations suggests that the computed final states apparently reveal the basic features of the thermodynamically equilibrated state(s).

Typical examples of spectral evolution of certain initial distributions of general interest have been discussed in Papers I and VII. Paper VII considers evolution of anisotropic spectra  $F(\vec{k}, 0) = A_1 \kappa \exp(-\kappa^2) \sin^4 \varphi$ ,  $G(\vec{k}, 0) = A_2 \kappa \exp(-\kappa^2) \sin^4 \varphi$  that represent a system of synoptic motions with predominating zonal component of both the modes. This case was chosen, because evolution of the corresponding purely barotropic wave system showed the most interesting behaviour. Paper I discusses the case of isotropic initial spectra  $F(\vec{k}, 0) = A_3 \kappa \exp(-\kappa^2)$ ;  $G(\vec{k}, 0) = A_4 \kappa \exp(-\kappa^2)$ . The energy balance between the modes follows the ratio of the layer’s thicknesses and the coefficients  $A_1 \dots A_4$  are chosen so that the total energy  $E = 1$ . Further analysis of spectral evolution of different combinations of initial spectra has been performed with the use of the solver in question and with supercomputers of the Deutsche Klimarechenzentrum in the middle of the 1990s (Soomere 1995, 1996 [112, 113]).

Behaviour of both the spectra and their time derivatives (Fig. 2.7.1, 2.7.2) is important in understanding the energy exchange processes. Examination of fields of  $\partial F / \partial T$  and  $\partial G / \partial T$  allows determining of areas of energy inflow and outflow (marked with ‘+’ and ‘-’, respectively). Configuration of these areas can help to establish the basic tendencies of energy redistribution.

In the calculations of the initially nearly zonal flow a complex pattern of energy exchange occurs. Most of the details of the evolution of the barotropic spectrum and its derivative resemble those of the pure barotropic case (Reznik and Soomere, 1984a [98]).

There are two areas of energy inflow I, III, placed near the  $l$ - and  $k$ -axis, respectively, and two areas of energy outflow II, IV. The absolute values  $\partial F / \partial T$  in area IV are at least of an order smaller than the analogous values in area II, and area IV does not play any essential role in the total energy exchange. The maximum values of  $\partial F / \partial T$  in relatively narrow inflow area I are much greater than in area III, but the total amount of inflow is greater in area III.

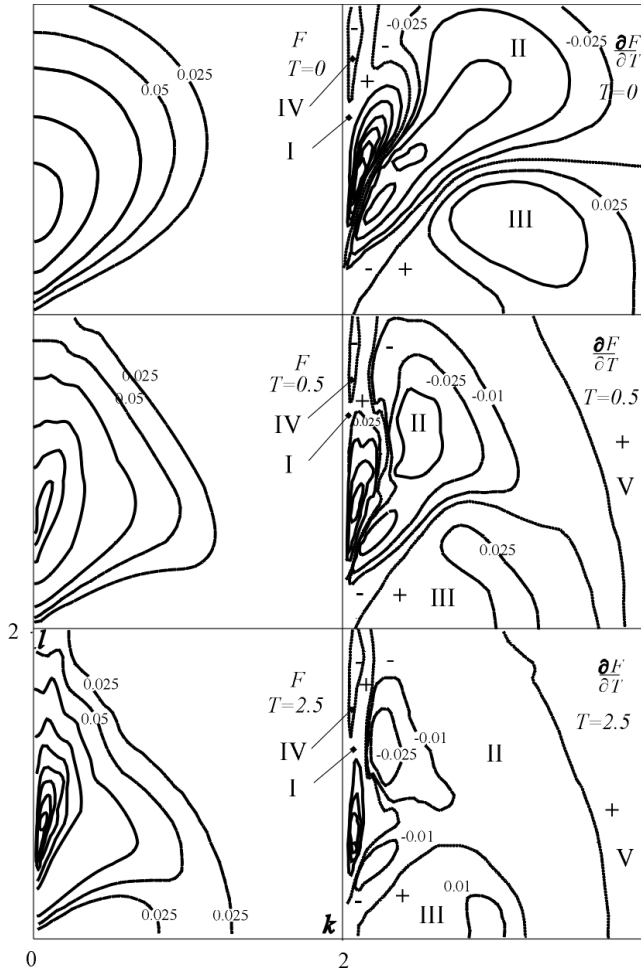


**Figure 2.7.1.** Temporal evolution of energy spectrum of the barotropic mode  $F$  (left) and its time derivative  $\partial F / \partial T$  (right) in experiments with initial conditions  $F(\vec{\kappa}, 0) = \alpha G(\vec{\kappa}, 0) = 16 [3\pi^{3/2}(1 + \alpha)]^{-1} \kappa \exp(-\kappa^2) \sin^4 \varphi$ . The main isolines (solid lines) are plotted from 0.1 with a step of 0.1 for  $F$  and from  $\pm 0.05$  with a step of 0.05 for  $\partial F / \partial T$ . The dotted line corresponds to  $\partial F / \partial T = 0$ . Area  $0 \leq k, l \leq 2$  is represented in each panel.

Physically, there exist two main directions of energy redistribution. A spectrally narrow almost-zonal flow with  $l \sim 1$  is generated and an almost-meridional flow with  $k \sim 1$  is supported to some extent.

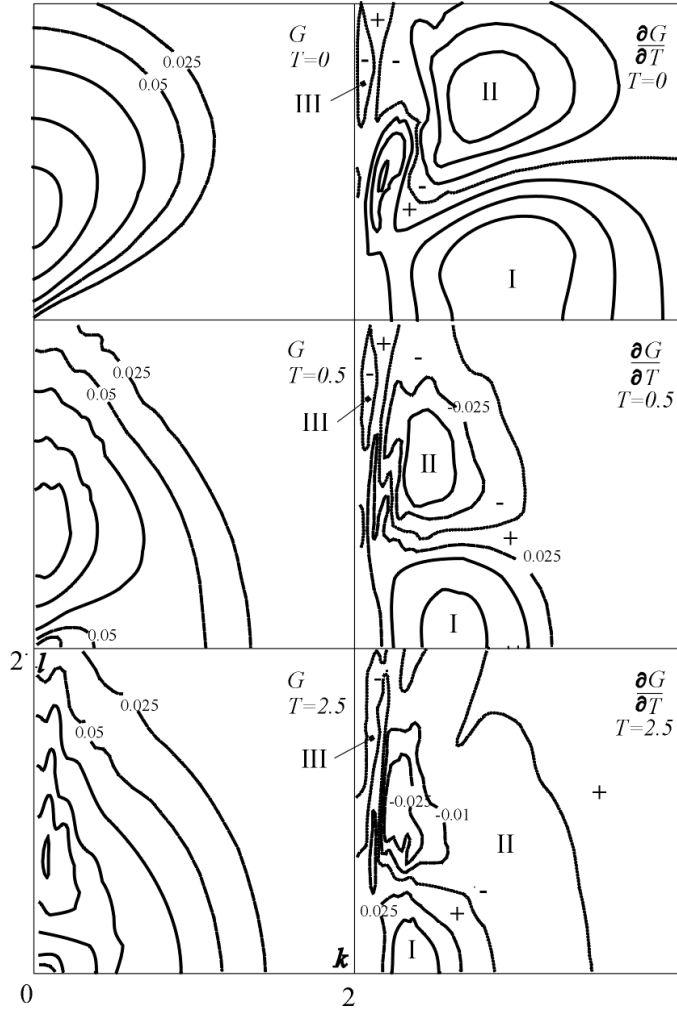


**Figure 2.7.2.** Temporal evolution of energy spectrum of the barotropic mode  $G$  (left) and its time derivative  $\partial G / \partial T$  (right) in experiments with initial conditions  $F(\vec{\kappa}, 0) = \alpha G(\vec{\kappa}, 0) = 16 [3\pi^{3/2}(1 + \alpha)]^{-1} \kappa \exp(-\kappa^2) \sin^4 \varphi$ . The main isolines (solid lines) are plotted from 0.1 with a step of 0.1 for  $G$  and from  $\pm 0.05$  with a step of 0.05 for  $\partial G / \partial T$ . The dotted line corresponds to  $\partial G / \partial T = 0$ . Area  $0 \leq k, l \leq 2$  is represented in each panel.

In the course of time the values of  $\partial F / \partial T$  decrease all over the wave vector plane. Areas I, III decrease as well and a new inflow area V remote from the origin, arises from the falling of area III into two parts. Area II increases to some extent and stretches out in the direction of the  $l$ -axis. However, the later changes of the  $\partial F / \partial T$  field have a negligible influence on the spectral evolution, which is mostly determined by areas of intensive inflow I, III and outflow II. The described processes result in a narrow and high spectral peak of the barotropic mode in the very close vicinity of the  $l$ -axis. We call it a zonal peak. An interesting peculiarity of the evolution of zonal peak is that, after some time, an “erosion” process of its upper right slope becomes evident, a typical phenomenon in all the experiments. It additionally enhances the steepness of the right-hand slope of the peak, in this way acting towards adjusting it towards a delta-like hump. Finally, the zonal peak appears to be quite a modest at  $\kappa > 1$ , but extremely sharp and high at  $\kappa \approx 0.6 - 0.7$ . Remote from the  $l$ -axis, the spectrum  $F$  apparently tends to an isotropic state.

At the outset, the evolution of the baroclinic mode is characterized by an intense energy inflow at  $l \leq 1$  (area I of distribution of  $\partial G / \partial T$ ) and an energy outflow at  $l \geq 1$  (area II). Energy exchange in areas III and IV is negligible. Area I has two inflow maxima, corresponding to the reinforcement of both the nearly zonal flow and the mostly meridional disturbances. The former process, however, rapidly ceases and the baroclinic zonal flow is suppressed starting from  $T \approx 0.5$ . Differently from the evolution of the barotropic mode, the latter process remains active during the whole experiment. The resulting spectrum is nearly isotropic, whereby the isotropization process acts much faster than in the barotropic case. Baroclinic energy mostly flows along the  $l$ -axis, while both in the 1-layer experiment and in the case of the barotropic mode energy exchange mainly occurs between waves of nearly equal length.

The temporal evolution of other initial spectra and their time derivatives in all the runs with comparable initial energies of both the modes shows similar features to the described ones. The fields of derivatives  $\partial F / \partial T$  and  $\partial G / \partial T$  always initially reveal a characteristic two-lobed (or three-lobed, in case of initial zonal anisotropy only) structure with an extensive inflow area close to the  $l$ -axis (cf. Fig. 2.7.3–2.7.4). To the end of simulations, energy is mostly transferred into the barotropic nearly zonal flow and (occasionally) into large-scale baroclinic mostly meridional motion components.

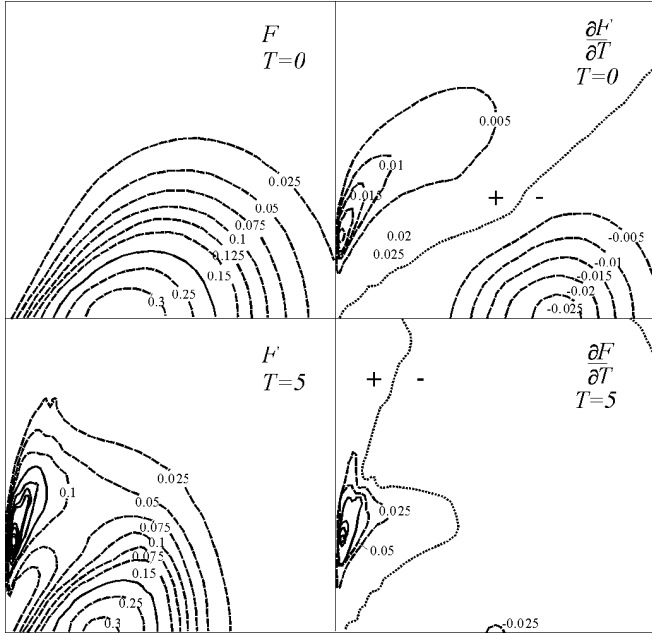


**Figure 2.7.3.** Temporal evolution of energy spectrum of the barotropic mode  $F$  (left) and its time derivative  $\partial F / \partial T$  (right) in experiments with initial conditions  $F(\vec{\kappa}, 0) = \alpha G(\vec{\kappa}, 0) = 2[\pi^{3/2}(1 + \alpha)]^{-1} \kappa \cos^4 \varphi \exp(-\kappa^2)$ . The main isolines (solid lines) are plotted from 0.2 with a step of 0.2 for  $F$  and from  $\pm 0.1$  with a step of 0.1 for  $\partial F / \partial T$ . The dotted line corresponds to  $\partial F / \partial T = 0$ . Area  $0 \leq k, l \leq 2$  is represented in each panel.



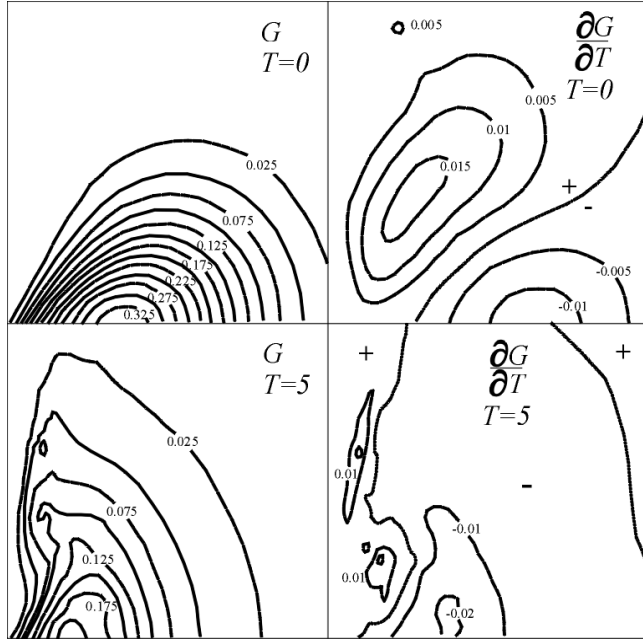


**Figure 2.7.4.** Temporal evolution of energy spectrum of the barotropic mode  $G$  (left) and its time derivative  $\partial G / \partial T$  (right) in experiments with initial conditions  $F(\vec{\kappa}, 0) = \alpha G(\vec{\kappa}, 0) = 2[\pi^{3/2}(1 + \alpha)]^{-1} \kappa \exp(-\kappa^2) \cos^4 \varphi$ . The main isolines (solid lines) are plotted from 0.1 with a step of 0.1 for  $G$ . The dotted line corresponds to  $\partial G / \partial T = 0$ . Area  $0 \leq k, l \leq 2$  is represented in each panel.

The temporal evolution of the barotropic mode always is similar to that in the barotropic experiments (Reznik and Soomere, 1984a,b [98, 99]; Reznik 1986 [100]) and reveals a coexistence of two basic tendencies. A portion of the energy is transferred into a well-defined spectral peak near the  $l$ -axis while remote from this axis the spectrum tends to become isotropic. As a result, a strong peak in the spectrum of the barotropic mode  $F$  near this axis emerges. This peak is quite narrow near the origin, widens to some extent at medium wavenumbers and has a general form of an elongated hogback with abrupt slopes near to the origin and with relatively gently sloping end at  $\kappa \approx 1$ . It has a characteristic enlargement at  $\kappa \approx 0.7$ . This form is universal within all experiments described here and in the following studies. It is interesting to notice that the evolution within the 2-layer model leads to a much more intense spectral peak of the barotropic mode, which is concentrated in a somewhat narrower vicinity of the  $l$ -axis compared to the purely barotropic case (Reznik, Soomere 1984a,b [98, 99], Reznik 1986 [100]).

Typically, the baroclinic spectrum soon takes a practically isotropic shape and preserves it until the end of experiments. This is a deeply interesting feature: the resonant interactions always form a powerful spectrally narrow zonal peak of the barotropic flow but usually do not enhance the zonal component of the baroclinic mode. In specific cases some increase of zonal component of the baroclinic motion takes place, but compared to barotropic mode  $F$  the relative height of the peak for  $G$  nearby the  $l$ -axis is much lower. Therefore, in most cases the weakly nonlinear interactions of Rossby waves in the 2-layer ocean lead to the generation of mostly barotropic nearly zonal flow.

Most of the initial spectra analysed above and in (Soomere 1995, 1996 [112, 113]) have the energy maximum at a fixed wavenumber  $\kappa \approx 0.7$ . The spectral maximum of the barotropic spectrum emerges at a comparable wavenumber suggesting that the energy exchange mostly occurs among waves of comparable length (cf. Reznik 1986 [100]). In order to make clear whether the location of the spectral maximum is determined by the shape of the initial spectra, a series of experiments was performed with initial spectra with maxima located at much smaller wavelengths.

Figures 2.7.5 and 2.7.6 present the initial and the final energy distributions with experiments with the initial spectra  $F(\bar{\kappa}, 0) = G(\bar{\kappa}, 0) \sim (\kappa - 0.5) \exp[-(\kappa - 0.5)^2]$ . The energy maximum in the relevant motions is located at  $\kappa = \sqrt{0.5} + 0.5 \approx 1.2$ . Initially the spectral peaks are formed at somewhat smaller wavelengths (larger  $\kappa$ ) and are somewhat wider than in the above-described experiments. However, in the course of time energy is intensely transferred to larger scales, and the spectral maximums are also gradually shifted closer to the origin. These results suggest that to the basic features of spectral evolution insignificantly depend on the initial location of the maximum at the  $(k, l)$ -plane, and that a dependence of the final result of the evolution on the location of the initial spectral maximum of the initial conditions is unlikely.

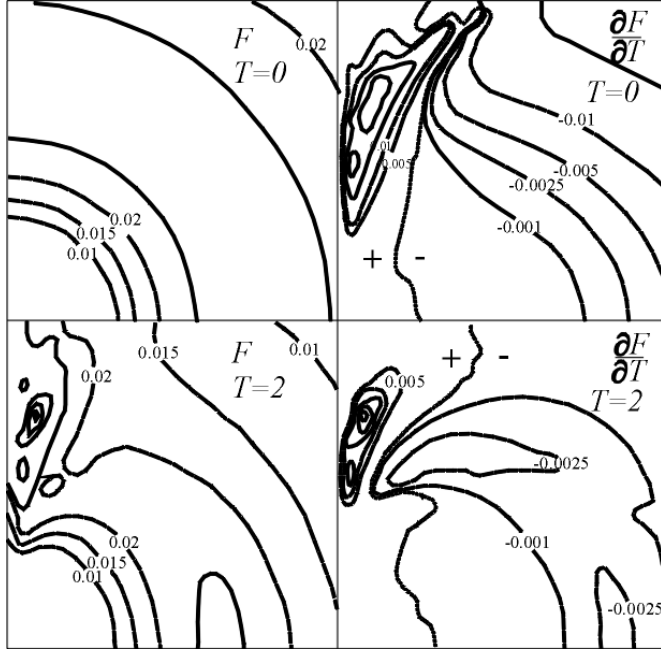


**Figure 2.7.5.** Temporal evolution of energy spectrum of the barotropic mode  $F$  (left) and its time derivative  $\partial F / \partial T$  (right) in experiments with initial conditions  $F(\vec{k}, 0) = G(\vec{k}, 0) \sim (\kappa - 0.5) \exp[-(\kappa - 0.5)^2]$  for  $\kappa > 0.5$ ,  $F(\vec{k}, 0) = G(\vec{k}, 0) \equiv 0$  for  $\kappa \leq 0.5$ . The spectra are normalised so that the total energy  $E = 1$ . The main isolines (solid lines) are plotted from 0.025 with a step of 0.025 for  $F$  and from  $\pm 0.02$  with a step of 0.02 for  $\partial F / \partial T$ . The dotted line corresponds to  $\partial F / \partial T = 0$ . Area  $0 \leq k, l \leq 2.0$  is represented in each panel.

The described and several other experiments, made with the use of largely different types of initial spectra, have demonstrated that the following main tendencies of the spectral evolution evidently are universal:

(i) in the course of time intensive almost-zonal nearly barotropic flow arises. It is remarkable that the peak in the spectrum of the barotropic mode is significantly higher and located closer to the  $l$ -axis than in the pure barotropic case;

(ii) although the zonal component of baroclinic motions increases to some extent, the relative height of the spectral peak near the  $l$ -axis still remains essentially lower than the analogous peak in the spectrum of the barotropic mode. Therefore, the almost-zonal flow generated by weakly nonlinear interactions of Rossby waves often should be practically barotropic;

(iii) in areas remote from the  $k$ -axis the spectra of the both modes become almost isotropic;

(iv) during all the numerical experiments the full spectrum of motion retains essentially its baroclinic nature.

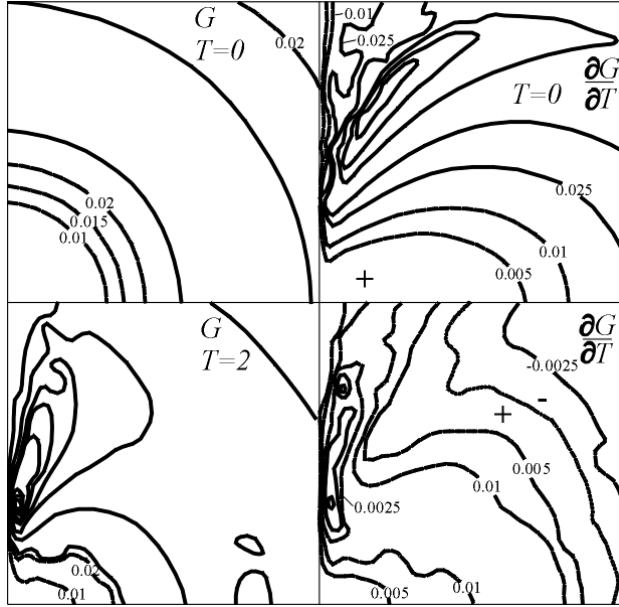


**Figure 2.7.6.** Temporal evolution of energy spectrum of the barotropic mode  $G$  (left) and its time derivative  $\partial G / \partial T$  (right) in experiments with initial conditions  $F(\bar{\kappa}, 0) = G(\bar{\kappa}, 0) \sim (\kappa - 0.5) \exp[-(\kappa - 0.5)^2]$  for  $\kappa > 0.5$ ,  $F(\bar{\kappa}, 0) = G(\bar{\kappa}, 0) \equiv 0$  for  $\kappa \leq 0.5$ . The spectra are normalised so that the total energy  $E = 1$ . The main isolines (solid lines) are plotted from 0.025 with a step of 0.025 for  $G$  and from  $\pm 0.05$  with a step of 0.05 for  $\partial G / \partial T$ . The dotted line corresponds to  $\partial G / \partial T = 0$ . Area  $0 \leq k, l \leq 2$  is represented in each panel.

The first feature suggests that the presence of the baroclinic mode acts as a catalyst in generation of large-scale almost-zonal barotropic flows in the oceans, a feature that has been confirmed by later research (Soomere 1995, 1996 [112, 113]). A conclusion of direct practical interest is that one may anticipate more intensive barotropic zonal currents in these areas of the ocean, in which well-defined stratification is present. This feature may partially explain the high persistency of a jet stream in certain layers of the Gulf of Finland (Andrejev et al. 2004a, b [4, 5]) where they mostly follow the bottom isolines. The two latter features suggest that the effect of barotropization of synoptic flows observed in oceans occurs mainly due to the formation of intensive large-scale almost-zonal flows; however, the field of relatively small-scale synoptic motions may retain a certain vertical structure.

Another important conclusion is that the resulting wave system only weakly depends on the choice of initial functions. This is not unexpected, because the wave systems described by the kinetic equation should evolve towards a thermodynamically equilibrated state. The resulting distributions of  $F$  and  $G$  are expected to reveal some information about the final state of evolution. The barotropic component of the latter apparently contains a delta-like part while the baroclinic one evidently has an isotropic shape. Some aspects of further evolution scenarios of Rossby wave systems to the equilibrium state have been discussed in (Soomere 1995, 1996 [112, 113]).

## 2.8. Layer formation in stratified medium

In nature, the air in the atmosphere and the water in the oceans, seas and lakes is usually stratified. The basic source of stratification in the ocean is the energy submitted to the ocean by the Sun. Including of stratification into models of geophysical flows usually drastically increases their complexity. The analysis performed in this Chapter shows that this consequence can be partially avoided if the stratification becomes evident in the form of well-defined layers of practically homogeneous fluid. This is frequently the case in the real ocean. In this case, assumptions made, *e.g.* in the theory of Rossby waves in the vertically homogeneous ocean are reasonable within each layer. Although interactions of motions within different layers make the layered model more complex, a multi-layer model is substantially simpler than full three-dimensional models. For example, the two-layer model and the relevant kinetic equation are applicable in cases when the vertical density distribution in the ocean (atmosphere) has one well-defined layer of large density gradients, and the rest of the medium is much more weakly stratified. Its generalisations can be applied also in cases when the water masses have more complex structure (see Section 1.4).

The stratification of a water column frequently becomes evident in the form of a series of homogeneous layers alternating with high gradient interfaces. Such a vertical structure is known as a stepped staircase or a stepwise thermohaline structure. Steplike vertical profiles with the typical height of the steps from a few centimetres to tens and hundreds of meters occur in many regions of the world's oceans, including tropical (Caribbean, Schmitt *et al.* 1987 [105]), arctic (Weddell Sea, Muench *et al.* 1990 [76]), and mid-latitude (Tyrrhenian Sea in the Mediterranean, Zodiatis *et al.* 1996 [147]) waters. A large number of experiments in the Red Sea (Swallow and Crease 1965 [129]), in the Arctic Ocean (Neal *et al.* 1969 [77]), the North Atlantic, in the Canada Basin (Padman and Dillon 1989 [81]), etc. suggest that the staircase-like structures are a common feature in the ocean. Layered structures can be found in some lakes also (*e.g.* lake Nyos in Cameroon where the contribution of  $\text{CO}_2$

to the stratification is much larger than that of temperature and dissolved salts, Schmid *et al.*, 2004 [104]).

There exist a large number of studies of formation of a staircase-like structure. Its mathematical modelling both in general fluid mechanics and in oceanography is supported by many laboratory experiments (Turner 1968 [133], Linden 1979 [63], Fernando 1987, 1989 [21, 22], among others) and with a large amount of experimental data. Many aspects of the origin of such a structure, in spite of long history of its studies, are still unclear.

There exist several mechanisms that can produce layered structures similar to those observed in the nature. A field of turbulence in a strongly stratified fluid, far from boundaries, being supported by a Reynolds stress and having a non-zero vertical flux of buoyancy or density, may be unstable to variations in the vertical density gradient (Phillips 1972 [91]). The vertical diffusion of salt (or heat) is a strongly nonlinear process, and the relevant non-linear differential equation has initially unstable solutions under certain conditions. The properties of such solutions have been analysed in (Posmentier 1977 [93]) who numerically demonstrated the possibility of development of initially smooth salinity profiles into staircase-like structures. Thermohaline intrusions may also create such structures (Feodorov 1976 [23], Walsh and Ruddick 1998 [139]). Even a simple one-dimensional numerical model demonstrates how intrusions generate inversions<sup>3</sup> in temperature and/or salinity. The medium seems to evolve toward an equilibrium state characterised by a chain of “convecting” (and thus well mixed) layers separated by interfaces containing large gradients. The resulting structure thus has staircase-like vertical profiles of temperature, salinity and/or density.

A well-defined layered structure means that large gradients appear in some areas below called interfaces. In extreme cases, the behaviour of the derivatives of the temperature, salinity and/or density at the interface(s) resembles delta-like peaks. This feature makes the numerical studies of the formation of step-like stratification a particularly difficult problem. On the one hand, the onset of numerical instability may be interpreted as a (non-realistic) layer in the modelling process. On the other hand, too high numerical viscosity can artificially damp the layer formation. The described problem resembles well-known difficulties appearing in numerical solving of stiff systems characterised by extensive variation of the magnitude of different terms in the equations to be solved. The stability and reliability of the numerical scheme is a central prerequisite in the relevant studies.

---

<sup>3</sup> A reversal of the normal behaviour of the density in the ocean, in which a layer of more dense water is overlaid by a less dense layer. Under normal conditions the density usually increases with depth.

Paper IV and some related conference papers<sup>4</sup> focus on a specific mechanism of the formation of the layered structure, triggered by the joint influence of the double-diffusion and the turbulent mixing. The double-diffusion is a phenomenon that occurs in fluids with two constituents of greatly different molecular diffusivities (*e.g.* Ruddick and Gargett 2003 [102]). In the oceans, such constituents, which also affect the water density, are the temperature and salinity. The molecular diffusivity of temperature is by two orders of magnitude larger than the molecular diffusivity of salinity. Equivalently, on the molecular scale heat diffuses much more rapidly than salt.

There exist two options of initially stable stratification for two water masses with different temperature and salinity above each other. First, the overall stratification is stable when the upper layer is cooler but much less saline compared to warmer and more salty lower layer. The interface is unstable with respect to the highly diffusive constituent (*i.e.* heat) and the changes of water properties in its vicinity occur by the molecular diffusion of both heat and salt. The molecular diffusion causes density inversions (see Fig. 2.9.2) that lead to the corresponding release of potential energy within the inversion region and initiate the mixing process and formation of new (more or less uniformly mixed) layers. An interface of this kind is known as a diffusive layering (DL) interface.

Second, the upper layer may be more saline but warm enough compared to the relatively cool and somewhat fresher lower layer. The interface is unstable with respect to a substance of lower diffusion (*i.e.* salt) and long, narrow finger-like convection cells with rising and sinking fluid motions that carry buoyancy flux will be created. These interfaces are called (salt) finger (SF) interfaces (Turner 1973 [134], Turner 1995 [135]; Feodorov 1976 [23], Fernando 1989 [22]).

Many oceanographers expect that the double-diffusion has major effects on oceanic water masses and circulation. Although the double-diffusion becomes evident mostly in small scales and the resulting vertical structure of water masses may be not directly applicable in the analysis of large-scale processes such as the Rossby waves, several leading experts have the opinion that “double-diffusive fluxes produce significant effects on various large-scale features of the ocean” (Ruddick and Gargett 2003 [102]).

---

<sup>4</sup> Rannat, K., Heinloo, J., 1999. The staircase-like vertical structure of hydrophysical fields: the model and numerical scenarios. *Paper presented at the 24<sup>th</sup> EGS General Assembly, The Hague, 19–23 April 1999*; Rannat, K., Heinloo, J., 1999. Model of vertical transport in stratified turbulent environment, considered as rotationally isotropic. In: *Fourth workshop on physical processes in natural waters, Roosta, 13–17 Sept. 1999, Estonia, EMI Report Series*, 10, 1999, 15–18.

## 2.9. Modelling of layer formation

The object of study in Paper IV is a one-dimensional model that reflects several aspects of formation of the staircase-like vertical structure of the density field owing to the joint influence of the double-diffusion (called DD below) and turbulent mixing. The central problem is the choice of the numerical scheme and its parameters for a reliable description of the layer formation. The basic result consists in establishing the range of parameters for which the numerical scheme is stable. A series of preliminary numerical experiments demonstrating certain features of layer formation were also performed.

The model is developed by Dr. Jaak Heinloo in the framework of the analysis of the turbulent mixing by means of the theory of rotationally anisotropic turbulence (RAT, Heinloo 1984, 2004 [37, 38]). It is an extension of the model used in (Võsumaa and Heinloo 1996 [138]) and embraces both DL and SF regimes. The model is related to the models of Phillips (1972) explaining the layering process as a result of instability of a turbulence field with respect to variations of the vertical density gradient and to the model of Posmentier (1977) stressing the essentiality of transport processes of salt and heat.

The quantities under consideration are the nondimensional turbulent energy  $K(z,t)$ , salinity  $S(z,t)$ , temperature  $T(z,t)$  and density  $\rho(z,t)$ . Assuming that the state equation  $\rho = 1 - \tilde{\alpha}(T - 1) + \tilde{\beta}(S - 1)$  is linear, the model equations read (Paper IV):

$$\frac{\partial K}{\partial t} = b \frac{\partial}{\partial z} \left( K \frac{\partial K}{\partial z} \right) - K \left[ 1 + rb \left( \beta \frac{\partial S}{\partial z} - \alpha \frac{\partial T}{\partial z} \right) \right], \quad (12)$$

$$\frac{\partial T}{\partial t} = \frac{\partial}{\partial z} \left[ (a + bK) \frac{\partial T}{\partial z} \right], \quad (13)$$

$$\frac{\partial S}{\partial t} = \frac{\partial}{\partial z} \left[ (d + bK) \frac{\partial S}{\partial z} \right], \quad (14)$$

where  $b = ct_K^2 K_0 z_0^{-2}$  has the meaning of the coefficient of turbulent diffusion,  $t$  is nondimensional time,  $t_K$  and  $z_0$  are the characteristic time and vertical scale, respectively,  $K_0$  is the characteristic scale of the turbulent energy,  $r = gz_0 K_0^{-1}$ ,  $a = k_T^{mol} t_K z_0^{-2}$ ,  $d = k_S^{mol} t_K z_0^{-2}$ ,  $k_T^{mol}$  and  $k_S^{mol}$  are the coefficients of molecular diffusion of heat and salt, respectively,  $\tilde{\alpha} = \alpha T_0 \rho_0^{-1}$ ,  $\tilde{\beta} = \beta S_0 \rho_0^{-1}$ , and  $\alpha$  and  $\beta$  are the coefficients of thermal expansion and salinity contraction, respectively. The model thus contains five physical



constants  $\alpha$ ,  $\beta$ ,  $k_T^{mol}$ ,  $k_S^{mol}$  and  $g$ . The derivation and discussion of the equations is presented in Paper IV and the value of the semi-empirical constant  $c = 0.05$  is suggested based on theoretical considerations of (Simpson *et al.* 1996 [108]).

The qualitative evolution of the vertical profiles of temperature, salinity, kinetic energy and density in the framework of Eqs. (12-14) is sketched on Figure 2.9.1. If at the outset the water density monotonously increases with the depth, the factor in square brackets at the right-hand side of Eq. (12)

$$B = 1 + rb \left( \beta \frac{\partial S}{\partial z} - \alpha \frac{\partial T}{\partial z} \right) = 1 + rb \frac{\partial \rho}{\partial z} > 0. \quad (15)$$

The turbulent energy is thus damped by the stable stratification and the molecular diffusion described by Eqs. (13,14) dominates in the system. It generally results in changes of local gradients of  $S$  and  $T$ , and if it is intense enough, it may change the sign of  $B$  for some range of depths after some time. The situation  $B < 0$  corresponds to a strong density inversion (unstable stratification) in which  $\partial K / \partial t \approx -BK > 0$  and the turbulent energy fast increases (Eq. (12)). In the DL case, one layer with density inversion is usually formed above and another below the original interface (Figure 2.9.1a). In the SF case (Figure 2.9.1b) only one area of density inversion, which embraces the original interface area, is occasionally formed.

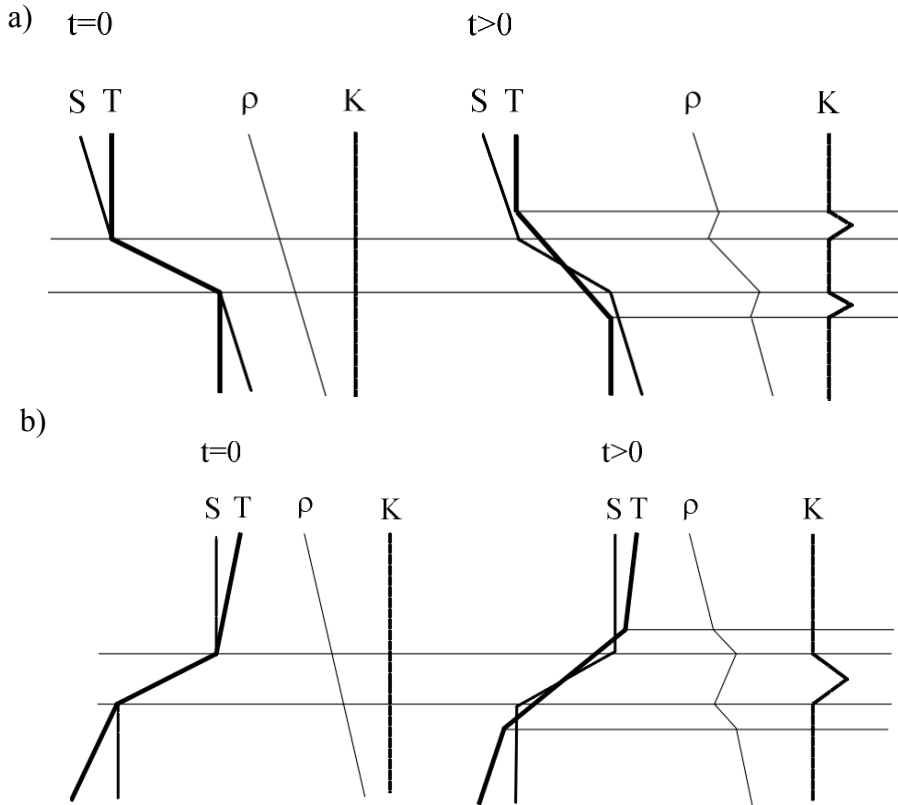


**Figure 2.9.1.** Evolution of the vertical profiles of temperature  $T$ , salinity  $S$ , density  $\rho$ , and turbulent kinetic energy  $K$  in the case of (a) the diffusive layering (DL) interface and (b) the salt finger (SF) -type interface.

The increase of  $K$  may resemble numerical instability but in fact it only reflects a rapid displacement (equivalently, intense mixing) of water masses in a certain sublayer. This process is accompanied by a fast decrease of  $\partial T/\partial z$  and  $\partial S/\partial z$  in this sublayer owing to Eqs. (13, 14). The quantity  $B$  soon becomes positive again and Eq. (12) implies a fast decrease of the turbulent energy in the layer where  $B > 0$ . The whole process can be interpreted as forming of a new mixed layer in the vicinity of the former interface. This layer is eventually separated from over- and underlying regions by new interfaces where the buoyancy gradients are big enough to suppress the turbulence energy.

This process may have a recurrent nature. After the turbulent energy has drastically decreased at the new interfaces, the double diffusion apparently becomes the governing process again and starts to initiate new inversions in the

density profile at the borders of the new mixed layer. Under favourable conditions the number of mixed layers will grow and the vertical profiles of  $\rho$ ,  $T$  and  $S$  may obtain a staircase-like shape.

The basic steps in establishing of what kind of numerical schemes are reasonable (numerically efficient and stable) for representing the layer-forming process governed by Eqs. (12–14) are described in Paper IV. The advantages of an explicit method, used in (Võsumaa and Heinloo 1996 [138]), consist in an almost trivial matrix inversion and a minimal number of arithmetic operations at each time step. They are counterbalanced by the stability and convergence conditions which impose severe restrictions on the time step. For that reason, we have used the implicit iterative method as recommended in (Stoer and Burlish 1993 [125]).

The stability criterion of discretized Eqs. (12–14) is studied in Paper IV for computations with the use of a regular time-space grid, with the time step  $\Delta\tau$  and the vertical step  $\Delta h$ . Its derivation is quite cumbersome but still straightforward. For the realistic maximum values of the turbulent kinetic energy and for typical values of temperature and salinity in the ocean, the ratio  $(\Delta h^2)/\Delta\tau > 0.01$  must hold.

A series of preliminary numerical experiments suggests that the layering process is only effective for a certain set of the parameters. For their many realistic combinations the layer-formation mechanism did not become evident within a reasonable computation time. However, in several cases it led to quite fast forming of new layers and interfaces (Figures 2.9.2–2.9.4). The essence of the model requires that  $0 < d \ll a \ll bK_{\max}$ , where  $K_{\max}$  denotes the maximum value of the turbulent energy. New layers only can be generated if the turbulent energy is initially nonzero; however, this is normally the case in natural conditions. The initial turbulent kinetic energy was set to constant  $K(z,0) = O(10^{-6})$ . The initial profiles  $T(z,0)$  and  $S(z,0)$  were chosen so that the fluid density varied linearly in the vertical direction but a thin interface layer with relatively large temperature and salinity gradients was located at the mid-depth of the computational domain.

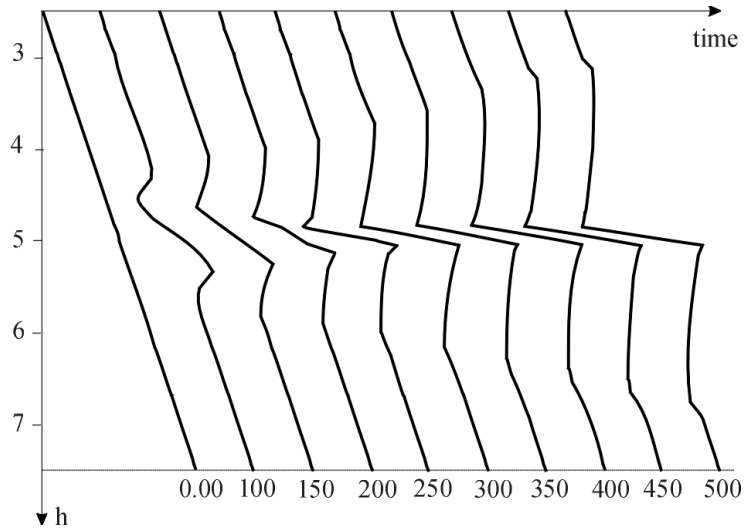


**Figure 2.9.2.** Temporal evolution of the vertical profile of water density.

For the following values of the physical parameters  $\tilde{\alpha} = 0.0003 \text{ K}^{-1}$ ,  $\tilde{\beta} = 0.0008 \text{ ‰}^{-1}$ ,  $k_T^{mol} = 1.3 \times 10^{-7} \text{ m}^2 \text{ s}^{-1}$ ,  $k_S^{mol} = 1.7 \times 10^{-9} \text{ m}^2 \text{ s}^{-1}$ , the molecular diffusion has generated inversion regions (represented by negative gradients of the density profile, Fig. 2.9.2), large enough to launch the turbulent mixing at  $t=100 \text{ s}$  (Fig. 2.9.3). The resulting mixing process forms two new well-defined mixed layers by  $t=500 \text{ s}$ .

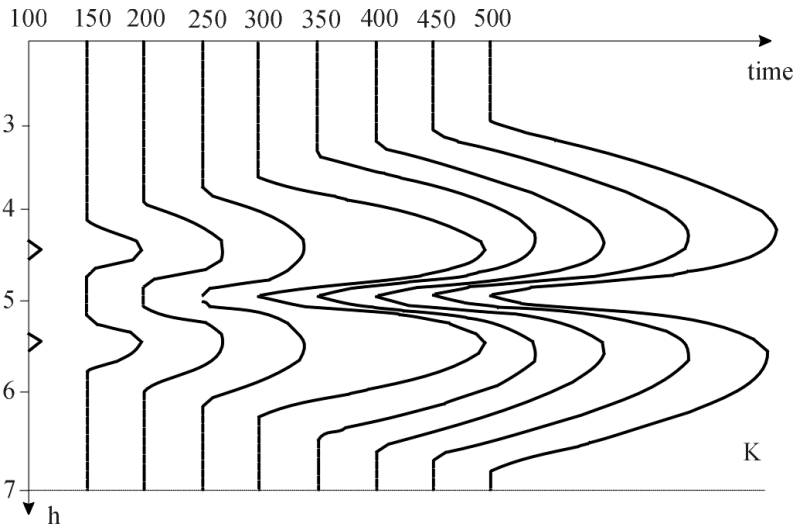


**Figure 2.9.3.** Temporal evolution of the vertical profile of the turbulent kinetic energy  $K$ .

The corresponding step-like structure can be identified also in salinity (Fig. 2.9.4) and temperature profiles.

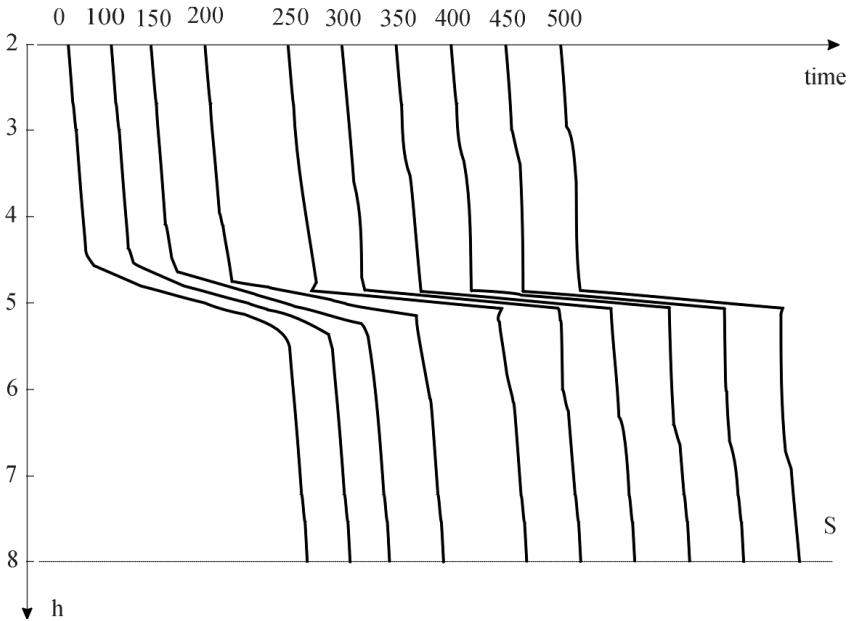


**Figure 2.9.4.** Temporal evolution of the vertical profile of water salinity.

The research in Paper IV and the presented numerical example serve as a first stage of the studies of the layer-generation mechanism described by Eqs. (12-14). For a certain set of realistic initial conditions the layered density structure is jointly generated by double-diffusion and turbulent mixing within an appreciable time. However, we were not able to identify which sets of parameters are the most favourable for large-scale layer generation process.

The experience with different sets of parameters and initial conditions suggests that the forming of such structures may have drastically different time scales in different regions, and that generally it is a long-term process. Validation of the relevant calculations against field or experimental data would be the next step for future research. Further studies are needed in order to establish what can be the thickness of the layers and how large can be the temperature, density and salinity jumps between the layers. The results obtained so far suggest that these studies require extensive computational efforts and are outside of the scope of this thesis. Research in this direction is clearly important, because as yet no modelling framework provides an integrated picture of DD-convection phenomena (Kerstein, 1999 [50]).

## 3. LONG WEAKLY NONLINEAR SURFACE WAVES

### 3.1. Kinetic theory in surface wave modelling

Many properties of nonlinear waves and their interactions have been studied in a most detailed manner for surface waves. These studies have a highly important practical output both in open sea where wind wave activity forms an important aspect of safety of marine transport and offshore structures, and in the coastal areas where wind waves are essential in many coastal engineering problems. In particular, the kinetic equation was first derived for surface waves by Hasselmann in 1962 [33]. Soon after this work, efforts towards spectral wave modelling were launched (The SWAMP Group 1985 [131], Komen *et al.* 1994 [55]).

The research on the properties of the surface-wave kinetic equation is much more complicated than in the case of Rossby waves because of (i) the complicated form of the dispersion relation for surface waves (which contains hyperbolic functions or, equivalently, a combination of exponents) and (ii) the occurrence of the 4-wave interaction. In particular, the analytical expressions for interaction coefficients for surface waves are extremely complicated (Krasitskii 1994 [57]). As a result, straightforward proofs of several properties of this equation as well as its numerical investigation are very complicated. The situation is largely the same today, and essential simplifications of the collision integrals are used in numerical wave models in order to obtain a reasonable performance (Komen *et al.* 1994 [55]).

Both the definitions of weak nonlinearity discussed in Chapter 1 have an important role in this chapter. The calculation of energy exchange owing to weakly nonlinear resonant interactions is a basic constituent of contemporary wave models, most of which are based on the Hasselmann's equation. One of such models, WAM cycle 4, has been used in studies of the wave climatology of the Baltic Sea and in the Tallinn Bay area (Soomere 2005 [121]). This and analogous wave models are based on specific solvers of the collision integral of the kinetic equation for surface waves. The difference from the studies described in Chapter 2 is that (i) realistic energy sources and sinks, and wave propagation is taken into account but (ii) only one wave mode is included into the equations. Numerical solving of the resulting forced-dissipative kinetic equation is out of the scope of this study, and the results concerning the wave regime in Tallinn Bay are taken from (Soomere 2005 [121]).

One of the major topics in this chapter is the influence of nonlinearity on wave-induced processes in shallow areas. Linear and kinetic approaches are widely used for description of surface waves and their interactions provided the wave height is small compared to the wave length and water depth. However, relatively long and appreciably high waves in shallow water cannot be correctly described within the linear theory. Their shape is no more sinusoidal and more

elaborated wave theories must be applied. As different from weakly nonlinear interactions where waves are supposed to satisfy the linear dispersion relation and nonlinearity becomes evident after a long time, now nonlinearity is intrinsically present in the equations describing the wave evolution, and may substantially affect the wave shape and properties.

### 3.2. Basic concepts of the linear surface wave theory

The major generating force for sea waves is wind that acts on sea-air interface and optionally disturbs the calm water surface. The gravitation serves as the restoring force that together with the laws of fluid motion govern the further behaviour of the disturbances that in most cases behave in the wavelike manner. Wave theories – approximations to reality – well describe some phenomena on the water surface provided the assumptions made in their derivation are satisfied. The numerical models of wave motion are usually based on simplified governing equations and boundary conditions. Their numerical counterparts may cause additional restrictions for practical applications. Solving the wave propagation problem exactly, involving all physical processes with the relevant temporal and spatial scales is still practically impossible.

The simplest surface wave theory is the so-called first-order, small-amplitude wave theory, developed by Airy (1845 [1]) and known as the linear theory. Many engineering problems can be easily handled with reasonable accuracy by this theory (Dean and Dalrymple 2004 [17]). However, the theory obviously fails in the cases, for example, where the wave crests are higher above the mean water surface than the troughs are below of it. For such asymmetric waves as well as for many other cases, more elaborated approaches have to be used, all of which contain certain elements on nonlinearity.

The simplest version of the linear theory of surface waves of appreciable length is based on a large number of assumptions: the fluid is homogeneous and incompressible ( $\rho = \text{const}$ ); the motion is irrotational, surface tension, viscosity and Coriolis effect are neglected; air pressure at the water surface is uniform and constant; the seabed is horizontal and rigid, fixed boundary and vertical velocity at the bed is zero; wave amplitude is small and waves are periodic plane or long-crested (1D) entities that do not interact with any other wave motions, only normal forces are important, shearing forces are negligible. These assumptions imply that the wave motion is governed by the Laplace equation (that is linear) with linearised boundary conditions and that the waveform is invariant in time and space.

The simplest surface wave of permanent form is a progressive linear wave propagating without experiencing any change in shape over a horizontal bottom. It is an infinite sequence of sinusoidal wave forms  $\eta(x, t) = a \cos(kx - \omega t)$  that move horizontally over the water. Here  $x$  and  $t$  stand for the spatial coordinate

and time, respectively. The linear wave form only depends the wave amplitude  $a$  and on the combination  $x$  and  $t$  called phase and defined as  $\Theta = kx - \omega t$ , where  $k = 2\pi/L$  is the wave number,  $L$  is the wave length,  $\omega = 2\pi/T$  is the angular frequency and  $T$  is the wave period. The phase velocity  $c_f$  (also called celerity) is the speed at which a wave form propagates – the speed of an individual wave in a group. The distance travelled by a wave during one period is equal to one wavelength, consequently,  $c_f = L/T = \omega/k$ . The wave energy propagates with the group velocity  $c_g = \partial\omega/\partial k$ . The energy  $E$  of a linear wave is proportional to the wave amplitude squared. This quantity is usually defined as the energy density per unit area or volume, averaged over the wave period. Its flux (wave power, also interpreted as the density of energy flux) is  $P = Ec_g$  and characterises the bulk power carried by the wave per unit of length of the wave crest (e.g., W/m). This description is generic for any kind of linear waves. The particular wave class is determined by the relation between the wave period (or angular frequency  $\omega$ ) and length (or wave number  $k$ ). This relation is called dispersion relation and it may involve several medium-specific parameters. An important feature of linear waves is that their amplitude is independent on other wave properties.

The dispersion relation for linear surface waves is  $\omega = \sqrt{gk \tanh kh}$ , where  $g$  is the acceleration due to gravity and  $h$  is the water depth. Their height is defined as  $H = 2a$  and their energy is  $E = \frac{1}{2}\rho g a^2$ . The dispersion relation is frequently given in terms of  $L$  and  $T$  as  $L = gT^2(2\pi)^{-1} \tanh(2\pi h L^{-1})$ . The hyperbolic tangent approaches to 1 for its large arguments and is approximately equal to its argument if the latter is small. Two practically useful approximations can be made based on this feature:

(i) *Deep-water approximation* is valid if  $kh \gg 1$  and  $\tanh kh \approx 1$ , that is, if the water depth  $h \gg L$  is much greater than the wave length  $L$ . The deep-water dispersion relation is  $\omega^2 = gk$ , while the phase and group velocities can be expressed as  $c_f = \sqrt{g/k} = g/\omega$  and  $c_g = c_f/(2\omega) = c_f/2$ , and the wave length  $L = gT^2/2\pi$ . This approximation is usually used when  $h > L/4$ .

(ii) *Shallow-water approximation* is valid if  $kh \ll 1$  and  $\tanh kh \approx kh$ , that is, the water depth  $h \ll L$  is much less than the wavelength. The dispersion relation simplifies to  $\omega = k\sqrt{gh}$ . The phase and group velocities can be expressed as  $c_f = c_g = \sqrt{gh}$  and the wavelength as  $L = T\sqrt{gh}$ . The wave speed is independent of the other wave properties and depends only on the water depth; therefore shallow-water waves are non-dispersive. This



approximation is usually used when  $h < L/11$ . Both approximations (i) and (ii) are accurate within 10% for the given limits of  $h$  and  $L$ .

For transitional water depths limited by  $1/25 < h/L < 1/2$  the phase speed can be expressed as  $c_f = gT(2\pi)^{-1} \tanh(2\pi h L^{-1})$ . The group velocity of waves propagating in deep or transitional water is smaller than the phase velocity. The interplay of the phase speed and the group speed can be vividly expressed with the use of an example from nature. An observer that follows a group of waves at group velocity will see waves that originate at the rear of the group, travel with the phase velocity and disappear at the front of the wave group. A wave field excited by a storm usually consists of waves with a wide range of frequencies. Stormy winds excite directly relatively short wave components while longer waves are gradually generated by resonant interactions. High and long waves thus only can develop if the storm blows long time from the same direction over a large sea area. The growth of the wind-generated waves is limited by breaking of shorter wave components whereas longer components may propagate over extremely large distances. Long waves have very small decrease when they propagate over water surface (Sorensen 1973 [124]). If an observer can stay reasonably far from the storm area then (s)he can notice the swell – relatively long waves that have propagated out from the area where they have been generated. Intense swell frequently occurs at the open ocean coasts but seldom dominates the wave regime in the Gulf of Finland or Tallinn Bay (Orlenko 1984 [79]).

In deep water the wind-generated waves are not affected by bottom bathymetry. Getting closer to the coastline, they start to lose part of the energy through near-bottom dissipation, the wave profiles become steeper and the wavelengths shorter. The dispersion relation of surface waves is such that the speed of propagation of a wave depends on its length: the longer waves propagate faster except in very shallow conditions where all the waves propagate with a constant speed. This feature is partially reflected in propagation of ship wave packages: the group of the longest waves first reaches the point of measurements.

Linear waves can be described also by certain dimensionless parameters such as the wave steepness  $H/L$  and the relative water depth  $h/L$ . The latter indicates whether waves are dispersive or not and whether the celerity, length and height are influenced by the water depth. Wave steepness implicitly indicates whether the linear assumption is valid. Large values of wave steepness correspond to situation where the linearity assumption may be questionable. The ratio  $H/h$  is called the relative wave height. Its large values also indicate that the small-amplitude assumption, a basic feature of linear waves, may be unacceptable.

An appropriate nondimensional parameter to characterise the nature of surface waves in shallow areas (where the wave height is an appreciable

fraction of the water depth) is the Ursell number – a combination of the relative wave height and the relative water depth (*e.g.* Massel 1989 [68]):

$$Ur = \left(\frac{L}{h}\right)^2 \frac{H}{h} = \frac{L^2 H}{h^3}. \quad (16)$$

The value of Ursell number is often used to select an adequate wave theory according to typical  $L$  (or  $T$ ) and  $H$  in a given water depth  $h$ . High values of  $Ur$  correspond to large, finite-amplitude, long waves in shallow water and suggest that the use of a nonlinear wave theory could be appropriate.

Natural wave fields are usually described in terms of (sometimes directional) wave spectra. In contemporary wave measurements and simulation the most important parameters – the wave height, period and, if directional properties are important, also the propagation direction – are obtained directly from measured or simulated spectra. The most common measure is the significant wave height  $H_S$  defined as the fourfold variance (standard deviation) of the water surface.

An estimate of the significant wave height  $H_S \approx H_{1/3}$  is defined as the average height of 1/3 of the highest waves. This can be estimated in various ways; for example, in Almagrundet data below it is found from the 10<sup>th</sup> highest wave in a record of about 10 minutes once an hour under the assumption that the wave heights are Rayleigh distributed (Paper III). The mean period is usually understood as the average period of waves over some time interval whereas the peak period is the period of the wave component with the largest amplitude.

### 3.3. Long nonlinear surface waves

For many coastal engineering tasks the non-linear models must be used as the waves cannot always be approximated as linear. For example, when waves of appreciable height travel into shallow water, higher order wave theories are often required to describe their behaviour.

The basic assumption of the linear wave theory is that  $ka \ll 1$  everywhere and  $a/h \ll 1$  in shallow water where  $kh \ll 1$ . For realistic finite amplitude waves these assumptions may become invalid. If  $ka \ll 1$  but not infinitely small, the equations and boundary conditions governing the wave properties can be expanded in a power series of  $ka$  (Stokes 1847 [126]). Different versions of the Stokes' theory that account for different number of terms in this expansion are used for short waves in deep water (Massel 1989 [68]).

For limited depths, the Stokes wave theory can be used provided the Ursell number is relatively small. Dean and Dalrymple (2004 [17]) suggest that the Stokes theory is only meaningful provided  $Ur < 8\pi^2/3 \approx 25$ . Massel (1989

[68]) expresses the opinion that when  $Ur \approx 1$  and  $L/h > 8-10$ , both the linear and the Stokes theory are useful in many aspects, even in some cases when the condition  $ka \ll 1$  is violated, and that the Stokes wave theory can be used up to  $Ur \approx 75$  in some cases. For even larger Ursell numbers (resp. for longer or higher waves, or for lesser depths) the Stokes wave theory is generally incorrect (Massel 1989 [68]).

The necessity to switch from the linear and/or Stokes description to another framework becomes evident in the analysis of properties, behaviour and influence of long components of surface waves. For storm waves in the Baltic Sea and in the Gulf of Finland that typically have periods of 5–6 s (Kahma *et al.* 2003 [47], Pettersson 2001 [88], Paper III), the threshold  $Ur \approx 75$  occurs for 1 m high waves at a depth of 1–2 m ( $Ur \approx 25$  at 3–4 m), and for a 3 m high wave at a depth of 3–4 m ( $Ur \approx 25$  at 6–7 m). Therefore, for storm waves the Stokes' theory can be applied up to the depth where the wave height is around 80% of the water depth, that is, practically up to the wave breaking. The typical storm waves in the coastal zone of Tallinn Bay are short enough to use the Stokes' approximation outside the surf zone.

For long-period open ocean swell and for waves from fast ferries the situation is different. The period of a typical wave from a fast ferry in the Tallinn Bay area is 10–15 s (Paper V). The length of a wave with a period of 10 s is  $L \geq 30\sqrt{h}$  m; thus water with depth  $h \leq 10$  m can be already considered as shallow. The Ursell number for such a wave in the coastal area ( $h \approx 3$  m) is  $Ur \approx 100H$  and already ship waves of moderate height ( $H \approx 0.5$  m) correspond to  $Ur \approx 50$ . Consequently, Stokes description clearly fails for even longer or higher ship waves that frequently occur in the area in question (Papers II, V), or for lesser depths.

An appropriate model for long finite-amplitude surface waves in shallow water is the Korteweg-de Vries (KdV) equation (Massel 1989 [68]). Its periodic solutions are called cnoidal waves, because they can be explicitly expressed in terms of so-called cnoidal (Jacobi elliptic) functions. This theory is based on the Boussinesq approximation and includes nonlinearity and dispersion effects but is restricted to waves progressing in one direction only. Cnoidal waves have more narrow crests, and more broad troughs than sine waves (Figure 3.3.1). The cnoidal wave theory is applicable provided  $L/h > 8-10$  and the Ursell number  $Ur > 20$  (Massel 1989 [68]).

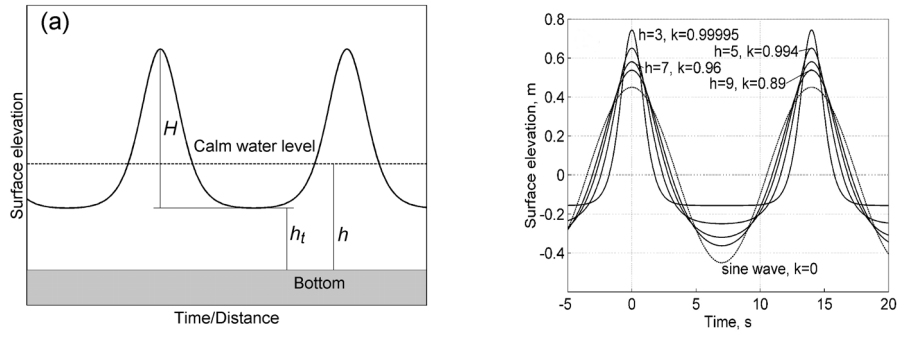


**Figure 3.3.1.** Sketch of a typical cnoidal wave profile (left); profile of a sine wave with 14 s period and a height of 0.9 m compared with the profile of cnoidal waves of the same height and length but propagating in water with a depth of 3–9 m.

If the wavelength infinitely increases, the period of the Jacobi elliptical functions also infinitely increases and their modulus  $k \rightarrow 1$ . For  $k = 1$  the cnoidal wave theory reduces to the theory of KdV solitons. For another limiting case  $k = 0$  the cnoidal wave approaches the sinusoidal wave. This happens if the wave height is small compared to water depth.

### 3.4. Wind wave observations and modelling in the Baltic Sea

Many Baltic Sea countries have performed extensive wave studies in the past and have implemented operational wave models nowadays. Contemporary wave measurements in the northern Baltic Sea were launched about three decades ago when several measurement devices were deployed in different parts of the sea. In particular, bottom-fixed devices were installed and operated by the Swedish Meteorological and Hydrological Institute (SMHI) near the caisson lighthouse of Almagrundet located in the western sector of the northern Baltic Proper, 59°09' N, 19°08' E (Fig. 3.4.1). The wave data from this site form the main object of study in Paper III.

An important step towards understanding open-sea wave conditions in the northern Baltic Proper (NBP) was made when the Finnish Marine Research Institute deployed a directional waverider there at a depth of about 100 m (Fig. 3.4.1, 59°15' N, 21°00' E, Buoy 1). The relevant data set now covers 10 years, starting from September 1996 but excluding ice seasons. The highest waves at this location ( $H_S = 7.7$  m) were recorded on 22 December 2004 ([www.fimr.fi](http://www.fimr.fi)). The significant wave height has exceeded 7 m only four times at this site: twice

in December 1999 and twice within three weeks – on 22 December 2004 (when the largest single wave ever recorded in the NBP has been registered with a height of 14 m) and on 9 January 2005 during windstorm Gudrun. The peak periods during these events slightly exceeded 12 s. An overview of wave statistics in the northern part of the Baltic Sea is presented by (Kahma *et al.* 2003 [47]).



**Figure 3.4.1.** Wind wave observation sites in the northern Baltic Proper (left panel), the Gulf of Finland (upper right panel) and in the vicinity of Tallinn Bay.

Unfortunately, hardly any instrumentally measured wave data are available from the coastal areas of Estonia, Latvia and Lithuania, except for visual observations from the coast and for sporadic measurements made with pressure-based sensors (Soomere 2005 [121]). Older publications such as (Rzheplinsky and Brekhovskikh 1967 [103]) are obsolete. The books published in the former Soviet Union (*e.g.* Davidan *et al.* 1985 [16]) contained valuable wave data but were available only in Russian language and discussed wave properties in certain regions only. This makes it virtually impossible to identify basic features of the spatial distribution of wave properties in the Baltic Proper from the measured data.

This gap has been partially filled by the use of numerical models that adequately represent the sea state of the northern Baltic Sea even in extreme conditions (*e.g.* Tuomi *et al.* 1999 [132], Soomere 2001a [115], Jönsson *et al.* 2002, 2005 [43,44]). The overall picture of wave activity follows the well-known anisotropy of the wind and wave regime in the Baltic Proper (Mietus

1998 [71], Soomere 2003 [117]). Statistically, the regions of the highest wave activity are found along the eastern coasts of the Baltic Proper. These areas are characterised by long fetches for the dominant winds and, consequently, the highest and longest waves of the northern Baltic Proper apparently occur in the vicinity of the entrance of the Gulf of Finland.

### 3.5. Trends and extremes in wave fields of the Baltic Sea

The longest regular wave measurements in the northern Baltic Sea have been carried out in 1978–2003 by the Swedish Meteorological and Hydrological Institute near a caisson lighthouse of Almagrundet (Fig. 3.4.1, Mårtensson and Bergdahl 1987 [69]). The extreme wave conditions and long-term trends of surface wave heights based on this data set are analysed in Paper III.

Wave properties at this site are determined with the use of data from an inverted echo-sounder and based on the classical zero-downcrossing method (IAHR 1989 [40]). An estimate of the significant wave height  $H_{1/3}$  (defined as the average height of 1/3 of the highest waves during a certain time interval) is found from the 10<sup>th</sup> highest wave in a record of about 10 minutes once an hour under the assumption that the wave heights are Rayleigh distributed. The significant wave height  $H_S \approx H_{1/3}$  is defined as the fourfold variance of the water surface (IAHR 1989 [40]). The highest  $H_{1/3}$  at this site was 7.82 m in January 1984 (Paper III; some sources mention the value  $H_S = 7.7$  m, e.g. Kahma *et al.* 2003 [47]) whereas the mean period (which generally is slightly less than the peak period) reached 11 s. This is formally the largest significant wave height ever instrumentally recorded in the Baltic Sea. This storm is the only one recorded at that site when  $H_{1/3} \geq 7$  m was registered.

The data for the years 1979–95, the period for which the data are the most reliable, show a linear rising trend of 1.8% per annum in the average wave height. The seasonal variation in wave activity follows the variation in wind speed. The monthly mean significant wave height varies from 0.5 m in May–July to 1.3–1.4 m in December–January (Paper III).

The most important conclusion in the context of the studies of ship-induced waves below is that typical mean wave periods are 4–5 s for wave heights below 1 m, about 6 s for wave heights around 2 m, and exceed 7 s only when wave heights are 3 m or higher. Note that the data set in question contains the mean period whereas the majority of other data sets and numerical simulations rely on the peak period. The corresponding values of the peak period, found from the recorded wave spectra, are about 20% larger than the mean period; however, not all spectra have a clear peak.

Long waves with periods over 10 s dominate in the wave field only in a few cases. This usually happens in the case of swell-dominated low wave conditions when the wave height  $H_{1/3}$  is well below 1 m. Large mean periods may also occur during extremely rough seas. For example, the mean period reached 11 s in one case of rough seas with  $H_{1/3}$  around 4 m, and also in the final stage of the January 1984 storm, when waves with periods 11 s dominated the wave field with  $H_{1/3}$  about 7 m.

### 3.6. Wave properties in the Gulf of Finland and in Tallinn Bay

There exist high-quality wave data sets measured by the FIMR starting from 1970s in areas surrounding Finland (Kahma *et al.* 1983 [45], Kahma and Pettersson 1993 [46], Pettersson 1994 [87], Pettersson 2001 [88], Kahma *et al.* 2003 [47]). A directional waverider has been deployed off Helsinki where measurements have been made in 1990–91, 1994 and from November 2001 at the location of buoy 2 in Fig. 3.4.1 (59°57.9' N, 25°14.1' E, water depth about 60 m) during the ice-free seasons. The highest  $H_s = 5.2$  m in the Gulf of Finland was measured at this site in November 2001 during a strong NNW storm (Pettersson and Boman 2002 [89], cf. hindcast for the Tallinn Bay area in Soomere 2005 [121]). The peak periods  $T_p$  reached 11 s during this event in the Gulf of Finland but were less than 10 s in Tallinn Bay.

Early wave measurements in the Gulf of Finland have suggested that the peak periods are typically 4–5 s in this area, reach 8–9 s in the roughest seas, and usually do not exceed 10 s (Kahma and Pettersson 1993 [46]). More recent observations indicate that  $T_p \approx 11$  s may occur in this area (Pettersson 2001 [88]). Yet the rough seas, with  $H_s \sim 4$  m, have peak periods of about 8–9 s. The number of observations of larger peak periods is very small: peak periods of 11 s only occurred three times during measurements in 1990–1994; since wave properties have been recorded once an hour, these three cases may reflect one event. Peak periods were also close to 11 s for a short time during the very strong storm in November 2001. The distribution of frequency of occurrence of different peak periods in (Pettersson 2001 [88]) suggests that  $T_p \geq 10$  s usually correspond to penetration of long-period swell of moderate height from the Baltic Proper to the Gulf of Finland (Paper III).

Only a few instrumentally measured wave data are available from the coastal areas of Estonia (Orlenko 1984 [79], Soomere 2005 [121]). Wave conditions in the recent exceptional storm Gudrun (Soomere 2006 [123]) were measured by a pressure-based wave sensor near the Island of Naissaar (buoy 3 in Fig. 3.4.1).

Although the wave and wind observations in Tallinn Bay extend back to 1805 (Soomere 2005 [121]), these visual data only represent the wave properties adequately in the immediate proximity of the Tallinn harbour (Orlenko, 1984 [79]). For example, the swell is often noticed in the western entrance to the bay and at the area of Miiduranna, but it only seldom reaches the Tallinn Harbour area.

The results of the above-described measurements in the Baltic Proper and in the Gulf of Finland cannot be directly extended to the Tallinn Bay area because of its extremely complex geometry and bathymetry. For that reason the basic features of the local wave climate, necessary for comparison of the properties and influence of ship and wind waves, were modelled with the use of the WAM model. This model, generally known as a deep-water ocean wave model, was verified in the area in question with the use of the measurements described in Paper V. Comparison of the modelled and observed data confirmed that this model can be used in the Tallinn Bay conditions up to a distance of 200–300 m from the coast and up to the depth of around 5 m (Soomere, 2005 [121]). The basic reason for such a favourable feature is that the waves in the Gulf of Finland area are relatively short and that the limited depth effects become evident only in very shallow areas.

The dimensions of Tallinn Bay are about  $10 \times 20$  km. Its wave regime is mostly governed by the interplay of the local geometry and winds in the northern part of the Baltic Proper and in the western part of the Gulf of Finland. The dominating winds in this area blow from southwest or northwest whereas strong west and east winds also frequently blow along the axis of the Gulf of Finland (Soomere and Keevallik 2003 [120]). Since Tallinn Bay is well sheltered for the eastern and southern winds, waves during such winds are small and short owing to short local fetch. The bay is partly protected from the western side by the island of Naissaar. The highest waves generated in remote areas can therefore only enter the bay from the North-West and North, or from West through the strait between Naissaar and the mainland (Soomere 2005 [121]). The northernmost part of the bay between Aegna and Naissaar is frequently affected by waves generated in other parts of the Gulf of Finland; however, they usually do not penetrate into the bay interior.

Strong long-lasting western winds are infrequent in the Gulf of Finland (Soomere and Keevallik 2003 [120]). The wave heights and periods during the northern and NW storms remain relatively small as the width of the gulf between Tallinn and Helsinki is 50–80 km in this area. The listed features suggest that high and long waves are infrequent at the coasts of Tallinn Bay. This is confirmed by both numerical analysis of the wind wave regime (Soomere 2005 [121]) as well as by observed wave field properties during experiments described in Paper V. The wave regime of Tallinn Bay follows the general properties of the wave fields in the Baltic Sea. It has significant annual variation, with a relatively stormy autumn and winter period and a calm spring and summer season. The wave regime also exhibits a strong spatial variability.



The reason is that the banks and shallow areas located at the entrances of the bay shelter certain parts of the bay from northern and western winds. A part of their effect is indirect: topographical refraction of longer waves at their underwater slopes redirects a part of the waves so that less wave energy enters the inner parts of the bay.

The highest waves occur in the vicinity of Tallinn-Helsinki ship line where significant wave height exceeds 2 m each year and may reach 4 m in extreme NNW storms. Quite rough seas may occur in the central part of the bay during extreme NW storms and at the western entrance during strong west storms (Soomere 2005, 2006 [121, 123]). Yet high waves occur infrequently and the wave climate is relatively mild compared to that in the open part of the Gulf of Finland (Soomere 2005 [121], Orlenko 1984 [79]). Both the wave heights and periods are usually moderate. The significant wave height  $H_S$  only exceeds 1 m if the mean wind speed exceeds  $10 \text{ m s}^{-1}$  during a few hours. The mean wave periods are 3–4 s in such wind conditions but a swell with a typical frequency of 4–5 s may appear if such winds persist at least 4–5 hours. Gales with the wind speed exceeding  $14\text{--}15 \text{ m s}^{-1}$  result in  $H_S \approx 2 \text{ m}$ . The wave periods vary largely according to the duration of the gales but the mean period normally does not exceed 4–5 s. Since swell of substantial height can enter into the bay only from the west, swell-dominated wave fields infrequently appear after strong storms. Wave fields with  $H_S > 1 \text{ m}$  only appear with a probability of about 1% whereas the peak periods remain well below 10 s even in the strongest storms.

## **3.7. Ship waves in Tallinn Bay**

### **3.7.1 Possibilities of description of ship waves**

When a ship passes through water surface, it produces a series of waves that are limited in both space and time, and are called ship wake. The properties of ship waves in the framework of the linear wave theory in an inviscid sea and without surface tension are well known (see, e.g., Lamb 1997 [58], §256, or Lighthill 1978 [62], §3.10). The stationary ship wave pattern in deep water is located within a triangular area past the ship and is independent of the ship's speed. It consists of one set of waves that move forward and out from the disturbance (diverging waves), and the other set of waves move in the direction of the disturbance (transversal waves, Fig. 3.7.1.1). The highest waves are found at the borders of the area filled with ship waves. The periods of the highest ship waves are roughly proportional to the ship speed (Sorensen 1973 [124]); consequently, the length of the highest ship waves also increases with the increase of the speed.

Navigational speeds in water of finite depth are distinguished according to the depth Froude number  $F_d = v/\sqrt{gh}$  that is the ratio of the ship speed  $v$  and the maximum phase speed of surface gravity waves. Generally, the effects of a finite depth become evident when the wavelength twice exceeds the water depth. For the highest diverging waves this corresponds to about  $F_d \approx 0.69$  and for transverse waves at the sailing line to about  $F_d \approx 0.56$  (Sorensen 1973 [124]). Therefore, at depth Froude numbers above 0.55–0.7 the ship-generated wave system should respond to the water depth.

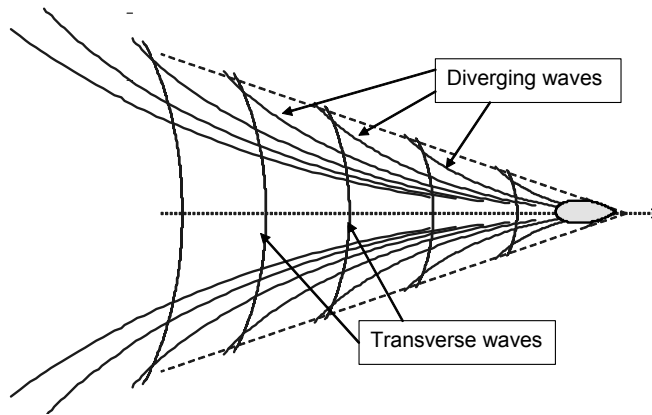


**Figure 3.7.1.1.** Wave crest pattern generated by a point pressure disturbance moving over deep water.

Operating at speeds resulting  $F_d < 1$  is defined as subcritical, at  $F_d > 1$  as supercritical and at  $F_d = 1$  as critical. There is a relatively wide transcritical speed range  $0.84 < F_d < 1.15$  in realistic conditions, where no clear distinction between sub- and supercritical regimes is possible (Hüsig *et al.* 2000 [39]). The ship wave pattern widens for increasing Froude numbers below 1 whereas the leading diverging waves become gradually long-crested and more accentuated compared with other wave components (Sorensen 1973 [124]). The wave heights increase particularly rapidly if  $F_d \rightarrow 1$ . Ships sailing at transcritical speeds may produce fundamentally different wave systems compared to conventional ships (Chen and Sharma 1997 [13], Guidelines 2003 [26], Sorensen 1973 [124]).

The waves from high-speed ships, in particular on the open sea, are relatively small in terms of wave amplitude compared to storm waves, but may have a very long wave period (Kirk McClure Morton 1998 [51], Kofoed-Hansen and Mikkelsen 1997 [54], Parnell and Kofoed-Hansen 2001 [83],

Whittaker *et al.* 2001 [142]). While frequently hardly visible in deep water like tsunamis, they have occasionally been found to cause violent impacts on the coast and energetic plunging breakers on beaches (Guidelines 2003 [26], Hannon and Varyani 1999 [30], Kirk McClure Morton 1998 [51], Kofoed-Hansen and Mikkelsen 1997 [54]). Since the wave height increases proportionally to the square root of the changes of the group velocity (Dean and Dalrymple 2004 [17]), wind waves, possibly having larger amplitude in deep water but often clearly shorter wavelengths undergo a much smaller amplification in the shallow coastal zone.

The motivation for detailed studies of features of the ship waves in Tallinn Bay comes from the fact that the periods of the highest waves excited by high-speed ships (10–15 s) are much longer than typical periods of wind waves (<6–7 s) in this area. Therefore, ship waves serve as a new component of hydrodynamic activity in this bay since natural waves with similar properties probably do not exist here even during strong storms. The longest ship-induced waves, with the length of about 100 m, also have considerable heights. They cannot be considered as linear in shallow water. The most important outcome from this fact is that the wakes may have significantly larger impact on the affected area than predicted by the linear theory (Paper VI).

The central objects of study in Papers II, V, and VI are (i) the properties of waves from high-speed ships in the coastal area of Tallinn Bay, (ii) their potential difference from the typical parameters of wind waves in this area, and (iii) the corresponding environmental effects. The name “high-speed ships” stands here for the ships that are able to sail in the transcritical regime along the fairway of Tallinn Bay; among which the large car-carrying high-speed ships are called fast ferries. The investigation is based on numerous field experiments in different coastal areas of Tallinn Bay. The comparison of waves of different origin is mostly performed with the use of numerically estimated parameters of wind wave climate of Tallinn Bay.

The studies described in Chapter 2 have been focussed on the ‘very’ weak non-linearity which only contributes to wave evolution in the long-term run. It was assumed that wave shape, properties and propagation features coincide with those of perfectly linear waves. This assumption, which frequently is not explicitly mentioned in the description of the kinetic theory, implicitly means that wave amplitudes have to be small. For description of spectral evolution of storm waves, violation of this assumption apparently is not essential, because the wave model based on the kinetic approach shows good results also for rough windseas where wave amplitudes and steepness are substantial. Another basic assertion in the kinetic theory is that the wave field consists of a large number of wave harmonics that are spread over large sea areas. Ideally, the kinetic theory even assumes that the wave systems have a continuous spectrum. Additionally, the kinetic equation is only valid when group velocities of resonantly interacting waves are different.

The listed assumptions are violated for ship wakes. In many cases of practical interest they have considerable heights, are concentrated in spatially localised wave groups and, in particular in shallow water, have nearly equal group velocities. Therefore, generally they cannot be considered as a part of the surface wave system in the kinetic approach. Formally, the structure of a ship wake can be examined with the use of the Fourier analysis. This technique allows identifying different wave components of the wake. Yet doing so is not always justified because a ship wake is a system of transient waves occasionally containing even solitary waves (Chen and Sharma 1997 [13], Sorensen 1973 [124]). For that reason, methods enabling analysis of single components of ship wakes generally have to be used in their analysis.

### **3.7.2. Properties of ship-generated waves in the Tallinn Bay area**

Extensive field studies of both wind wave and ship wave properties in Tallinn Bay are described in Paper V. The main goal was to identify the typical and extreme parameters of wake waves of different types of ships and to describe their potential influence in different coastal areas of the bay. Nearly 1000 ship wakes were traced during about 200 hours on 15 days. In the frame of the studies, only the properties of wakes necessary for estimates of the bulk influence of ship waves on coastal processes of Tallinn Bay have been analysed. Many other important questions, for example, the dependence of the properties of wakes on the navigation details (vessel speed, distance from the ship track, ship load and vessel trim), were not considered.

Since the periods of waves generated by fast ferries may vary from 3 s up to 40 s (Kirk McClure Morton 1998 [51]; Kirkegaard *et al.* 1999 [52]), appropriately positioned pressure sensors can be used for description of their basic parameters. During the field experiments in 2002, the wave properties were measured in areas with the depth of about 5 m in different parts of Tallinn Bay and at different distances (2–8 km) from the ship lane (Paper V). The wave recorder SBE26 (Sea-Bird Electronic) was positioned at the depth of 2–2.5 m in the water column in order to adequately represent even the largest waves. This configuration allows to trace wave components with the periods  $>1.5$ –2 s. This resolution is also suitable for wind wave measurements in the case of moderate and strong winds when wave energy is mostly concentrated in components with larger periods.

The study of the recordings comprised an analysis of the raw pressure signal (from which the longest waves are identified with the use of the zero-upcrossing analysis, IAHR 1989 [40]), spectrally filtered pressure signal, water surface time series (reconstructed on the basis of the Fast Fourier Transform method) and spectral properties of the wave field. The details on the measurement technique and sites are described in Paper V. The estimates of the relative role

of ship waves (based on both the experimental data and numerically estimated natural wave) in wave climate and a comparison of the influence of waves of different origin are described in Paper II.

The measurements were performed during spring and summer seasons. This period contains the most intense navigation of fast ferries. Also, the relatively mild weather conditions were favourable for experimental work: less background noise from wind waves to be filtered out, and it was easier to operate with the experimental setup in calm seas. The structure of wake patterns of different ships is analysed and the maximum and mean values as well as the spatial variability of the wake heights of fast ferries are described. As a new development in the ship wave analysis, the daily average frequency spectra of wakes have been constructed (Fig. 3.7.2.1). The extensive wave measurements in Tallinn Bay give also an impression of wind wave properties for different wind conditions and the general features of natural wave fields during the relatively calm spring and summer season.

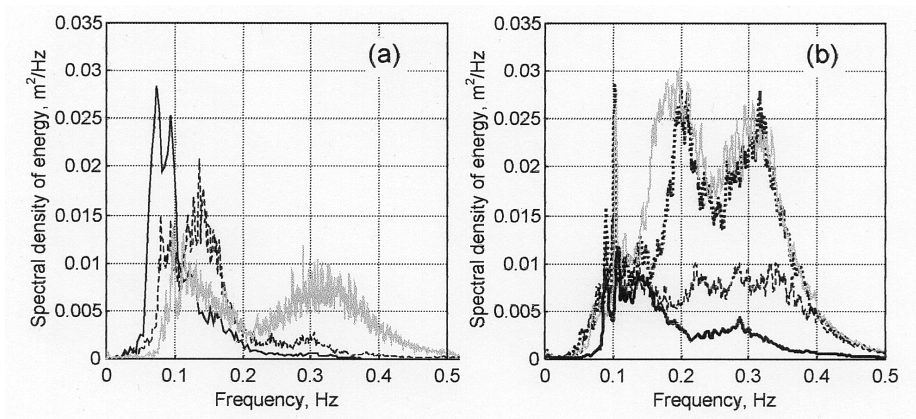


**Figure 3.7.2.1.** (a) The daily average spectral energy density at Aegna jetty on 14.04 (solid line), at Pringi jetty 12.05 (dashed line) and at the Viimsi museum on 31.05–01.06 (grey line). (b) The daily average spectral energy density at the western coast of Aegna on 17.07 (dotted line), on 18.06 (dashed line) and on 20.06 (grey line), and at Naissaar harbour on 06–08.08 (bold line).

The wakes of hydrofoils is practically indistinguishable from the natural background even on calm days. The wakes of conventional ferries were very similar to natural waves occurring in typical wind conditions of Tallinn Bay; since their heights are smaller than the heights of storm waves, such wakes do not present any specific features or influence compared with the natural background. For that reason, we only describe properties of wakes from fast ferries in what follows.

Waves caused by fast ferries generally are higher than those excited by hydrofoils or conventional ferries. Yet their heights are usually moderate. The daily highest examples are about 1 m in several sections of the eastern coast of Tallinn Bay. The typical heights increase with the distance from the harbour and are the largest at the coasts of Aegna. The heights of waves generated jointly by two or three ships (optionally, in a superposition with a background wind wave field) may reach in extreme cases 1.7–2.3 m at the 5 m isobath of the eastern coast of Tallinn Bay. In the remote areas such as the nearshore of Naissaar their height usually does not exceed 70 cm.

The fast ferries' wakes usually have a group structure in the coastal area (Paper V). A wake arrives the eastern coast of the bay (about 2–3 km from the ship lane) approximately 10 min after a ship has passed. Its total duration is about 10–15 min. The majority of the wave energy of fast ferries' wakes is concentrated in two parts. The fragments are well separated in both time and space domain but also in the spectral domain (Figure 3.7.2.2 and Figure 3.7.2.3). The first one is the group of leading waves that have typical periods of 10–15 s and lasts about 3–5 minutes. These waves usually are the highest and have the largest periods. Their daily maximum height at a depth of 5 m is 80–108 cm, depending on the site. Such waves extremely seldom exist in natural conditions in the area in question.

The highest leading waves have been measured near Aegna jetty in relatively deep (6.7 m) water (Figure 3.7.2.4). Theoretically, this area may be hit by large waves generated by ships sailing at transcritical speeds. The number of wave crests with the heights close to 1 m may be many tens per day in certain parts of the coast. The typical height of the highest waves from individual wake patterns, however, is moderate and in most cases equals to 60–80 cm. In a more remote coastal zone of Naissaar (about 8 km from the ship lane) the leading waves arrive several tens of minutes after a ship has passed. Their maximum and typical height is ~50 and 20–30 cm, respectively.

Another energetically important wake component consists of the waves of the second wave group arriving a few minutes after the leading waves. Their periods (7–8 s, at times up to 10 s) and amplitudes are generally less than those of the leading waves. However, the bulk energies of these groups are comparable with each other.

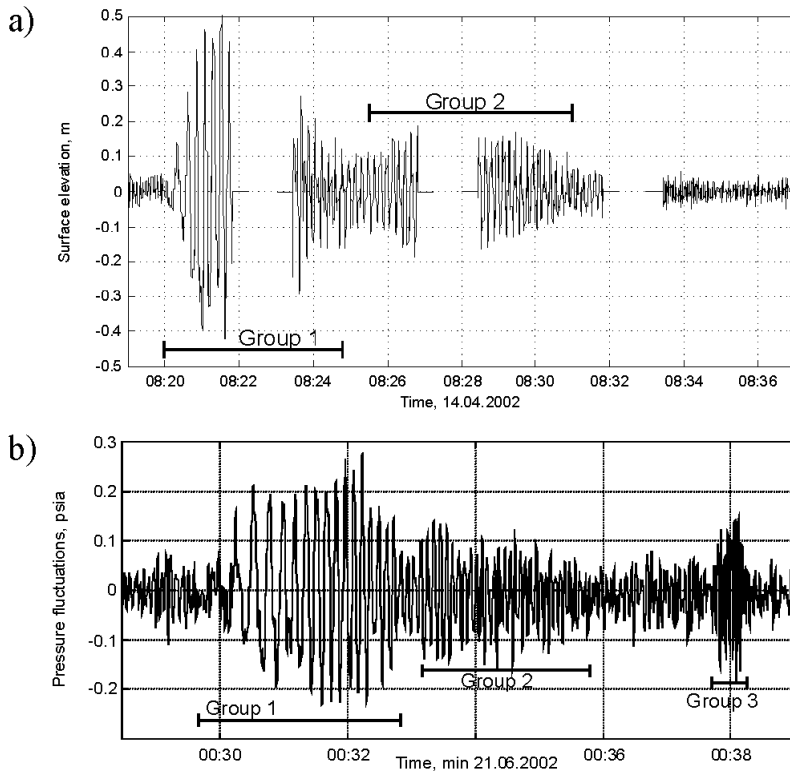


**Figure 3.7.2.2.** (a) Waves generated by AutoExpress/2 near Aegna jetty with two well-defined groups of waves. (b) Pressure fluctuations caused by the wake of SuperSeaCat IV near the western coast of Aegna at 00:27–00:39 on 21.06. The first wave group has the maximum height of 45 cm, the second group – of 25 cm. The highest is the third group (52 cm). The significant height of the natural wave background is about 30 cm. The wave height derived from pressure signal depends remarkably on the wave frequency. This is the reason why relatively small-amplitude pressure signal of shorter waves corresponds to relatively large wave amplitudes.

The closing part of a wake optionally consists of short and steep waves with periods of 3–4 s. They may arrive much later than the leading waves. In a few cases (more frequently at Naissaar) they are the highest part of a wake pattern. The duration of this segment is about one minute. It consists of about ten to fifteen wave crests. It carries a small fraction of the total wake energy but may remain compact during a long time. Owing to its small wavelengths, it may penetrate into the vicinity of the shoreline and is visually easily detectable. The actual mechanism of their generation is not clear (Brown *et al.* 1989 [11]). Since it contains relatively steep waves, in certain conditions it is the most dangerous group for the small boat traffic.

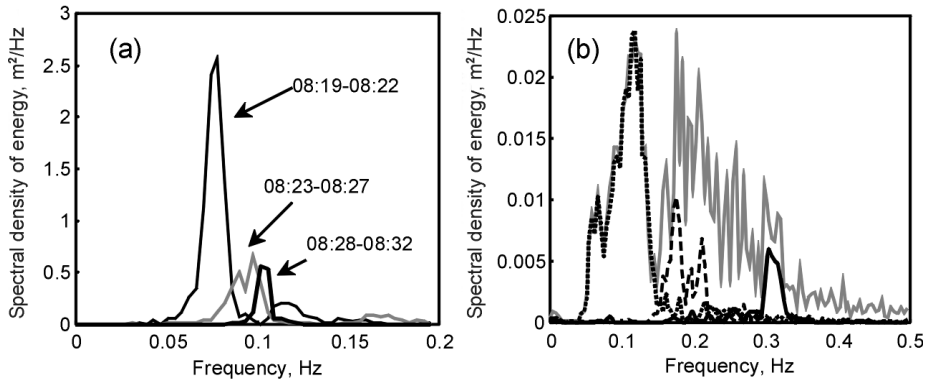


**Figure 3.7.2.3.** (a) Spectral density of energy for the wave groups of Autoexpress/2 from Fig. 3.7.2.2a. The highest waves leading the wake had periods 13–14 s and the final part – about 9 s. The spectrum of waves at 08:33–08:39 represents the natural wave background and is not distinguishable in the scale of the figure. (b) Spectral density of the energy of three wake pattern components of SuperSeaCat IV near the western coast of Aegna at 00:05-00:39 on 21.06 (see Fig. 3.7.2.2b). The dotted line represents the first wave group, the dashed line – the second group and the bold line – the third group. The grey line describes the spectrum of the whole wave field. The long wave components have the dominating periods about 16 s and 9–10 s. The wake is superposed by a relatively intense mixed wave field with the significant wave height about 30–35 cm and the mean period about 4 s. Although the group of short waves has a duration of only 1 minute from the 34-minute trace, it is still clearly visible in the wave spectrum as a double peak at the frequency of about 0.3 Hz.

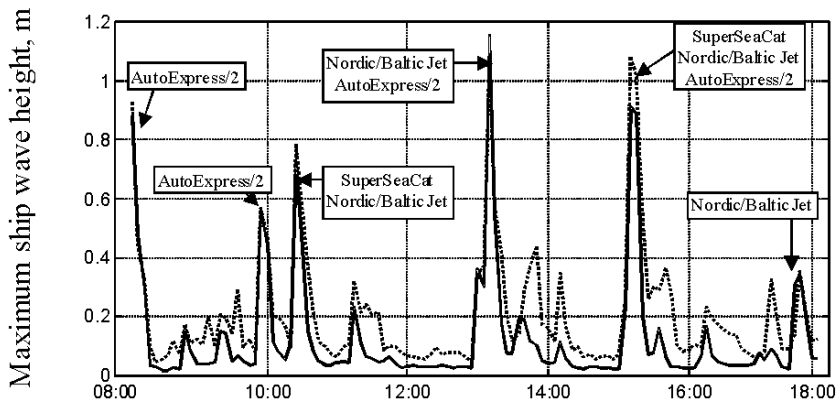


**Figure 3.7.2.4.** Heights of the long-wave components (periods  $> 8$  s; bold line) and the whole wash of fast ferries (dotted line) near the island of Aegna, 14.04.2002. Names of ships are indicated for several peaks.



The comparison of the natural wave climate with the results of the described studies of ship wave properties leads to some impressive results. The daily highest examples of ship waves (~1 m) are mostly found in the range of the annual highest 1–5% of wind waves (Paper II, V). The annual mean energy of ship waves at the 5 m isobath of Tallinn Bay (Fig. 3.7.2.5) is about 5–8% from the annual mean (6–12% during the spring and summer seasons) wind wave energy (Papers II, V, Soomere *et al.* 2003 [118]). This share is not very unusual: much larger portion of ship-generated waves in the total wave activity is identified in certain well-sheltered microtidal basins (Schoellhamer 1996 [106]). Yet the unique situation is that ship waves form an appreciable part of total wave energy at sea coasts partially open to dominating winds.

Comparison of the energy of ship and wind waves is equivalent to an evaluation of the squared wave heights. The wave energy flux (wave power, see Section 3.2) implicitly accounts for the wave periods since longer waves have higher group velocities. The annual mean power of ship waves constitutes 18–35% (27–54% during the summer season) from the annual wind wave power at the distance of 2–3 km from the fairway, and about 12% (17%) at sites located about 10 km from the fairway in the coastal area of Tallinn Bay (Fig. 3.7.2.5, Papers II, V). The reason for the excessive portion of the ship-wave power is the moderate dominating period of wind waves.

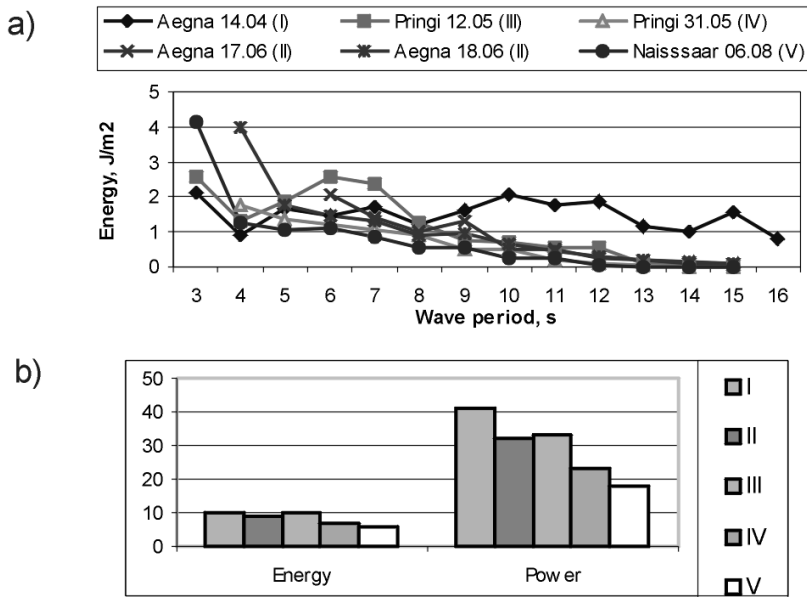


**Figure 3.7.2.5.** (a) Energy of wake components with different periods. (b) The share (%) of the energy and power of ship waves compared with the wind wave energy and power. Detailed description of the measurement sites I-V is in Paper V.

### 3.7.3. Multisensor analysis of the surface waves

The main shortages of the experiments in Tallinn Bay described in Papers V, VI are that they (i) consist of one-point measurements and that (ii) only pressure signal has been recorded. Several important properties of waves such as their propagation direction or the length of the wave crests cannot be established from one-point pressure data. Also the wave shape generally cannot be exactly restored from pressure data, because the processing of raw pressure data, which includes direct and inverse Fourier transformation of sine harmonics of the data, neglects high-frequency wave components and potentially distorts the geometry of the water surface. This is a general shortage of pressure-sensor-based wave measurements and direct recordings of the water surface presented in the next section generally are necessary in order to correctly describe the wave shape.

Usually the directional parameters of wave fields are obtained by using wave riders equipped with inertial sensors (Datawell Directional Waverider MK III, for example) or wave motion sensors based on GPS (Datawell DWR-G). These and analogous devices usually do not store the raw data and only export the directional wave spectrum (see, *e.g.* Kahma *et al.* 2003 [47]). For that reason, they cannot be used for the analysis of ship wakes that consist of groups of short duration.

The directional parameters of surface waves can be measured by the use of an array of sensors (Dean and Dalrymple [17], Chapter 7, Panicker and Borgman 1970 [82]). Although similar equipment was missing during the Aegna experiments and we had to rely on one-point data, efforts were made towards the simultaneous use of several pressure sensors for the detailed survey of directional properties and crest lengths of different groups of the ship wakes with implementing the methods of statistical calibration of the sensors (Paper VIII). This approach is a particular case of the use of a multisensor system.

Usually the multisensor technique means using different technical equipment simultaneously, acquiring data from the same (wave) field (in certain cases from the same point). Its main advantage in surface wave matters is the possibility to get data from different sea points. Their comparison may give some impression not only about the wave propagation direction but also about the geometry of the water surface and characteristics of single wave crests. Multisensor experiments are potentially able to distinguish the wave components coming from different ships as well as components reflected from coastal structures and bottom inhomogeneities. It might also be possible to analyse the challenging but not detected yet interactions of soliton-like ship waves in shallow water (Peterson *et al.* 2003 [86]).

The disadvantages of the multisensor system are the complexity of data processing and the calibration of the sensors. Usually sensors tend to give a certain bias; the situation is more complex in the realistic sea where moored sensors may drift to some extent owing to the influence of waves and currents. Different sensors may have also different sensitivity to noise characteristics. For

example, optical instruments such as laser-based wave height detectors are known to be sensitive on spray from the wave crests. Yet multisensor wave measurements (for example, from the North Sea oil platforms (Forristall *et al.* 2002 [24]), where wave radars, laser, wave gauges and video technique were used simultaneously) have given promising results in obtaining better knowledge of the statistical distribution of crest heights according to the given wave spectrum. The relevant results are of key value in solving the problem of setting the correct deck (platform) heights.

The most important problems to solve for an efficient use of a multisensor system are (i) the intercalibration of the sensors and (ii) data synchronisation. For a small number of sensors of the same type (e.g. system of three wave sensors analysed in Dean and Dalrymple [17]) the solution is straightforward. If the system grows larger and/or consists of equipment based on different detecting technology (Dean and Dalrymple [17]), and if the sensors are sparsely distributed, one has to employ the methods of statistical calibration. This is a viable alternative to *in situ* physical calibration in several cases where the latter is too expensive or technically impossible (especially in case of large systems and/or severe environmental conditions, which is the case of storm wave measurements).

An attempt to construct a data analysis technique for such multi-sensor experiments is described in Paper VIII. The suggested statistical calibration method is based on the Kalman filtering (KF) approach. This technique resolves the central question: getting accurate information using inaccurate data. It allows filtering unwanted noise out from a data stream. For a system of pressure sensors the noise consists of the thermal drift of electronics, non-tidal water level instabilities, wave-induced changes of the sensor etc.

The idea employed in Paper VIII was to use Extended Kalman Filtering for processing the raw data. As a first approximation, it was assumed that the conditions of observability and controllability are not violated and that the KF algorithm converges. Also the error estimates (obtained, e.g., from additional modelling activities or from another series of measurements) were assumed to be correct. This set of assumptions is somewhat optimistic; for example, it is not always possible to guarantee the stability of the conventional KF algorithm. The basic advantage of the proposed method is that it provides a numerical measure for making it sure whether the system suffers from any serious divergence of filtering. In other words, the outcome of this sort of filtering allows deciding whether seemingly unusual data from a certain set of sensors reflect the factual unusual behaviour of the sea surface or a failure of sensors. The latter is a key question in interpretation of extreme wave conditions. This technique is planned to be implemented in multi-sensor measurements of ship wave patterns.

The central problem in using this kind of technique is that the sea surface is extremely irregular. For that reason, in wave measurements it is impossible to determine the probability that a measurement of the sea surface position at a certain instant was correct. The problem is even more complicated if the truth

must be evaluated at every measurement point and we have to rely on statistical methods without knowing how much we can trust the results. A feasible way to overcome this difficulty consists in the use of the Fast Kalman Filtering (FKF) method (Lange 1997 [59]) that is supposed to be appropriate to resolve this shortage and to improve the quality of multi-sensor wave data. The FKF method is also attractive due to its numerical efficiency (it is based on a semianalytical solution), stability and capabilities of error analysis.

### 3.7.4. Shape of long ship waves

The shape of the water surface in a wave field (called the wave shape below) is one of the most important features of long waves, because many wave-induced effects directly depend on it. In particular, velocity of water particles follows the shape of long waves. Shapes of ship waves were recorded during joint Estonian-Finnish measurements of fast ferries' wakes in September 2001 (Bengston *et al.* 2003 [9], Peltoniemi *et al.* 2002 [85]) but the results are neither published nor available by other means. The shape of the pressure signal in records described in Paper V suggests that the leading waves of a wake are asymmetric: the crest elevation clearly exceeds the depth of the trough. Experimental evidence in analogous experiments (Parnell and Kofoed-Hansen 2001 [83], Whittaker *et al.* 1999 [141]) also indicates that the shape of ship waves in shallow water is not sinusoidal.

The properties and influence of ship waves usually are calculated assuming that they can be described by the linear wave theory (Soomere *et al.* 2003 [118], Parnell and Kofoed-Hansen 2001 [83]). The length of the leading waves of wakes from fast ferries exceeds 100 m in areas with a depth of  $\leq 10$  m. At smaller depths, such waves with a height of about 1 m cannot be considered as linear. As discussed in Section 3.3, even higher-order classical theories, for instance the Stokes wave theory (*e.g.* Massel 1989 [68]), are not applicable for waves with such properties. Theoretically, the shape and properties of long waves with appropriate parameters propagating in a shallow region with an ideal flat bottom should match those of the corresponding solution of the KdV equation. The single waves formed at the critical velocity may also have features of cnoidal or solitary waves (Li and Sclavonous 2002 [61]). The sea bottom is never perfect and in real conditions it is not clear in advance what exactly happens when waves approach coastal areas that have two-dimensional bottom with many imperfections.

As discussed above, the wave shape is universal for sine waves but depends on wave parameters in the cnoidal framework. This feature makes it possible to estimate the 'level' of nonlinearity of ship waves from measurements of the wave geometry. To some extent, the results allow to choose an adequate wave theory to estimate the wave impact on the coast. The non-linearity of the waves

has to be taken into account in many engineering calculations (not only at the coastal area, but for the oil platforms as well, for example, in the analysis of the maximum elevation of the water surface) and is a generic feature affecting wave properties. Another important issue is that the slope of the water surface in cnoidal or soliton-like waves may exceed that in linear surface waves of the same height and length (Massel 1989 [68]). Therefore, such waves may be particularly dangerous for small boats.

The appearance of long ship waves approaching shallow coastal areas of Tallinn Bay was studied in Paper VI. The technique used for wave profile measurements was the most robust: the instantaneous position of the water surface was determined from its location (recorded with a video camera) on the pillar that was rigidly fixed to the bottom and held a meter scale. Additionally, the waves were registered with the use of the pressure sensor fixed to the same pillar. The shape of ship waves was established from the water surface time series, digitized from the video recordings (Figure 3.7.4.1). The measurements of the wave shape needed a lot of patience and time because of the changing wind conditions and unexpectedly passing small ships and boats (the pilot boat to and from Rohuneeme plus numerous holiday-makers) generating the background noise that accomplished the measurements and made more complex the separation of the fast ferries' wakes.

Analysis of the water surface records in Paper VI shows that a large part of long components of waves from fast ferries are clearly non-linear in the test area. The wave shape considerably differs from the sine function but almost perfectly fits to the theoretical shape of cnoidal waves. Ship waves of already relatively small height (over 0.4 m, Figure 3.7.4.1) considerably differ from sine waves at a depth of about 4 m. The parameter  $k$  in the Jacobi elliptic functions (called elliptic modulus) is very close to 1 (mostly 0.95–0.99) for many waves, the shape of which practically coincides with that of the solitary wave solution of the KdV equation. These waves cannot automatically be considered as solitons, because not only the instantaneous shape but preserving it in time and in collisions are the distinguishing features of solitons. Yet cnoidal waves of relatively large amplitude preserve their identity and shape fairly well in time, and partially also during interactions (Svendsen and Veeramony 2001 [128]).

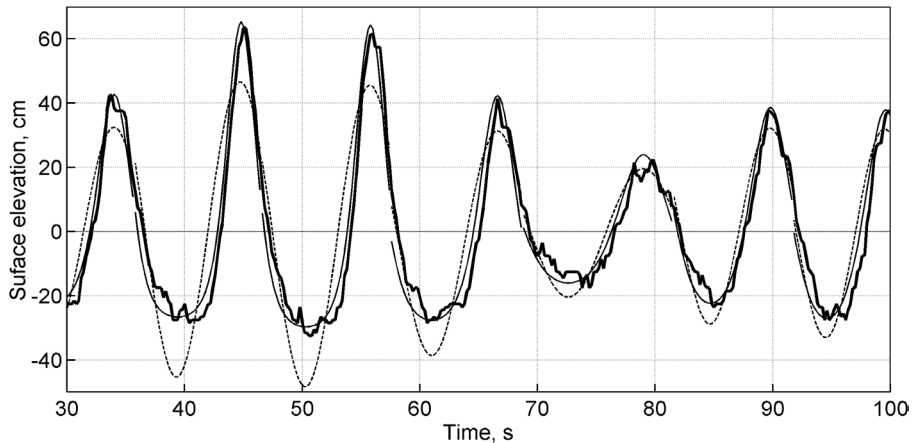


**Figure 3.7.4.1.** Water surface time series (bold line) in a ship wake with a maximum wave height of 0.95 m, the shape of the best-fitting cnoidal waves (solid line), and the corresponding sine wave (dashed line).

The results in Paper VI confirm that the shape of water surface in a large part of ship-generated waves reaching the coastal area of Tallinn Bay well matches that of the cnoidal waves even in conditions of the non-perfect sea bottom. Thus it is likely that the dynamics of a certain part of ship wakes in the shallow areas (at least, at the depth of experiments, about 4 m) is very close to that of cnoidal waves whereas the longer and higher ship waves may behave as ensembles of KdV solitons. For wind waves of comparable height the linear theory yet is applicable at this depth, because they are much shorter than ship waves (Paper V, Soomere 2005 [121]; see also Section 3.3).

For a wave with a given height and length the cnoidal wave theory predicts considerably larger velocities of water particles than the linear theory (Paper VI). Consequently, velocities of water particles in long ship waves in the coastal area of Tallinn Bay apparently are much larger than expected from the classical approach. A large difference may frequently occur in areas where the cnoidal wave theory is preferable, i.e., for depths less than 10–15 m, depending on the wave period and height. The ratio of maximal vertical and horizontal velocities in cnoidal waves compared with these velocities in the linear approximation for the waves with identical parameters is presented in Figure 3.7.4.2. The difference is at times substantial; for example, at the depth of 5 m the near-bottom velocity of water particles for cnoidal waves (with a period  $T = 15$  s and wave height 1 m, that is, for waves that occur several times a day near Aegna jetty, Paper V) can excite by 50–60% larger horizontal velocities of water particles than predicted by the linear theory (Figure 3.7.4.2a). The difference of the vertical speed (at the height of half-depth of the water column) may be more than two times (Figure 3.7.4.2b). Therefore, the possible adverse

influence of long ship-generated waves may be much larger than its estimates based on the classical wave theory.

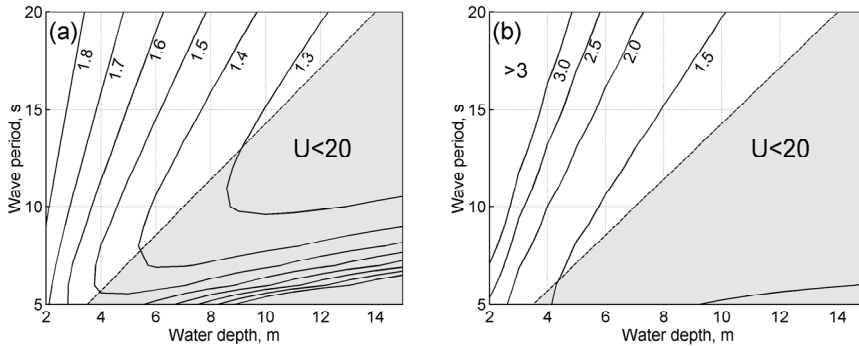


**Figure 3.7.4.2.** a) Ratio of the maximal near-bottom velocities ( $v_{cnoidal} / v_{sine}$ ). b) Ratio of the maximal vertical velocities at the 1/2 depth of the water column.

The described results are not unexpected. For example, the shape and properties of long waves in shallow areas with flat bottom should exhibit nonlinear features and resemble those of cnoidal waves for certain combinations of wave parameters and the water depth. However, the sea bottom is not perfect and may greatly affect the actual wave shape. The influence of bottom topography on ship waves may be decisive in some cases (see, for example, Jiang *et al.* 2003 [41]) and it will certainly be a subject for future research.

### 3.8. Environmental implications of ship wave activity

The influence of ship waves may be critical for certain processes in semi-enclosed estuaries or in areas usually not exposed to swell or severe windseas (Guidelines 2003 [26], Kirkegaard *et al.* 1999 [52]). Tallinn Bay is an example of a partially sheltered sea region; however, very rough seas may occasionally occur in this area and a large part of its coast show features of high natural wave intensity. The above has demonstrated that wakes of the particularly intense fast ferry traffic form an appreciable part of the total wave intensity. The traffic is very intensive indeed. Nearly 70 crossings of the bay take place daily. A variety of different types of high-speed ships operated there during the measurements. The potential implications of the heavy fast ferry traffic are described and discussed in Paper II.

The first impression one can get from Section 3.2 and Figure 3.7.2.5b is that the ship wave energy is small compared with the total wave activity. The fact that 70–80% of the energy of fast ferries' wakes is concentrated in wave

components with the periods exceeding 5–6 s (Figure 3.7.2.5a) becomes first evident in comparison of natural and wave-induced wave power. Another important feature is that the daily highest ship waves belong to the annual highest 1–5% of wind waves. These features suggest that ship waves still may play a remarkable role in the hydrodynamic activity of Tallinn Bay.

A specific influence of wakes of high-speed ships occurs when wake waves are much longer than wind waves (Parnell and Kofoed-Hansen 2001 [83], Soomere and Kask 2003 [119]). The typical wind wave periods in Tallinn Bay are 2–4 s and rarely reach 6–7 s (Section 3.6). The leading wake waves frequently have a height of about 1 m and a period of 10–15 s (Paper V). Such waves extremely seldom occur in natural conditions in Tallinn Bay as well as in certain regions of other semi-enclosed seas. They are qualitatively similar to long-period ocean swell. Together with wind waves, they may form bi-modal wave systems, impact of which on coastal processes may be much higher compared with that of wave systems with a single spectral peak and a comparable total energy (Coates and Hawkes 1999 [15], Hawkes 1999 [36]).

The majority of the energy of ship waves is concentrated in waves with periods exceeding 8 s and frequently reaching 10–15 s. This seemingly insignificant contrast between the prevailing periods of natural waves and ship waves causes highly a diverse impact of the waves of different origin at certain depths (5–20 m). The reason is that for a fixed wave height, the wave-induced near-bottom velocity depends essentially on the wave period. For the mentioned depths, the highest variation of this velocity occurs when the wave period increases from 5 s to 8 s (Figure 3.8.1).

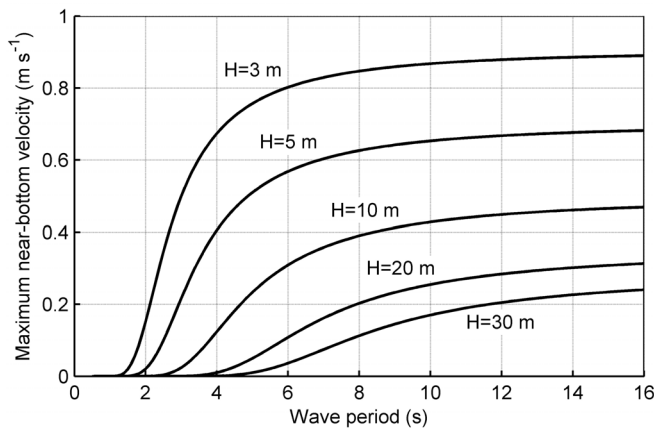


**Figure 3.8.1.** The maximum wave-induced near-bottom velocity *versus* wave period for the sine wave height of 1 m and water depth of H=3–30 m



A typical ship wave with the height 1 m and the period of 10 s induces the near-bottom velocity as high as about  $45 \text{ cm s}^{-1}$  at the depth of 10 m whereas the maximum velocity imposed by a wind wave with the period 4 s is only about  $10 \text{ cm s}^{-1}$ . A 2 m high wave with a period of 5 s or a 4 m high wave with a period of 4 s excites velocity  $45 \text{ cm s}^{-1}$  at this depth. Thus, the impact of a typical ship wake on bottom sediments and aquatic wildlife is comparable with that of the waves occurring in very strong storms. At certain depths, the near-bottom orbital velocities in the leading (the longest and highest) ship waves may be considerable larger than described here because of the nonlinear effects (Section 3.7.4). The described features suggest that ship waves may serve as a new forcing factor in this bay.

Although species that prefer rocky or sandy bottom may benefit from the increased hydrodynamic activity, the concern is that abrupt changes in forcing conditions usually have an adverse effect on the local ecosystem. The primary reaction of the sea bottom (the benthic layer and fine bottom sediments) to the increased hydrodynamic activity usually consists in intense (re)suspension of bottom sediments (Erm and Soomere 2004 [20], Soomere and Kask 2003 [119]). The accompanied reduced water transparency (Osborne and Boak 1999 [80], Erm and Soomere 2004 [20]) may have strong suppressing feedback on the bottom vegetation, and suspension and re-sedimentation of finer sediments may considerably worsen fish spawning conditions.

An important factor in associated questions of maritime safety is the increase of the wave height when the wake proceeds into shallow water. The conservation law of wave energy flux prescribes that the height increase is roughly inverse proportional to the square root of the decrease of the group velocity (Dean and Dalrymple 2004 [17]). Therefore the increase in height is much stronger for the long waves generated by a fast ferry, than for the shorter ones of a conventional ship or for the short-wave part of the wake. This increase may have played a role in the some phenomena. For example, New Scientist reported that in August 1999, holidaymakers on a beach at Felixstowe, three miles north of Harwich, UK, were forced to "flee for their lives when enormous waves erupted out of a millpond-smooth sea" (Hamer 1999 [27]). The possibility of forming highly monochromatic packets of short waves which propagate much more slowly than the leading ship waves means that the most dangerous (short but steep) waves might unexpectedly arrive a long time (even more than an hour) after the leading waves (Paper V).

The specific features of ship waves only become evident in Tallinn Bay because they are much longer than natural waves. Both the length and height of waves generally increase with the ship speed (Guidelines 2003 [26], Kirk McClure Morton 1998 [51], Sorensen 1973 [124]). Large high-speed ships frequently sail in the transcritical velocity range in Tallinn Bay (Paper V). The dependence of the properties of the wave pattern on the depth Froude number (see Section 3.7.1) suggests that the transcritical speeds are generally accompanied by high and long ship waves. Therefore keeping the ship speed

well below the critical one along the sailing line (either by reducing the speed of certain types of the ships or by shifting the fairway for fast ferries into deeper water) is a reasonable way to reduce the environmental impact of fast ferry traffic and to achieve environmentally friendly navigation in Tallinn Bay. Starting from 1997, several countries and communities have involved regulations (primarily based on wave height criteria in the nearshore environment, Parnell and Kofoed-Hansen 2001 [83]) for the fast ferry traffic. Relevant restrictions for Tallinn Bay have been discussed many times but no decision has been made yet.

Some specific effects may become evident when ship waves start to behave as KdV solitons. A moving disturbance in open sea areas seldom forms solitary waves of considerable height (Li and Sclavonous 2002 [61], Hammack *et al.* 1995 [29], Neuman *et al.* 2001 [78]). The results of Paper VI suggest that long ship waves that approach shallow regions eventually become highly nonlinear or even soliton-like structures (cf. Stumbo *et al.* 1999 [127]). Recently it has been shown that certain dramatic effects (incl. possibility of fourfold amplification of wave amplitudes and eightfold amplification of wave slopes) may occur when two trains of soliton-like waves intersect under a certain angle (Peterson *et al.* 2003 [86], Soomere and Engelbrecht 2005 [122]).

## REFERENCES

1. Airy, G., 1845. Tides and waves, *Encyclopedia Metropolitana*, 241–396.
2. Aitsam, A., Hansen, H.P., Elken, J., Kahru, M., Laanemets, J., Pajuste, M., Pavelson, J. and Talpsepp, L., 1984. Physical and chemical variability of the Baltic Sea: a joint experiment in the Gotland Basin, *Cont. Shelf Res.*, 3, pp. 291–310.
3. Amundsen, D.E. and Benney, D.J., 2000. Resonances in dispersive wave systems, *Studies in Applied Mathematics*, 105, 3, pp. 277–300.
4. Andrejev, O., Myrberg, K., Alenius, P. and Lundberg, P.A., 2004a. Mean circulation and water exchange in the Gulf of Finland – a study based on three-dimensional modelling, *Boreal Environment Research*, 9, pp. 1–16.
5. Andrejev, O., Myrberg, K. and Lundberg, P.A., 2004b. Age and renewal time of water masses in a semi-enclosed basin – Application to the Gulf of Finland, *Tellus*, 56A, pp. 548–558.
6. Axelsson, P., 1998. Three-wave coupling in a stratified MHD plasma, *Nonlinear Processes in Geophysics*, 5, pp. 105–110.
7. Balk, A.M., 1991. A new invariant for Rossby-wave systems, *Physics Letters, A* 155, 1, pp. 20–24.
8. Balk, A.M., 1997. New conservation laws for the interaction of nonlinear waves, *SIAM Review*, 39, 1, pp. 68–94.
9. Bengtson, A., Peltoniemi, H. and Rytönen, J., 2003. *Measurements of fast ferry waves in Helsinki–Tallinn run*, Research Report No BTUO34–031143, VTT Technical Research Centre of Finland, VTT Industrial Systems, Espoo 20.02.2003, 37 pp.
10. Benney, D.J. and Newell, A.C., 1969. Random wave closures, *Stud. Appl. Math.*, 48, pp. 29–53.
11. Brown, E.D., Buchsbaum, S.B., Hall, R.E., Penhune, J.P., Schmitt, K.F., Watson, K.M. and Wyatt D.C., 1989. Observations of a nonlinear solitary wave packet in the Kelvin wake of a ship, *J. Fluid Mech.*, 204, pp. 263–293.
12. Carnevale, G.F., 1982. Statistical features of the evolution of two-dimensional turbulence, *J. Fluid Mech.*, 122, pp. 143–153.
13. Chen, X - N. and Sharma, S., 1997. On ships at supercritical speeds. In *21 st Symposium on Naval Hydrodynamics. Trondheim, 1996*. National Academy Press, Washington, D. C., pp. 715–726.
14. Chung, Y.K. and Lim, J.S., 1991. A review of the Kelvin ship wave pattern, *Journal of Ship Research*, 35, 3, pp. 191–197.
15. Coates, T.T. and Hawkes, P.J., 1999. Beach recharge design and bi-modal wave spectra. In *Coastal Engineering 1998: Proc. 26<sup>th</sup> International Conference*. Copenhagen, 1998 (Edge, B.L., ed.). *American Society of Civil Engineers*, 3, pp. 3036–3045.
16. Davidan, I.N., Lopatoukhin, L.I. and Rozhkov, V.A. [Давидан, И.Н., Лопатухин, Л.И., Рожков, В.А.] 1985. [*Wind waves in the world oceans*]. Gidrometeoizdat, Leningrad, (in Russian).
17. Dean, R.G. and Dalrymple, R.A., 2004. *Water wave mechanics for engineers and scientists*, World Scientific, Singapore, 353 pp.
18. Dolotin, V.V. and Fridman, A.M., 1990. The Correlation Between the Main Parameters of the Interstellar Gas (Including Salpeter’s Spectrum of Masses) as a Result of the Development of Turbulent Rossby Waves, in *Dynamics of*

- Astrophysical Disks*, edited by J. Sellwood, Cambridge University Press, Cambridge, pp. 71–72.
19. Drazin, P.G. and Johnson, R.S., 2002. *Solitons: an introduction*, Cambridge Texts in Applied Mathematics, Cambridge University Press, 226 pp. (First printing 1989).
  20. Erm, A. and Soomere, T., 2004. Influence of fast ship waves on optical properties of sea water in Tallinn Bay, Baltic Sea. *Proc. Estonian Acad. Sci. Biol. Ecol.*, 53, pp. 161–178.
  21. Fernando, H.J.S., 1987. The formation of layered structure when a stable salinity gradient is heated from below. *J. Fluid Mech.*, 182, pp. 525–541.
  22. Fernando, H.J.S., 1989. Oceanographic implications of laboratory experiments on diffusive interfaces. *Journal of Physical Oceanography*, 19, pp. 1707–1715.
  23. Feodorov, K.N., 1976. *Thermohaline fine structure of oceans*, Gidrometeoizdat, 184 pp, (in Russian).
  24. Forristall, G.Z., Barstow, S.F., Krogstad, H.E., Prevosto, M., Taylor, P.H., Tromans, P.S., 2002. Wave crest sensor intercomparison study: an overview of WACSYS, *Transactions of the ASME: Journal of Offshore Mechanics and Arctic Engineering*, 126, pp. 26–34.
  25. Forsman, B., 1997. High-Speed ferries – environmental impact and safety assessment. *PIANC Bulletin*, 96, pp. 23–24.
  26. *Guidelines for managing wake wash from high-speed vessels*, 2003. Report of the Working Group 41 of the Maritime Navigation Commission, International Navigation Association (PIANC), Brussels, 32 pp.
  27. Hamer, M., 1999. Solitary killers, *New Scientist*, 163, No 2201, pp. 18–19.
  28. Hammack, J., Scheffner, N. and Segur, H., 1989. Two-dimensional periodic waves in shallow water, *J. Fluid Mech.*, 209, pp. 567–589.
  29. Hammack, J., McCallister, D., Scheffner, N. and Segur, H., 1995. Two-dimensional periodic waves in shallow water. Part 2. Asymmetric waves, *J. Fluid Mech.*, 285, pp. 95–122.
  30. Hannon, M.A. and Varyani, K.S., 1999. The wash effect of high speed ferries in coastal and inland waterways. *International Conference on Coastal Ships and Inland Waterways*. London, 1999. RINA, London, CD.
  31. Hasegawa, A., MacLennan, C.C. and Kodama, Y., 1979. Nonlinear behaviour and turbulence spectra of drift waves and Rossby waves, *Phys. Fluids*, 22, pp. 2122–2129.
  32. Hasegawa, A. and Mima, K., 1978. Pseudo-three-dimensional turbulence in magnetized nonuniform plasma, *Phys. Fluids*, 21, pp. 87–92.
  33. Hasselmann, K., 1962. On the nonlinear energy transfer in a gravity-wave spectrum. Part 1. General theory, *J. Fluid Mech.*, 12, pp. 481–500.
  34. Hasselmann, K., 1963. On the nonlinear energy transfer in a gravity-wave spectrum. Part 2. Conservation theorems, wave-particle analogy, irreversibility, *J. Fluid Mech.*, 15, pp. 273–281.
  35. Hasselmann, K., 1967. Nonlinear interactions by methods of theoretical physics, *Proc. Roy. Soc.* A299, pp. 77–100.
  36. Hawkes, P.J., 1999. Mean overtopping rate in swell and bimodal seas. *Proceedings of the Institution of Civil Engineers: Water, Maritime and Energy*, 136, pp. 235–238.

37. Heinloo, J., 1984. *Phenomenological mechanics of turbulence*, Valgus, Tallinn, (in Russian).
38. Heinloo, J., 2004. Formulation of turbulence mechanics. *Physical Review*, E 69, Paper 056317.
39. Hüsigg, A., Linke, T. and Zimmermann, C., 2000. Effects from supercritical ship operation on inland canals, *J. Waterw. Port Coast. Ocean Eng. – ASCE*, 126, pp. 130–135.
40. IAHR working group on wave generation and analysis: 1989, List of sea-state parameters, *J. Waterway, Port, Coastal Ocean Eng.*, 115, pp. 793–808.
41. Jiang, T., Henn, R. and Sharma, S.D. 2003, Wash wave generated by ships moving on fairways of varying topography, *24th Symposium on Naval Hydrodynamics, Fukuoka, Japan, 8-13 July 2002*, National Academy Press, Washington DC, pp. 441–457 (web only: www.nap.edu).
42. Jones, S., 1979. Rossby wave interactions and instabilities in a rotating, two-layer fluid on a beta-plane. Part I: Resonant interactions, *Geophys. Astrophys. Fluid Dyn.*, 11, pp. 289–332.
43. Jönsson, A., Broman, B. and Rahm, L., 2002. Variations in the Baltic Sea wave fields, *Ocean Engineering*, 30, pp. 107–126.
44. Jönsson, A., Danielsson, A. and Rahm, L., 2005. Bottom type distribution based on wave friction velocity in the Baltic Sea, *Continental Shelf Research*, 25, pp. 419–435.
45. Kahma, K., Rantanen, E. and Saarinen, J., 1983, *Wave data from the southern Bothnian Sea 1973–1975, 1981*, Finnish Institute of Marine Research, Internal report 1/1983, (in Finnish with English summary).
46. Kahma, K. and Pettersson, H., 1993. *Wave statistics from the Gulf of Finland*, Finnish Institute of Marine Research, Internal report 1/1993, (in Finnish with English summary).
47. Kahma, K., Pettersson, H. and Tuomi, L., 2003. Scatter diagram wave statistics from the northern Baltic Sea, *MERI – Report Series of the Finnish Institute of Marine Research*, 49, pp. 15–32.
48. Kamenkovich, V.M., Koschlyakov, V.N. and Monin, A.S., 1986. *Synoptic eddies in the ocean*, Reidel, Dordrecht, Holland, 433 pp.
49. Kenyon, K., 1964. Nonlinear energy transfer in a Rossby-wave spectrum, In *Notes on the 1964 Summer Study Program in Geophysical Fluid Dynamics at the Woods Hole Oceanographic Institute*, Student lectures, 11, pp. 69–83.
50. Kerstein, A.R., 1999. One-dimensional turbulence Part 2. Staircases in double-diffusive convection. *Dynamics of Atmospheres and Oceans*, 30, pp. 25–46.
51. Kirk McClure Morton, 1998. *Investigation of high speed craft and routes near to land or enclosed estuaries*. Research Report JR226. The Maritime and Coastguard Agency, UK.
52. Kirkegaard, J., Kofoed-Hansen, H. and Elfrink, B., 1999. Wake wash of high-speed craft in coastal areas. In *Coastal Engineering 1998. Proc. 26th International Conference*. Copenhagen, 1998 (Edge, B.L., ed.). *American Society of Civil Engineers*, vol. 1, pp. 325–337.
53. Kofoed-Hansen, H. and Kirkegaard, J., 1996. *Technical Investigation of Wake Wash from Fast Ferries*. Report No. 96–5012. Danish Hydraulic Institute, Copenhagen.

54. Kofoed-Hansen, H. and Mikkelsen, A.C., 1997. Wake wash from fast ferries in Denmark. In *Proc. Fourth International Conference of Fast Sea Transportation*. Sydney, 1997. Baird Publications, Hong Kong, vol. 1, pp. 471–478.
55. Komen, G.J., Cavaleri, L., Donelan, M., Hasselmann, K., Hasselmann, S. and Janssen, P.A.E.M., 1994. *Dynamics and modelling of ocean waves*, Cambridge University Press, Cambridge, 532 pp.
56. Kozlov, O.V., Reznik, G.M. and Soomere, T., 1987. Weak turbulence on the  $\beta$ -plane in a two-layer ocean, *Izv. Acad. Sci. USSR. Atm. Oceanic Phys.*, 23, pp. 869–874.
57. Krasitskii, V.P., 1994. On the reduced equations in the Hamiltonian theory of weakly nonlinear surface waves, *J. Fluid Mech.*, 272, pp. 1–20.
58. Lamb, H., 1997. *Hydrodynamics*, 6th edition, Cambridge University Press, 738 pp.
59. Lange, A., 1997. Method for adaptive Kalman filtering in dynamic systems, World Intellectual Property Organization, International Bureau, Patent WO 97/18442, PCT/FI96/00621, 22 May 1997.
60. LeBlond, P.H. and Mysak, L.A., 1978. *Waves in the ocean*, Elsevier, 602 pp.
61. Li, Y. and Sclavounos, P.D., 2002. Three-dimensional nonlinear solitary waves in shallow water generated by an advancing disturbance. *J. Fluid Mech.*, 470, pp. 383–410.
62. Lighthill, J., 1978. *Waves in fluids*, Cambridge University Press, 1978.
63. Linden, P.F., 1979. Mixing in stratified fluids. *Geophysical and Astrophysical Fluid Dynamics*, 13, pp. 3–23.
64. Longo, S., Petti, M. and Losada, I.J., 2002. Turbulence in the swash and surf zones: a review, *Coastal Engineering* 45 (3–4), pp. 129–147.
65. Longuet-Higgins, M.S. and Gill, A.E., 1967. Resonant interactions between planetary waves, *Phil. Trans. Roy. Soc. London*, 294, pp. 120–140.
66. Majda, A.J., McLaughlin, D.W. and Tabak, E.G., 1997. A one-dimensional model for dispersive wave turbulence, *J. Nonlinear Sci.*, 7, pp. 9–44.
67. Marshall, H.G., 1986. A note on the direction of energy movement in wavenumber of a two-layer model, *Dyn. Atm. Oceans*, 10, pp. 253–257.
68. Massel, S.R., 1989. *Hydrodynamics of coastal zones*. Elsevier, Amsterdam, 336 pp.
69. Mårtensson, N. and Bergdahl, L., 1987. *On the wave climate of the Southern Baltic*, Report Series A:15, Department of Hydraulics, Chalmers University of Technology, Göteborg.
70. Merilees, P.E. and Warn, H., 1975. On energy and entropy exchanges in two-dimensional non-divergent flow, *J. Fluid Mech.*, 69, pp. 625–630.
71. Mietus, M. (co-ordinator), 1998. *The climate of the Baltic Sea Basin*, Marine meteorology and related oceanographic activities, Report No. 41, World Meteorological Organisation, Geneva, 64 pp.
72. Miles, J.W., 1977a. Obliquely interacting solitary waves, *J. Fluid. Mech.* 79, pp. 157–169.
73. Miles, J.W., 1977b. Resonantly interacting solitary waves, *J. Fluid. Mech.* 79, pp. 171–179.
74. Mirabel, A.P., 1985. The effects of triad-resonance interaction of Rossby waves in the ocean, *Okeanologiya* 25 (4), pp. 558–562. (In Russian).
75. Monin, A.S. and Yaglom, A.M. 1967. *Statistical hydromechanics. Mechanics of turbulence*, Moscow (in Russian).

76. Muench, R.D., Fernando, H.J.S. and Stegen, G.R., 1990. Temperature and salinity staircases in the northwestern Weddell Sea. *Journal of Physical Oceanography*, 20, pp. 295–306.
77. Neal, V. T., Neshyba, S. and Denner, W., 1969. Thermal stratification in the Arctic Ocean. *Science*, 166, pp. 373–374.
78. Neuman, D.G., Tapio, E., Haggard, D., Laws, K.E. and Bland, R.W., 2001. Observation of long waves generated by ferries, *Canadian Journal of Remote Sensing*, 27, pp. 361–370.
79. Orlenko, L.R., 1984. *Studies of the hydrometeorological regime of Tallinn Bay*, Gidrometizdat, Leningrad, (in Russian).
80. Osborne, P.D. and Boak, E.H., 1999. Sediment suspension and morphological response under vessel-generated wave groups: Torpedo Bay, Auckland, New Zealand. *J. Coastal Res.*, 1999, 15, pp. 388–398.
81. Padman, L. and Dillon, T.M., 1989. Thermal microstructure and internal waves in the Canada Basin diffusive staircase. *Deep-Sea Research*, 36, pp. 31–542.
82. Panicker, N.N. and Borgman, L.E., 1970. Directional spectra from wave gage arrays, *Proc. 12th Conf. Coastal Eng.*, ASCE, pp. 117–136.
83. Parnell, K.E. and Kofoed-Hansen, H., 2001. Wakes from large high-Speed ferries in confined coastal waters: Management approaches with examples from New Zealand and Denmark. *Coastal Manage.* 29, pp. 217–237.
84. Pedlosky, J., 1998. *Geophysical fluid dynamics*, 2<sup>nd</sup> edition, Springer Verlag, 728 pp.
85. Peltoniemi, H., Bengston, A., Rytönen, J. and Kõuts, T., 2002. Measurements of fast ferry waves in Helsinki-Tallinn route. In *Abstracts, Symposium "The changing State of the Gulf of Finland Ecosystem"*. Tallinn, 2002, p. 32.
86. Peterson, P., Soomere, T., Engelbrecht, J. and van Groesen, E., 2003. Soliton interaction as a possible model for extreme waves in shallow water. *Nonlinear Processes in Geophysics*, 10, pp. 503–510.
87. Pettersson, H., 1994. *Directional wave statistics from the southern Bothnian Sea 1992*, Finnish Institute of Marine Research, Internal report 5/1994, (in Finnish with English summary).
88. Pettersson, H., 2001. Directional wave statistics from the Gulf of Finland 1990–1994, *MERI – Report Series of the Finnish Institute of Marine Research*, 44, pp. 1–37, (in Finnish with English summary).
89. Pettersson, H. and Boman, H., 2002. High waves and sea level during the November storm. In *Annual report 2001*, Finnish Institute of Marine Research, Helsinki, p. 7.
90. Phillips, O.M., 1966. The dynamics of the upper ocean, *Cambridge University Press*, 266 pp.
91. Phillips, O.M., 1972. Turbulence in a strongly stratified fluid—is it unstable? *Deep-Sea Research*, 19, pp. 79–81.
92. Piterbarg, L.I., 1998. Hamiltonian formalism for Rossby waves, in *Nonlinear waves and weak turbulence*, ed. Zakharov, V.E., Amer. Math. Soc. Transl. (2), 182, pp. 131–166.
93. Posmentier, E.S., 1977. The generation of salinity finestructure by vertical diffusion. *Journal of Physical Oceanography*, 7, pp. 298–300.
94. Read, P.L., Yamazaki, Y.H., Lewis, S.R., Williams, P.D., Miki-Yamazaki, K., Sommeria, J., Didelle, H. and Fincham, A., 2004. Jupiter's and Saturn's

- convectively driven banded jets in the laboratory, *Geophysical Research Letters* 31 (22): Art. No. L22701.
95. Reznik, G.M. and Kozlov, O.V., 1981. Weakly non-linear interactions of Rossby waves in a barotropic ocean, *Izvestiya Akademii Nauk SSSR, Fizika atmosfery i okeana* 17 (6), pp. 632–638 (in Russian).
  96. Reznik, G.M. and Soomere, T., 1983. On a method for solving kinetic equation for Rossby waves, *Izvestiya akademii nauk ESSR. Physics. Mathematics*, 32, (3), pp. 294–299 (in Russian).
  97. Reznik, G.M., 1984. On the energy transfer equation for weakly interacting waves, *Int. J. Nonlin. Mech.*, 19, pp. 95–113.
  98. Reznik, G.M. and Soomere, T., 1984a. Numerical investigation of the spectral evolution of weakly nonlinear Rossby waves. *Oceanology*, 24, pp. 373–384 (in Russian), pp. 287–294 (English translation).
  99. Reznik, G.M. and Soomere, T., 1984b. On the evolution of an ensemble of Rossby waves to an anisotropic equilibrium state, *Oceanology*, 24, pp. 558–565, (in Russian), pp. 424–429 (English translation).
  100. Reznik, G.M., 1986. Weak turbulence on a  $\beta$ -plane, in *Synoptic eddies in the ocean*, eds. Kamenkovich, V.M., Koschlyakov, V.N. and Monin, A.S., Reidel, Dordrecht, Holland, pp. 73–108,
  101. Rhines, P.B., 1979. Geostrophic turbulence, *Annual Rev. Fluid Mech.* 11, pp. 401–441.
  102. Ruddick, B. and Gargett, A.E., 2003. Oceanic Double-diffusion: Introduction, *Progress in Oceanography*, 56, pp. 381–393.
  103. Rzhaplinsky, G.V. and Brekhovskikh, Yu.P. [Ржеплинский, Г.В., Бреховских, Ю.П.] (eds.), 1967. [Wave atlas for Gulf of Finland]. Gidrometeoizdat, Leningrad, (in Russian).
  104. Schmid, M., Lorke, A., Dinkel, C., Tanyileke, G. and Wüest, A., 2004. Double-diffusive convection in Lake Nyos, Cameroon. *Deep-Sea Research I*, 51, pp. 1097–1111.
  105. Schmitt, R.W., Perkins, H., Boyd, J.D. and Stalcup, M.C., 1987. C-SALT: an investigation of the thermohaline staircase in the western tropical North Atlantic. *Deep-Sea Research*, 34, pp. 1655–1665.
  106. Schoellhamer, D.H., 1996. Anthropogenic sediment resuspension mechanisms in a shallow microtidal estuary, *Estuar. Coast. Shelf Sci.*, 43, pp. 533–548.
  107. Segur, H. and Finkel, A., 1985. An analytical model of periodic waves in shallow water, *Stud. Appl. Math.*, 73, pp. 183–220.
  108. Simpson, J.H., Crawford, W.R., Rippeth, T.P., Campbell A.R. and Cheok, J.W.S., 1996. The vertical structure of turbulent dissipation in shelf seas, *Journal of Physical Oceanography*, 26 (8), pp. 1579–1590.
  109. Soomere, T., 1992a. Geometry of the double resonance of Rossby waves, *Ann. Geophys.*, 10, pp. 741–748.
  110. Soomere, T., 1992b. *Kinetic theory of Rossby waves*. Dissertationes Mathematicae Universitatis Tartuensis, 5, 32 pp.
  111. Soomere, T., 1993. Double resonance and kinetic equation for Rossby waves, *Ann. Geophys.*, 11, pp. 90–98.
  112. Soomere, T., 1995. Generation of zonal flow and meridional anisotropy in two-layer weak geostrophic turbulence, *Phys. Rev. Lett.*, 75, pp. 2440–2443.



113. Soomere, T., 1996. Spectral evolution of two-layer weak geostrophic turbulence. Part I: Typical scenarios. *Nonlinear Proc. Geophys.*, 3, pp. 166–195.
114. Soomere, T., 2001. New insight into classical equilibrium solutions of kinetic equations, *J. Nonlinear Sci.*, 11, pp. 305–320.
115. Soomere, T., 2001a. Wave regimes and anomalies off north-western Saaremaa Island. *Proc. Estonian Acad. Sci. Eng.*, 7, pp. 157–173.
116. Soomere, T., 2003. Coupling coefficients and kinetic equation for Rossby waves in multi-layer ocean, *Nonlinear Processes in Geophysics*, 10, pp. 385–396.
117. Soomere, T., 2003. Anisotropy of wind and wave regimes in the Baltic Proper, *J. Sea Res.*, 49, pp. 305–316.
118. Soomere, T., Elken, J., Kask, J., Keevallik, S., Kõuts, T., Metsaveer, J. and Peterson, P., 2003. Fast ferries as a new key forcing factor in Tallinn Bay. *Proc. Estonian Acad. Sci. Eng.*, 9, pp. 220–242.
119. Soomere, T. and Kask, J., 2003. A specific impact of waves of fast ferries on Sediment transport processes of Tallinn Bay. *Proc. Estonian Acad. Sci. Biol. Ecol.*, 52, pp. 319–331.
120. Soomere, T. and Keevallik, S., 2003. Directional and extreme wind properties in the Gulf of Finland. *Proc. Estonian Acad. Sci. Eng.* 9, 73–90.
121. Soomere, T., 2005. Wind wave statistics in Tallinn Bay, *Boreal Environment Research*, 10, pp. 103–18.
122. Soomere, T. and Engelbrecht, J., 2005. Extreme elevations and slopes of interacting solitons in shallow water. *Wave Motion*, 41, 2, pp. 179–192.
123. Soomere, T., 2006. Unikaalsed lainetuse tingimused Läänemerele 2005.a. jaanuaris [Unique wave conditions in the Baltic Sea in January 2005], *Publicationes Geophysicales Universitatis Tartuensis*, 50, pp. 215–224.
124. Sorensen, R.M., 1973. Ship-generated waves. *Adv. Hydrosci.*, 9, pp. 49–83.
125. Stoer, J. and Burlish, R., 1993. *Introduction to Numerical Analysis*. Springer-Verlag, New York.
126. Stokes, G.G., 1847. *On the theory of oscillatory waves*. *Trans. Camb. Phil. Soc.*, 8, pp. 441–455.
127. Stumbo, S., Fox, K., Dvorak, F. and Elliot, L., 1999. The prediction, measurement, and analysis of wake wash from marine vessels. *Marine Technology and SNAME News*, 36, pp. 248–260.
128. Svendsen, I.A. and Veeramony, J., 2001. Wave breaking in wave groups. *Journal of Waterway, Port, Coastal, and Ocean Engineering*, 127, pp. 200–212.
129. Swallow, J. and Crease, J., 1965. Hot salty water at bottom of Red Sea. *Nature*, 205, pp. 165–166.
130. Tapp, M.C., 1989. Kinetic equations for 2-D turbulent flow. *Quart. J. Roy. Met. Soc.* 115 (485), pp. 173–199.
131. The SWAMP Group, 1985. *Ocean wave modelling*. Plenum Press, New York.
132. Tuomi, L., Pettersson, H. and Kahma, K., 1999. Preliminary results from the WAM wave model forced by the mesoscale EUR-HIRLAM atmospheric model. *Report series of the Finnish Institute of Marine Research*, 40, pp. 19–23.
133. Turner, J.S., 1968. The behaviour of a stable salinity gradient heated from below. *J. Fluid. Mech.*, 33, pp. 183–200.
134. Turner, J.S., 1973. *Buoyancy Effects in Fluids*. Cambridge University Press, 368 pp.

135. Turner, J.S., 1995. Laboratory models of Double-Diffusive Processes, Double diffusive Convection, Ed. Brandt, A., Fernando, H.J.S., *Geophysical Monograph 94, AGU*, pp. 11-30.
136. Vallis, G.K. and Maltrud, M.E., 1993. Generation of mean flows and jets on a beta plane and over topography, *J. Phys. Oceanogr.*, 23, pp. 1346–1362.
137. Varyani, K.S. and Krishnankutty, P., 2002. Wave Wash of Stena Explorer in Dublin Bay. *EU Project TOHPIC, Document No 1.2.08.01*, 2002, Wave Wash of NGV Liamone in Nice Port. *EU Project TOHPIC, Document No 1.2.08.02*, 2002, Wave Wash of INCAT96 in Barcelona. *EU Project TOHPIC, Document No 1.2.08.03*, 2002.
138. Vösumaa, Ü. and Heinloo, J., 1996. The model of the vertical structure of the turbulent active layer of the sea. *J. Geophys. Res.*, 101, C10, pp. 25635–25646.
139. Walsh, D. and Ruddick, B.R., 1998. Nonlinear evolution of thermohaline intrusions. *J. Phys. Oceanogr.*, 28, pp. 1043–1070.
140. Watson, G., Chapman, R.D. and Apel, J.R., 1992. Measurements of the internal wave wake of a ship in a highly stratified Sea Loch, *J. Geophys. Res.* 97, pp. 9689–9703.
141. Whittaker, T.J.T., Doyle, R. and Elsässer, B., 1999. A study of the leading long period waves in fast ferry wash. In *Proc. Int. Conf. Hydrodynamics of High Speed Craft – Wake Wash and Motions Control*, London, 2000. RINA, London, paper 7 (CD).
142. Whittaker, T.J.T., Doyle, R. and Elsässer, B., 2001. An experimental investigation of the physical characteristics of fast ferry wake. In *2nd International Euroconference on High-Performance Marine Vehicles HIPER'01*. Hamburg, 2001. Technical University Hamburg-Harburg, 2001, pp. 480–491.
143. Wiklund, K., 1999. Wave interactions in a shallow-water model, *Nonlinear Processes in Geophysics*, 5, pp. 137–144.
144. Zakharov, V.E. and Schulman, V.G., 1980. Degenerative dispersion laws, motion invariants and kinetic equations, *Physica D*, 1, pp. 192–202.
145. Zakharov, V.E., Lvov, V.S. and Falkovich, G., 1992. *Kolmogorov spectra of turbulence I: Wave turbulence*, Springer, Berlin, Heidelberg, New York.
146. Zakharov, V.E. and Pushkarev, A.N., 1999. Diffusion model of interacting gravity waves on the surface of deep fluid, *Nonlinear Processes in Geophysics*, 6, pp. 1–10.
147. Zodiatis, G. and Gasparini, G.P., 1996. Thermohaline staircase formations in the Tyrrhenian Sea, *Deep-Sea Research*, Vol. 43, No. 5, pp. 655–678.

## **Approbation of results**

The results of the studies have been presented at the following international conferences:

1. The 4th USSR Conference “Contribution of young scientists and specialists towards solving contemporary problems of oceanology and hydrobiology”, Sevastopol, 1989.
2. The XVII Conference of Baltic Oceanographers, SMHI, Norrköping, Sweden 1990.
3. The 3rd USSR Conference “Vortices and turbulence in the oceans”, Kaliningrad, 1990.
4. The 3rd USSR symposium “Fine structure and synoptic variability of seas and oceans”, Tallinn, 1990.
5. The 24th General Assembly of the European Geophysical Society, The Hague, The Netherlands, 19–23 April 1999.
6. The 7th Mechatronics Forum International Conference and Mechanics Education Workshop, US, Atlanta, 6–8 September 2000.
7. EGS-AGU-EUG Joint Assembly, Nice, France, 06–11 April 2003.
8. The 6th International Conference Coastal Engineering 2003, Cadiz, 2003.
9. The 4th Baltic Sea Science Congress, Helsinki, 24–28 August 2003.
10. The 3rd General Assembly of the European Geosciences Union, Vienna, Austria, 24–29 April 2005.
11. The 5th Baltic Sea Science Congress, Sopot, Poland, 20–24 June 2005.

## Summary

This thesis mostly deals with two adjacent topics of propagation and evolution of long weakly nonlinear waves in geophysical applications and consist of two major parts. The first part is dedicated to resonant interactions of weakly nonlinear Rossby waves on a  $\beta$ -plane in the framework of the kinetic approach. The key development consists in accounting for the vertical structure of the motions, which are treated as a two-layer flow. The second part treats long weakly nonlinear waves excited by fast ferries. The key conclusion is that long waves from fast ferries may serve as the qualitatively new factor of hydrodynamic activity in certain types of open sea areas.

The main object of the first part of the study form the energy redistribution patterns in different Rossby wave systems and between different modes in a two-layer ocean. The relevant kinetic equation describing interactions of different modes and slow energy exchange between different wave components is analysed numerically. The principles of the solver for the particular kinetic equation and the estimates of its accuracy are shortly described. The possibility of occurrence of the double resonance (corresponding to the case when interacting wave components have equal group velocities and the kinetic equation fails) is analysed in some detail and its influence is removed from the numerical scheme. Several simulations of long-term evolution of Rossby-wave systems and the physical consequences of the spectral evolution are discussed in detail. The basic common features of the evolution of largely different initial flows are (i) the generation of a relatively intense preferably barotropic zonal flow and (ii) a tendency for the rest of the wave system towards a spectrally isotropic state. Several aspects of the problem of emerging of layered structures in realistic ocean are treated in the framework of a one-dimensional model of the vertical structure of the ocean. Numerical stability of a model of emerging layered structures owing to the interplay of double diffusion and turbulent mixing is analysed and an example of developing layers is presented.

The second part of the thesis concentrates on properties and potential environmental influence of long weakly nonlinear waves excited by fast ferries. The analysis is based on (i) estimates of the typical and extreme local wind wave conditions obtained with the use of a spectral wave model based on the kinetic theory in an adjacent study and (ii) the results of *in situ* measurements of properties of ship waves, performed as a part of this thesis. The name "fast ferries" stands here for large car-carrying ships that are able to sail with a speed close to the maximum phase speed of long waves  $\sqrt{gh}$  in Tallinn Bay. They frequently excite long waves, periods of which largely exceed the periods of the storm waves in this area. The parameters of ship waves in different coastal areas of Tallinn Bay are discussed based on a two-year measurement campaign largely performed by the author. A part of the results are interpreted in the framework of the cnoidal wave theory and the Korteweg-de Vries equation.

The mostly theoretical results of the first part of the study have been used in parallel studies of some features of evolution of more complex Rossby wave systems. The results of the studies into ship wave properties can be (and partially have been) used in various coastal engineering and environmental impact assessment problems in Tallinn Bay. They can be also directly applied to other shallow water bodies that are sheltered from long waves such as lakes hosting fast ferry traffic, Azov Sea, some areas of the Black Sea and the Mediterranean where they can be used for (i) quantifying the influence of the fast ferry traffic, (ii) working out recommendations for limitations of the fast ferry traffic, and (iii) for constructing coastal structures in areas affected by ship waves.

## Abstract

Two adjacent topics of long waves in geophysical applications are considered: (i) evolution of weakly nonlinear Rossby waves on a  $\beta$ -plane in the framework of the two-layer kinetic equation and (ii) comparison of properties of waves from fast ferries with wind waves, key parameters of which are estimated from historical data and from the kinetic equation for surface waves.

Energy redistribution patterns in different baroclinic Rossby wave systems and between different modes in a two-layer ocean are studied numerically under an assumption that the double resonance can be ignored. The basic common features of the evolution of largely different initial flows are that (i) a relatively intense mostly barotropic zonal flow is generated from very different initial conditions, and (ii) the rest of the wave system, incl. the whole baroclinic mode, tends to evolve towards a spectrally isotropic state. Numerical stability of a model of emerging layered structures owing to the interplay of double diffusion and turbulent mixing is analysed.

Properties and shape of long weakly nonlinear waves from fast ferries are established from a series of *in situ* measurements in Tallinn Bay. Their comparison with typical and extreme wind wave conditions, extracted from long-term measurements in the open Baltic Sea and from simulations of the local wave climate in an adjacent study with the use of the WAM wave model based on the kinetic equation for surface waves, shows that fast ferries often excite long waves of substantial height, periods of which largely exceed the periods of the storm waves in this area. Shown is that the cnoidal wave theory is the proper tool for description of long ship waves in shallow areas. The key conclusion from the analysis of the potential environmental influence of ship waves is that long waves from fast ferries may serve as a qualitatively new factor of hydrodynamic activity in certain types of open sea areas such as the Azov Sea and some areas of the Black Sea or the Mediterranean.

## Pikad nõrgalt mittelineaarsed lained geofüüsikalistes rakendustes

Käesolev väitekiri on pühendatud pikkade, nõrgalt mittelineaarsete geofüüsikaliste lainete levimise ja interaktsiooni kahele probleemipaketile ning jaguneb vastavalt kaheks suuremaks osaks.

Uuringute esimene osa käsitleb Rossby lainete omavahelisi interaktsioone nn kineetilise teooria raames  $\beta$ -tasandi lähenduses nõrga mittelineaarsuse tingimustes. Kontsentreerutakse lainetevahelist aeglast energiavahetust kirjeldava kineetilise võrrandi numbrilisele lahendamisele. Põhimõtteline erinevus varasemate analoogiliste töödega seisneb keskkonna vertikaalse struktuuri arvestamises, mida vaadeldakse kahekihilisena.

Peamiseks uurimisobjektiks on erinevate Rossby lainete komponentide ja moodide vahel aset leidev energia ümberjaotumine. Identifitseeritakse algselt erinevate lainesüsteemide evolutsiooni põhijooned – tsonaalse voolamise tekkimine ja lainesüsteemide ülejäänud osa muutumine isotroopseks. Analüüsitakse nn topeltresonantsi esinemise võimalust (mille puhul interakteeruvate lainete rühmakiirused on võrdsed ning kineetiline võrrand üldiselt pole korrektne). Lühidalt kirjeldatakse uuringuteks koostatud programmipaketti. Analüüsitakse erinevat tüüpi lainesüsteemide evolutsiooni põhilisi jooni ning esitatakse autori poolt läbiviidud numbriliste arvutuste tulemuste füüsikalised tõlgendused. Leitakse turbulentsse segunemise ja topeltdifusiooni vastasmõjul kihtide tekkimist kirjeldava mudeli stabiilsuse tingimused.

Töö teine osa hõlmab pikki, mittelineaarseid, kiirlaevade tekitatud laineid ja nende potentsiaalset mõju looduskeskkonnale. Pinnalainete kineetilisel võrrandil baseeruvate lainekliima hinnangute ja autori poolt läbi viidud in situ lainemõõtmiste alusel on teostatud võrdlev analüüs Tallinna lahes domineeriva tuulelaineruse ja kiirlaevade poolt põhjustatud lainetuse vahel. Kiirlaevadeks nimetatakse selles kontekstis laevu, mis sõidavad Tallinna lähel kriitilisele kiirusele (pinnalainete leviku maksimaalne kiirus antud sügavusega vees  $\sqrt{gh}$ ) lähedase kiirusega. Selliste laevade tekitatud lained on sageli märksa pikemad kui tormilained Tallinna lahes. On antud ülevaade autori isiklikul osalusel teostatud kiirlaevalainete põhiliste parameetrite mõõtmistest Tallinna lähel ja tulemuste tõlgendamisest mittelineaarsete pikkade pinnalainete teooria valgusel Korteweg-de Vriesi võrrandi raames.

Töö teises osas saadud tulemused on praktiliselt rakendatavad nii Tallinna lahes kui ka teistes suhteliselt madala loodusliku lainetuse intensiivsusega piirkondades (kiirlaevaliiklusega järved, Aasovi Meri, Musta Mere loodepiirkond ja mõningad alad Vahemeres) kiirlaevade keskkonnamõju ja insenertehniliste rajatistele tekkiva mõju kvantifitseerimisel ning kiirlaevaliiklust reguleerivate eeskirjade väljatöötamisel, aga ka insenertehniliste rajatiste projekteerimisel rannavööndis.

## Väitekirja tulemused

1. On välja töötatud efektiivne arvutuskeem Rossby lainete kineetilise võrrandi numbriliseks lahendamiseks kahekihilise ookeanimudeli jaoks ja vormistatud see programmipaketina. On lahendatud mitmed matemaatiliste tehnilised probleemid, sh resonantsikõverate geomeetria kirjeldamine, vastavate singulaarsete päratute integraalide teisendamine arvutuslikult sobivale kujule, topeltresonantsi käsitlemine, peaaegu tsonaalsele voolamisele vastavas arvutuspiirkonna osas kõrgema lahutusega skeemi rakendamine ning optimaalse arvutuspiirkonna valiku küsimus.
2. On teostatud erinevat tüüpi Rossby lainete süsteemide (algselt isotroopne, algselt tsonaalse ülekaaluga, algselt meridionaalse ülekaaluga) pikaajalise evolutsiooni arvutus ning identifitseeritud erinevat tüüpi lainesüsteemide evolutsiooni põhijooned. Arvutused on tehtud tüüpiliste ookeani tingimuste jaoks, kus ülemise ja alumise kihi paksuste suhe on 1:5.
3. On näidatud, et Rossby lainete barotroopse moodi evolutsioon kahekihilises mudelis sarnaneb põhijoontes barotroopsete Rossby lainete evolutsioonile. Kõikidel vaadeldud juhtudel esineb teatava osa energia ülekannet neile liikumise komponentidele, mis on suunatud peaaegu piki laiuskraade. Teisisõnu, on näidatud, et ka kahekihilises mudelis tekib peaaegu tsonaalne voolamine (liikumine geograafiliste paralleelide suunas).
4. On näidatud, et väga erinevate algtingimuste puhul tekib suhteliselt kiiresti selline lainete süsteem, mis vastab tugevale barotroopsele peaaegu tsonaalsele voolamisele. Seejuures ei pruugi barokliinse moodi puhul ilmnedas selget tendentsi tsonaalse komponendi ülekaalu tekkimisele ning see mood paljudel juhtudel muutub praktiliselt isotroopseks. Peamise osa tsonaalse voolamise kujunemisse annavad Rossby lained, mille pikkus on samas suurusjärgus nn. barokliinse Rossby raadiusega, mis iseloomustab sünoptiliste liikumiste iseloomulikku mastaapi konkreetsel merealal. Selliste lainete pikkus on avaookeanis mõnikümmend kuni 100 km ja perioodi mõnikümmend ööpäeva. Läänemere avaosas on tõenäoline, et tsonaalse voolamise asemel tekib piki põhja samasügavusjooni suunatud liikumine, mille kujundavad 10–20 km (Soome lahes 1–5 km) pikkusega topograafilised Rossby lained.
5. Arvutustulemuste alusel on püstitatud hüpotees, et Rossby lainete süsteemid mitmekihilises keskkonnas evolutsioneeruvad üldiselt sellise liikumiste süsteemi suunas, mille barotroopses moodis domineerib tsonaalne voolamine, kuid ülejäänud moodid on põhiosas isotroopsed (Märkus: paralleelsed uuringud sama numbrilise meetodi baasil (Soomere, *Phys. Rev. Lett.* 1995) näitasid, et kõrgemates moodides on teatavatel tingimustel võimalik ka meridionaalse voolamise ülekaalu tekkimine ja mitmeastmeline arenemine termodünaamilise tasakaalu suunas). Selline mehhanism võib osutada olu-



liseks jugavoolude asendi muutumisel ja polaarfrondi meandrite tekkimisel.)

6. On näidatud, et multimodaalse (antud juhul barotroopsest ja ühest barokliinsest moodist koosneva) Rossby lainete süsteemi evolutsioon toimub üldjuhul kiiremini kui sama energiaga, kuid puhtalt barotroopse lainesüsteemi evolutsioon. Teisisõnu, barokliinne mood mängib Rossby lainete evolutsioonis 'katalüsaatori' rolli.
7. On analüüsitud turbulentsse segunemise ja topeltdifusiooni koosmõjus kujuneva merekeskkonna vertikaalse struktuuri matemaatilise mudeli omadusi. On leitud vastava ilmutatud arvutuskeemi stabiilsust tagavad skeemi parameetrite väärtused ning numbriliselt demonstreeritud kihtide tekkimist realistlikel eeldustel. Ookeani ja Läänemere tingimuste jaoks tüüpiliste temperatuuri ja soolsuse ning turbulentsi kineetilise energia hinnanguliste ekstreemsete väärtuste korral on piisav jälgida tingimust  $(\Delta h)^2 / \Delta \tau > 0.01$ , kus  $\Delta h$  tähistab ruumi- ja  $\Delta \tau$  ajasammu.
8. On leitud looduslike lainete tüüpilised ja ekstreemsed parameetrid Läänemere avaosa põhjapoolses sektoris teostatud ligikaudu 25 aasta pikkuse lainemõõtmiste aegrea alusel. On näidatud, et tuulelainete perioodid isegi Läänemere avaosas on tavaliselt 4–6 sekundit ning ulatuvad 10 sekundini vaid ekstreemsetes tormides ning on seega tavaliselt väiksemad kõrgeimate kiirlaevalainete perioodidest.
9. Otseste lainemõõtmiste alusel on määratletud laevalainete põhilised parameetrid Tallinna lahe rannavööndis. On näidatud, et kiirlaevalainete maksimumne kõrgus Tallinna lahel on suhteliselt tagasihoidlik absoluutarvudes (päeva kõrgeimad lained ligikaudu 1 m). On demonstreeritud, et suur osa kiirlaevalainete energiast on koondunud lainetes, mille periood 10–15 sekundit ja kõrgus kuni 1 m.
10. Laevalainete parameetreid on võrreldud pinnalainete kineetilise võrrandi baasil toimiva lainemudeli abil arvutatud Tallinna lahe looduslike lainete režiimiga. On näidatud, et
  - looduslik lainetuse intensiivsus on nii madal, et päeva kõrgeimad kiirlaevalained kuuluvad aasta 1–5% kõrgeimate lainete hulka;
  - ligikaudu 1 m kõrgusi ja 10–15 s perioodiga looduslikke laineid esineb Tallinna lahel äärmiselt harva, mistõttu kiirlaevalained võivad endast kujutada kvalitatiivselt uut hüdrodünaamilist mõjutegurit.
11. On näidatud, et kiirlaevalainete pikemate ja kõrgeimate komponentide (kõrgus üle 0,5 m, periood üle 10 s) puhul muutuvad mittelineaarsed efektid märkimisväärseks sügavusel 10–15 m. Eksperimentide käigus salvestatud veepinna kuju aegjadade alusel on näidatud, et:
  - pikkade ja kõrgete kiirlaevalainete kuju madalas vees on väga lähedane Korteweg-de Vriesi (KdV) võrrandi perioodiliste lahendite – knoidaalsete lainete – kujule;

- kõrgeimad kiirraevalained kujutavad endast peaaegu täpseid Korteweg-de Vriesi solitone.  
Seega võib soovitada KdV võrrandit kiirraevalainete omaduste kirjeldamiseks rannalähedases vööndis.
12. Knoidaalsete ja siinuslainete omaduste võrdlemise kaudu on demonstreeritud, et kiirraevalainete pikemate ja kõrgemate komponentide poolt tekitatud põhjalähedased kiirused teatavates sügavustes Tallinna lahe rannavööndis on tõenäoliselt märksa suuremad võrreldes klassikalise siinuslainete teooria alusel leitud hinnangutega.

## ACKNOWLEDGEMENTS

I would like to begin by expressing my gratitude to my supervisor Prof. Tarmo Soomere, for his support and advice since my first years in science. Thanks for the patience and support during the long time of preparation of the thesis.

Thanks to my supervisor, Assoc. Prof. Hanno Ohvril, for any kind of support from the side of the Tartu University and for help in explaining many aspects of physics.

Thanks to Prof. Rein Rõõm and the excellent colleagues from the Institute of Environmental Physics for support at many different stages of preparation of the thesis.

Thanks to Dr. Jaak Heinloo for interesting tasks in modeling. It has helped me a lot to understand the differences between a model and the possibilities of its numerical realization.

Thanks to Dr. Rein Tamsalu and Dr. Vladimir Zalesny for consultations in numerical methods and stability.

Thanks to Dr. Peep Miidla and Prof. Peep Uba for consulting and teaching different aspects in math.

Thanks to the long-term colleagues from the Marine Systems Institute. Thanks to the PTR Grupp for the help with instrumentation.

Thanks to Prof. Jüri Engelbrecht and the colleagues from the Institute of Cybernetics for their support and motivation.

Special thanks to my family, Ragner for IT-support and Christine for valuable remarks and corrections.

## CURRICULUM VITAE

**Name** Kalev Rannat  
**Date of birth** 22.10.1958, Tallinn  
**Phone** +372 50 54 209  
**E-mail** kr@litefix.com, rannat@cs.ioc.ee  
**Home address** Tartu mnt. 19, 61505 Elva  
**Education** Tallinn University of Technology (1982), engineer (electronics).  
**Scientific degree** MSc, Tartu University, 1994 (Interaction of weakly nonlinear Rossby waves in 2-layer ocean, Tartu University, sup. T. Soomere).  
**Employment** TUT, Institute of Cybernetics, scientist.  
**Professional experience** TUT, TU sector, laboratory assistant, 1977–1982;  
Special Design Office of the Acad. of Sci., sector of micro-processor-techniques: engineer, constructor, 1982–1983, 985–1989; military service, 1983–1985;  
Institute of Therm. and Electrophysics, Institute of Ecology and Marine Research, scientist, 1989–1992;  
Estonian Marine Institute, scientist: 1992–2002;  
TUT, Marine Systems Institute, scientist, 2002–2005;  
TUT, Institute of Cybernetics, scientist, 2005– ...  
**Research areas** Adaptive, multisensor surveillance systems. Double-diffusion in the ocean. Waves and nonlinear effects. Applications of GPS-method in meteorology.  
**Self-education, trainings, expeditions** Coriolis Laboratory at Grenoble University, EU program Human Capital and Mobility – Access to Large Devices, Rossby waves and their interactions, March–April 1997.  
Short-term missions in FIMR (Finnish Institute of Marine Research) and FIM (Finnish Institute of Meteorology).  
Intermediate-level short course in GPS analysis using GAMIT/GLOBK software, Toulouse, France, November, 2002.  
Luxembourg University, GAMIT/GLOBK advanced courses, Nov. 2006.  
Participation in sea expeditions on research vessels, organized by the Estonian Marine Institute, up to 2002.  
**Projects** Participation in international projects SEAMOCS and ECONEt.  
Wind wave climate of the Baltic Sea and nonlinear effects (TUT).  
Nonlinear dynamics and stress analysis (TUT).  
Tomographical Surveillance of the Troposphere (collaboration with the Institute of Applied Math, TU).  
Ontologies of interactivity, multi-agent systems and time (collaboration with the Institute of Technology, TU).  
**Languages** English, Russian, Finnish, German.

## ELULOOKIRJELDUS

<b>Nimi</b>	<b>Kalev Rannat</b>
<b>Sünniaeg ja -koht</b>	22.10.1958, Tallinn
<b>Telefon, E-post</b>	+372 50 54 209, kr@litemfix.com, rannat@cs.ioc.ee
<b>Kodune aadress</b>	Tartu mnt 19, 61505 Elva
<b>Haridus</b>	Tallinna Tehnikaülikool (1982), elektroonikainsener.
<b>Teaduskraad</b>	MSc, Tartu Ülikool, 1994 (Nõrgalt mittelineaarsete Rossby lainete interaktsioon 2-kihilises ookeanis, Tartu Ülikool, juh. T. Soomere).
<b>Töökoht</b>	Tallinna Tehnikaülikool, Küberneetika Instituut, teadur.
<b>Teenistuskäik</b>	Tallinna Tehnikaülikool, TU sektor, laborant, 1977–1982; TA SKB mikroprotsessortehnika sektor, insener, vaneminsener, ins.-konstruktor, 1982–1983, 1985–1989; armeeteenistus, 1983–1985; TA TEFI, TA ÖMI, nooremteadur, 1989–1992; Eesti Mereinstituut, merefüüsika sektor, teadur, 1992–2002; TTÜ Meresüsteemide Instituut, teadur, 2002–2005; TTÜ Küberneetika Instituut, teadur, 2005– ...
<b>Uurimissuunad</b>	Adaptiivsed ja paljuandurilised seiresüsteemid. Topeltdifusioon meres. Lained ja mittelineaarsed efektid. GPS-meetodi rakendused meteoroloogias.
<b>Enesetäiendamine, stažeerimine, ekspeditsioonid</b>	Grenoble'i Ülikooli Coriolis' laboratoorium, EU programm Human Capital and Mobility – Access to Large Devices Rossby lained ja interaktsioonid, märts–aprill 1997. Lähetused Soome Mereinstituuti ja Soome Meteoroloogia-instituuti. GPS-kursus Prantsusmaal: Intermediate-level short course in GPS Analysis using GAMIT/GLOBK Software, Toulouse, France, November, 2002. GPS-GAMIT/GLOBK-kursus Luxembourg'i Ülikoolis, november 2006. Osalemine Eesti Mereinstituudi korraldatud mereekspeditsioonidel uurimislaevadega, aastani 2002.
<b>Osalus projektides</b>	Tuulelainete uurimine ja modelleerimine (koostöö Euroopa mereuurimiskeskustega: SEAMOCS, ECO-NET). Läänemere lainetus ja mittelineaarsed efektid (TTÜ). Mittelineaarne dünaamika ja pingeanalüüs (TTÜ). Troposfääri seire tomograafiliste meetoditega (koostöö TÜ Rakendusmatemaatika Instituudiga). Interaktiivsuse ontoloogiad, multiagentsüsteemid ja aeg (koostöö TÜ Tehnoloogiainstituudiga).
<b>Võõrkeeled</b>	Inglise, vene, soome, saksa.

# DISSERTATIONES GEOPHYSICALES UNIVERSITATIS TARTUENSIS

1. **Andres Kuusk.** The hot-spot effect in plant canopy reflectance. Tartu, 1991.
2. **Tiit Nilson.** Radiative transfer in non-homogeneous plant canopies. Tartu, 1991.
3. **Helgi Arst.** Atmosfääri ja mere kiirguskarakteristikud looduskeskkonna seisundi informatoritena (vene keeles). Tartu, 1991.
4. **Juha Sarkkula.** Measuring and modelling water currents and quality as a part of decision making process for water pollution control. Tartu, 1992.
5. **Piia Post.** On the two radiatively effective cloud parameters. Tartu, 1993.
6. **Aadu Mirme.** Electric aerosol spectrometry. Tartu, 1994.
7. **Aare Luts.** Mathematical simulation of the evolutions of air ions. Tartu, 1995.
8. **Tiit Kutser.** Estimation of water quality in turbid inland and coastal waters by passive optical remote sensing. Tartu, 1997.
9. **Ülle Kikas.** Atmospheric aerosol in the Baltic region. Tartu, 1998.
10. **Tarmo Kõuts.** Processes of deep water renewal in the Baltic sea. Tartu, 1999.
11. **Anu Reinart.** Underwater light field characteristics in different types of Estonian and Finnish lakes. Tartu, 2000.
12. **Marko Kaasik.** Parameterisation of atmospheric boundary layer in the numerical model of air pollution transport. Tartu, 2000.
13. **Janek Laanearu.** Topographically constrained deep-water flows in channels. Tartu, 2001.
14. **Urmas Raudsepp.** Wind-driven circulation in the gulf of Riga. Tartu, 2001.
15. **Urmas Hõrrak.** Air ion mobility spectrum at a rural area. Tartu, 2001.
16. **Marko Vana.** Formation and evolution of atmospheric aerosol size spectrum by the occurrence of nucleation burst events in the atmospheric boundary layer; transport of the climatically active particulate air pollution. Tartu, 2002.
17. **Veljo Kimmel.** Analysis of methods of air quality assessment. Applications in Estonia. Tartu, 2002.
18. **Oleg Okulov.** Variability of atmospheric transparency and precipitable water in Estonia. Tartu, 2003.
19. **Aarne Männik.** Implementation and validation of the nonhydrostatic adiabatic core of the numerical weather prediction model hirlam. Tartu, 2003.
20. **Matti Mõttus.** Shortwave solar radiation field inside willow canopy. Tartu, 2004.



